

THE EFFECTS OF FLOW RATE AND ECCENTRIC DISCHARGE  
ON VERTICAL LOADS IN A MODEL GRAIN BIN

by

Darryl Glenn Pokrant

A thesis  
presented to the University of Manitoba  
in partial fulfillment of the  
requirements for the degree of  
Master of Science  
in  
Agricultural Engineering

Winnipeg, Manitoba

(c) Darryl Glenn Pokrant, 1987



National Library  
of Canada

Acquisitions and  
Bibliographic Services Branch

395 Wellington Street  
Ottawa, Ontario  
K1A 0N4

Bibliothèque nationale  
du Canada

Direction des acquisitions et  
des services bibliographiques

395, rue Wellington  
Ottawa (Ontario)  
K1A 0N4

*Your file* *Votre référence*

*Our file* *Notre référence*

The author has granted an irrevocable non-exclusive licence allowing the National Library of Canada to reproduce, loan, distribute or sell copies of his/her thesis by any means and in any form or format, making this thesis available to interested persons.

L'auteur a accordé une licence irrévocable et non exclusive permettant à la Bibliothèque nationale du Canada de reproduire, prêter, distribuer ou vendre des copies de sa thèse de quelque manière et sous quelque forme que ce soit pour mettre des exemplaires de cette thèse à la disposition des personnes intéressées.

The author retains ownership of the copyright in his/her thesis. Neither the thesis nor substantial extracts from it may be printed or otherwise reproduced without his/her permission.

L'auteur conserve la propriété du droit d'auteur qui protège sa thèse. Ni la thèse ni des extraits substantiels de celle-ci ne doivent être imprimés ou autrement reproduits sans son autorisation.

ISBN 0-315-86141-X

**Canada**

THE EFFECTS OF FLOW RATE AND ECCENTRIC DISCHARGE ON  
VERTICAL LOADS IN A MODEL GRAIN BIN

BY

DARRYL GLENN POKRANT

A thesis submitted to the Faculty of Graduate Studies of  
the University of Manitoba in partial fulfillment of the requirements  
of the degree of

MASTER OF SCIENCE

© 1987

Permission has been granted to the LIBRARY OF THE UNIVERSITY OF MANITOBA to lend or sell copies of this thesis, to the NATIONAL LIBRARY OF CANADA to microfilm this thesis and to lend or sell copies of the film, and UNIVERSITY MICROFILMS to publish an abstract of this thesis.

The author reserves other publication rights, and neither the thesis nor extensive extracts from it may be printed or otherwise reproduced without the author's written permission.

I hereby declare that I am the sole author of this thesis.

I authorize the University of Manitoba to lend this thesis to other institutions and/or individuals for the purpose of scholarly research.

Darryl Glenn Pokrant

I further authorize the University of Manitoba to reproduce this thesis by photocopying or by other means, in total or in part, at the request of other institutions and/or individuals for the purpose of scholarly research.

Darryl Glenn Pokrant

## ABSTRACT

Vertical loads imposed on a 1.0 m diameter by 1.5 m smooth-walled model grain bin filled with wheat were measured in a series of dynamic tests to determine the effects of discharge rate and eccentricity. A high-speed data acquisition system recorded both vertical wall and total loads for each combination of the four discharge rates and locations used. Discharge rates of 0.48, 1.13, 2.10 and 4.58 kg/s were obtained using 45, 60, 75 and 100 mm diameter orifices located at the bin centre, 150 and 300 mm from the bin centre and at the bin wall.

An increase in vertical wall load from the static to the dynamic condition was measured for each test. Analysis of variance of the peak loads on the wall nearest the outlet indicated the significance of both flow rate and location effects with no interaction between the two.

Total vertical wall load was linearly proportional to flow rate with a 9.5 fold increase in discharge rate causing a 12% increase in wall load. With centre discharge, this load increase was uniform around the bin circumference. With eccentric discharge, load on the wall section nearest the outlet increased while a decrease occurred on the far wall. In both cases, total wall load was similar, indicating that the effect of eccentric discharge was to simply redistribute the basic dynamic load without causing any additional increase. Partially eccentric discharge produced the largest near wall loads and regression analysis suggested the maximum would occur at an eccentricity of 70%.

## ACKNOWLEDGMENTS

Throughout this project, I received encouragement and assistance from many individuals and I would like to thank them for their kindness and inspiration to keep pursuing that "light at the end of the tunnel"

First, I want to acknowledge Dr. M.G. Britton, my major professor, for initially intriguing me with this topic. His positive attitude and guidance was always a source of motivation and it was most sincerely appreciated. Thank you also to Dr. Jayas and Dr. Stimpson for serving on my thesis advisory committee.

I am grateful to Jack Putnam and Ben Mogan for their expertise and helpful suggestions offered during the building stage of the project. The electronic wizardry of Henry Kroker was invaluable and his time spent in late night repair sessions went far beyond the call of duty. A special thank you to Donna Weiss and Debby Allston for their cheery smiles every time I came to the office to settle "yet another bill!"

A sincere thank you to all of my friends and fellow students for allowing me to bounce ideas off them when I needed a second opinion. A special thank you to Mike Burns and Patrick Versavel. Thanks also to Andrew C. Eisbrenner for his photography and binary code expertise.

Finally, I would like to thank my parents and family for their encouragement and understanding over the past four years. I could not have completed this thesis without their love, care and concern.

## TABLE OF CONTENTS

ABSTRACT . . . . .		iii
ACKNOWLEDGMENTS . . . . .		iv
<u>Chapter</u>		<u>page</u>
I. INTRODUCTION . . . . .		1
II. LITERATURE REVIEW . . . . .		3
Historical Review . . . . .		3
Current Research Trends . . . . .		8
Factors Influencing Dynamic Pressure . . . . .		9
Variation and Change in Material Properties . . . . .		9
Pressure State . . . . .		12
Type of Flow . . . . .		13
Pulsations and Oscillations . . . . .		16
Discharge Rate . . . . .		17
Location of the Discharge Outlet . . . . .		20
Model Testing . . . . .		28
Instrumentation . . . . .		30
Summary . . . . .		31
III. EXPERIMENTAL EQUIPMENT . . . . .		33
Test System . . . . .		33
Main Frame and Base Table . . . . .		33
Model Bin . . . . .		36
Discharge Outlets . . . . .		37
Load Measurement . . . . .		39
Vertical Load Transducers . . . . .		40
Transducer Calibration . . . . .		41
Instrumentation . . . . .		45
Materials Handling . . . . .		48
IV. PROCEDURE . . . . .		50
Experimental Design . . . . .		50
Bin Wall Surface Conditioning . . . . .		50
Testing Procedure . . . . .		51
Dynamic Tests . . . . .		52
Settling Tests . . . . .		57
Dead Weight Tests . . . . .		58
Grain Quality Control . . . . .		59
Discussion . . . . .		60

V.	DATA ANALYSIS AND COMPUTER PROGRAMS . . . . .	63
	Introduction . . . . .	63
	Computer Programs . . . . .	63
	CALBRAT6 . . . . .	63
	REGRESS6 . . . . .	64
	COLLECT . . . . .	64
	ACQUIRE1 . . . . .	65
	NOISE . . . . .	66
	CHANGES . . . . .	67
	CONVERTS . . . . .	67
	STATICS . . . . .	69
	STATDYNA . . . . .	70
	FLOWBULK . . . . .	70
	GRAPHS . . . . .	71
	SEARCH and RESULTS . . . . .	72
	PEAKS . . . . .	73
	ANOVA . . . . .	74
	SAS . . . . .	74
VI.	RESULTS AND DISCUSSION . . . . .	75
	Static Loads . . . . .	75
	Dynamic Tests . . . . .	75
	Settling Tests . . . . .	77
	Pre-flow Static Load Comparison . . . . .	80
	Grain Flow Observations . . . . .	82
	Flow Rate . . . . .	82
	Flow Patterns . . . . .	86
	Dynamic Loads . . . . .	88
	Load vs. Time Graphs . . . . .	88
	Peak Loads . . . . .	98
	Dynamic/Static Ratios . . . . .	108
	Time of Peak Load . . . . .	109
	Weight of Discharge at Peak Load . . . . .	112
VII.	CONCLUSIONS . . . . .	114
VIII.	RECOMMENDATIONS . . . . .	116
	LIST OF REFERENCES . . . . .	117
	<u>Appendix</u>	<u>page</u>
A.	WALL STRAIN GAGE LOCATIONS AND CALIBRATION . . . . .	125
B.	TRANSDUCER CALIBRATION RESULTS . . . . .	131
C.	TRANSDUCER-TO-BIN LOAD CONVERSION EQUATIONS . . . . .	132
D.	BIN LOADS VS. TIME GRAPHS - SERIES #1 . . . . .	136
E.	STATIC LOAD ANALYSIS RESULTS . . . . .	153
F.	DYNAMIC LOAD ANALYSIS RESULTS . . . . .	157
G.	DATA ACQUISITION PROGRAM . . . . .	175

LIST OF TABLES

<u>Table</u>	<u>page</u>
6.1. Peak Dynamic Load on Wall Section B . . . . .	98
6.2. Peak Dynamic Load on Wall Section C . . . . .	99
6.3. Peak Average Dynamic Load on Wall Sections B and C . . . . .	99
6.4. Peak Dynamic Load Imbalance Between the Near and Far Wall Sections . . . . .	103
6.5. Peak Average Dynamic/Static Ratio on Wall Sections B and C	108
6.6. Time of Peak Average Dynamic Load on Wall Sections B and C	110
6.7. Discharge Weight at Peak Average Dynamic Load on Wall Sections B and C . . . . .	112

## LIST OF FIGURES

<u>Figure</u>	<u>page</u>
3.1. Test system - front elevation . . . . .	34
3.2. Test system 3-point support - plan view . . . . .	35
3.3. Typical discharge plates . . . . .	38
3.4. Adjustable pneumatically controlled slide gate . . . . .	38
3.5. Transducer mounting configurations . . . . .	42
3.6. Calibration setup arrangement . . . . .	43
3.7. Data acquisition instrumentation . . . . .	46
4.1. Measurement of the filling angle of repose . . . . .	54
5.1. Model bin floor and wall sections . . . . .	68
6.1. Wall transducer loads vs. settling time - test D60E1S0 . . .	79
6.2. Total grain load vs. discharge time for the four flow rates .	83
6.3. Total grain load vs. discharge time - magnified scale . . . .	85
6.4. Grain surface profiles for four discharge eccentricities . .	87
6.5. Wall transducer loads vs. discharge time - test D60E0S2 . . .	90
6.6. Wall transducer loads vs. discharge time - test D60E1S2 . . .	90
6.7. Wall transducer loads vs. discharge time - test D60E2S2 . . .	91
6.8. Wall transducer loads vs. discharge time - test D60E3S2 . . .	91
6.9. Floor and wall loads vs. discharge time - test D60E0S2 . . .	93
6.10. Floor and wall loads vs. discharge time - test D60E1S2 . . .	94
6.11. Floor and wall loads vs. discharge time - test D60E2S2 . . .	95
6.12. Floor and wall loads vs. discharge time - test D60E3S2 . . .	96
6.13. Wall loads vs. discharge time - dynamic test D60E1S2 . . .	107
6.14. Wall loads vs. discharge time - settling test D60E1S0 . . .	107

## CHAPTER I

### INTRODUCTION

The North American and European grain handling industry has seen many changes since the early days when sacks of wheat were filled by hand and manually stacked in large warehouses waiting to be shipped to local buyers. Today, farm sizes and machinery are large with increased grain storage capacity and high-throughput bulk handling systems being required to supply worldwide grain export markets. As material costs rise, the term "efficient" is often stretched to its full definition by bin manufacturers as they attempt to meet these growing grain handling requirements at the lowest cost.

All this has caused concern among bin designers since most design code specifications are very vague with respect to static grain loads and the dynamic increases associated with discharge. The problem was summarized by Ross et al. (1979) who suggested that the "difficulty of accurately estimating the stresses within . . . axially loaded, thin-walled shells with a unique form of internal pressure and axial bending moment is confounded by the problem of accurately predicting the loads imposed on the structure by the stored grain."

Two factors which are thought to have an effect on these loads are discharge rate and the location of the discharge outlet. As capacity of grain handling systems increase, so does the rate at which the grain must be conveyed. Some researchers have suggested that dynamic bin

loads are unaffected by increasing flow rates, but bin failures that occurred when higher flow rates were used appear to contradict this opinion. If the current trend continues, higher flow rates will become the norm and bin designers will therefore need to know if and/or how they should account for them.

It has also been known for many years that locating the centre of discharge in a flat-bottomed bin away from the centre of the bin tends to cause higher bin loads. Research results have been very qualitative however, and opinions are still varied as to where load maximums occur and even if the loads increase or decrease near a given wall section. Many bin design codes have allowed for eccentric discharge by applying an overpressure factor proportional to the degree of eccentricity, but recent studies indicate that partially eccentric discharge creates the most critical situation. It is clear that more work with respect to eccentric discharge load effects needs to be done.

With these thoughts in mind, it was decided to undertake a study to investigate the effects of discharge rate and discharge location on the vertical wall loads in a smooth steel wall model grain bin. The specific objectives of this model study were:

1. to determine the effect on vertical wall loads of increasing the discharge rate, and
2. to outline more clearly the pattern of vertical wall load change associated with eccentric discharge.

## Chapter II

### REVIEW OF LITERATURE

#### 2.1 HISTORICAL REVIEW

It was suggested by Kramer (1944) that the first account of grain storage was recorded in the Bible in the 41st Chapter of Genesis, where Joseph, in anticipation of an impending famine, decreed that one fifth of the grain harvest should be stored. This event took place in Egypt around 1700 B.C. and proved to be a turning point in history since over the 3700 years to follow, countless numbers of grain and bulk material storage structures were built.

Prior to 1850, storage requirements were small and grain bins were relatively shallow. Many designs were based on Rankine's formula for a retaining wall using hydrostatic pressure theory (Ketchum, 1919). This theory assumed that lateral wall load increased linearly with depth and that vertical load was carried by the floor. As agricultural production began to increase, large scale marketing and export of grain soon became popular giving rise to a need for larger and deeper storage structures.

Deep bins were first built around 1860 and hydrostatic theory was also used in their design (Jenike and Johanson, 1968). Deep bins have been defined as having heights greater than anywhere from 3/4 to 5 times the diameter (Ketchum, 1919; Isaacson and Boyd, 1965; NRCC, 1977 & 1983) although most authors suggest height to diameter ratios between 1 and 2.

In 1882, Roberts made the first measurements of grain pressure and he observed no increase in bin floor pressure after the height of fill exceeded twice the bin diameter (Ketchum, 1919). This discovery was significant since it contradicted the hydrostatic design practice and pointed to the existence of wall friction which transfers vertical load from the bulk material to the bin walls.

The first theoretical analysis of grain pressures was performed by Janssen in 1895 (Ketchum, 1919). Janssen modeled the grain mass as a series of horizontal differential elements subjected to uniform vertical pressure with an additional vertical shear force due to friction between the grain and the bin wall acting along the elements' outside edges. The frictional shear force related to an assumed uniform lateral pressure by a coefficient of friction  $\mu'$ , which was assumed to be constant. Lateral pressure related to vertical pressure at any similar depth by a ratio  $k$ , which was also assumed to be constant. Static analysis of the forces resulted in a differential equation which Janssen solved using an exponential solution. The additional assumption of a constant bulk density yielded the following equations:

$$V = \frac{w \cdot g \cdot R}{\mu' \cdot k} \left[ 1 - e^{\mu' \cdot k \cdot Y/R} \right] \quad [2.1]$$

$$L = k \cdot V \quad [2.2]$$

where:  $V$  = vertical grain pressure at depth  $Y$ , Pa  
 $L$  = lateral grain pressure at depth  $Y$ , Pa  
 $w$  = grain bulk density,  $\text{kg/m}^3$   
 $g$  = gravitational acceleration,  $9.81 \text{ m}^2/\text{s}$   
 $R$  = hydraulic radius of bin, m  
 $\mu'$  = coefficient of friction of grain on the bin wall  
 $k$  = ratio of lateral to vertical pressure  
 $Y$  = depth of grain, m

In 1896, Koenen suggested the Janssen k ratio could be estimated using the Rankine theory for active earth pressure which defined k as a function of the internal friction angle  $\phi$  (Smith and Simmonds, 1983):

$$k = \frac{1 - \sin \phi}{1 + \sin \phi} \quad [2.3]$$

The formula assumed that the bulk grain mass reached an active state of failure, which Smith and Simmonds noted as being reasonable. This led, however, to a lower bound on the pressures predicted using Janssen's equation and Cowin (1979) suggested the above equality was in fact a lower limit with  $k=1$  being the upper limit.

Two years after Janssen published his equations, Airy proposed a formula for calculation of grain pressure based on Coulomb's theory of sliding wedges, which was a theory borrowed again from soil mechanics. Airy's solution gave results similar to Janssen's but it never gained wide acceptance due to its very complex nature (Ketchum, 1919).

At this early stage of grain pressure research, investigation focussed primarily on static loads. Little attention was given to dynamic unloading effects since most researchers assumed the static condition resulted in the greatest bin loads. A major discrepancy, however, was noted by Prante in 1896 after measuring lateral pressures up to four times the static values while discharging wheat from his full size bins (Ketchum, 1919). Ketchum questioned the validity of the results since the discharge outlets were located near the edge of the bin. Later research, however, confirmed Prante's results and thus the existence of overpressures or pressures over and above static values was established.

The state-of-the-art for grain pressures was summarized by Ketchum (1919) in his classic design text. Generally, Janssen's results for static pressures were confirmed by most researchers, but again, there was disagreement as to the effect of grain in motion.

Pleissner (Ketchum, 1919) obtained lateral pressure increases up to two times static values but his results, like Prante, were attributed to the use of eccentric discharge outlets. Jamieson (Ketchum, 1919) noted pressure increases during discharge of no greater than 10% provided the discharge orifice was no larger than 1/150th of the bin area. This was the first report to indicate of possible "dynamic" effects when using higher flows. Lufft (1904) stressed that grain was not homogeneous and that subsequent variability in material properties should be accounted for.

Over the period from 1920 to 1960, there was little new information to come from North America. Researchers generally ignored dynamic overpressures even though it was concluded by Bovey (1904) that "grain in motion produces far greater stresses than the grain at rest." Most of the work basically confirmed the accuracy of Janssen's equation provided a proper choice of "constants" was made. Sundaram and Cowin (1979) classified these years as a period of misconceptions and misinformation.

Although North American research was sparse, there was significant European and Russian research conducted during these middle years. In the 1940's, Marcel and Andre Reimbert developed a second set of grain pressure prediction equations. The derivation was outlined in detail in Reimbert and Reimbert (1976). The equations were similar to Janssen's, with the basic difference being that the Reimberts assumed a hyperbolic

solution whereas Janssen used the exponential form. The equations were as follows with the variables the same as per equations [2.1] and [2.2]:

$$V = w \cdot g \cdot Y \left[ \frac{Y \cdot \mu' \cdot k}{R} + 1 \right]^{-1} \quad [2.4]$$

$$L = \frac{w \cdot g \cdot R}{\mu'} \left[ 1 - \left[ \frac{Y \cdot \mu' \cdot k}{R} + 1 \right]^{-2} \right] \quad [2.5]$$

Turitzin summarized additional work by the Reimberts, Taktamishev, Kovtun and Platonov and V.S. Kim and he concluded that:

1. Two distinct patterns of flow can occur during emptying:  
dynamic (mass) flow, which is accompanied by lateral pressure increases, and  
non-dynamic (funnel) flow, which causes no lateral overpressures,
2. Filling pressures are less than emptying pressures,
3. Lateral pressures predicted by the equations of Janssen or Reimbert are only valid for the static case or the non-dynamic flow condition,
4. Dynamic pressure increases up to 2.4 times the values predicted using Janssen theory can be obtained,
5. Factors affecting the type of flow are: wall roughness, grain density and bin height to diameter ratio,
6. Dynamic overpressures can be eliminated by inducing non-dynamic flow through the use of flow tubes or wall rings,
7. There is no agreement among researchers as to the magnitude or location of dynamic overpressures, and
8. Neglect of dynamic pressure in design may result in bin wall failures

## 2.2 CURRENT RESEARCH TRENDS

Over the last 25 years, there has been renewed interest in grain pressure studies, prompted primarily by an increasing number of failures of large grain and other bulk solid storage structures. Many authors have derived new theories or modified existing ones to predict static pressures (Cowin, 1977; Jofriet et al., 1977; Ross et al., 1979; Bishara et al., 1983), but despite its obvious shortcomings, Janssen's equation still remains the simplest most direct method for predicting static grain pressures (Smith and Simmonds, 1983). Evidence of this is seen in that most design codes use either the Janssen or Reimbert formulae to determine static loads (Safarian and Harris, 1985).

The majority of recent research on grain pressures has dealt with the subject of dynamic effects since they result in large overpressures. However, as pointed out by Britton in 1977, "It seems a shame that we are now in pursuit of this new problem (dynamic overpressures) but have not succeeded in fully understanding the static problem." The results of all the individual authors are too numerous to mention in this review of literature, but general conclusions and observations can be made.

The most obvious observation to be made is that a large number of reports contradict each other. Haaker and Scott (1983), in a paper presented to the 2nd International Conference on Design of Silos for Strength and Flow stated, "the reviewer cannot help but notice the wide disparity that exists between the various theories, methods and codes of practice that have been proposed . . . Recent advances have appeared to further this disparity rather than clarifying the position."

### 2.3 FACTORS INFLUENCING DYNAMIC GRAIN PRESSURE

Due to the unpredictability of many of the factors involved with dynamic pressures, Jenike (1954) did not see the possibility of a mathematically derived formula being developed and suggested that an empirical solution was required. Twenty-one years later, McLean and Bravin (1985) arrived at the same conclusion when they wrote, "So great are the complexity and variations possible, that it is doubtful whether a general fundamental analysis procedure will ever be published."

Theories that have been advanced to account for the larger dynamic pressures during grain flow usually apply to a specific condition which requires a specific type of flow. Most of the theories were reviewed in three recent publications (Gaylord and Gaylord, 1985; Safarian and Harris, 1985; Singh and Moysey, 1985). Many theories make use of complicated design charts and graphs and appear, at best, unclear.

Although current literature appears contradictory at times, most researchers seem to be in general agreement that there are six major factors to be considered in the analysis of dynamic grain pressure:

1. Variation and change in material properties,
2. Pressure state: active or passive,
3. Flow type: mass, funnel or combination,
4. Pulsations and oscillations,
5. Discharge rate, and
6. Location of the discharge outlet

### 2.3.1 Variation and Change in Material Properties

Janssen's original assumptions of a constant friction coefficient (grain on the bin wall), a constant bulk density and a constant ratio of lateral to vertical pressure enabled a simple analysis of the static equilibrium equations. Unfortunately, the assumptions were incorrect as the properties in question have been shown to vary with pressure, method of filling the storage bin, moisture content, settling time and surface conditioning (Bickert and Bakker-Arkema, 1968; Brubaker and Pos, 1965; Klassen and Britton, 1986; Moysey, 1984; Versavel, 1985). Ross et al. (1979) rederived Janssen's equation allowing for variation in  $k$ ,  $\mu'$  and  $w$  as functions of vertical pressure and moisture content. Although the functions were based on an empirical analysis, they were able to account for variation in material properties in the static case.

When grain discharges from a bin, some or all of the bulk material starts to move. Although the increased wall pressures are referred to as "dynamic" overpressures, it is generally agreed that the velocities and accelerations of the individual particles are small enough to be neglected and the equilibrium equations for the grain/bin system can still be based on statics (American Concrete Institute, 1969; Jenike and Johanson, 1968; Sokol, 1986). Equations for predicting dynamic pressure are similar in principle to the Janssen approach. The major difference is that smaller and differently shaped differential elements are used in the derivation of the dynamic equations and allowance is made for change in material properties associated with flowing grain. There are various reasons why material properties ( $\mu'$ ,  $k$  and  $w$ ) change under dynamic conditions but there is still disagreement as to how they change.

When the discharge gate in a bin opens, vertical pressure over the outlet decreases due to the unrestricted pull of gravity. This results in a loosening of the material, with a corresponding decrease in bulk density near the outlet. Granular material characteristically displays a slip-stick flow pattern which is often the source of bin vibrations. These vibrations cause the bin walls to expand and contract laterally, thus altering the material bulk density (Kmita, 1985).

Under mass flow discharge conditions, when grain slides down along the bin wall, the coefficient of friction changes from the static value to the lower dynamic value (Jenkyn, 1978). Taktamishev (as cited in Turitzin, 1963) suggested that mass flow of grain resembles liquid flow, thus  $\mu'$  should decrease and a corresponding increase in lateral pressure should occur. On the other hand, grain caught inside the pockets formed by a corrugated bin wall remains static even during unloading by mass flow. For this reason, it was suggested that the larger coefficient of grain on grain friction be used rather than the smaller grain on bin wall friction coefficient (Haaker and Scott, 1983; Pieper, 1969).

In evaluating  $k$ , the ratio of lateral to vertical pressure, Jenkyn (1978) suggested that owing to the fluid-like motion of flowing grain, the internal pressure distribution would become more hydrostatic with  $k$  increasing to a value approaching unity. The German Standard DIN 1055 suggests  $k=1$  for emptying conditions (Fankhauser, 1977). Suzuki et al. (1985) suggested that the Janssen equation could be used to predict dynamic pressures provided  $\mu'$  and  $k$  are modified to give isotropic pressures.

### 2.3.2 Pressure State

Although the lateral and vertical pressure distribution within a stored grain mass can vary considerably, the overall state of pressure is generally classified as being active or passive. As implied by the name, active pressure occurs when a grain mass pushes outwardly against the restraining surface, which in this case is a bin wall. Conversely, passive pressure occurs when the bin wall pushes into the grain mass (Colijn and Peschl, 1981). A grain mass is said to be in the active state of pressure both while the bin is being filled and during the static condition. The vertical pressure is greater than the lateral pressure and thus the major pressure lines lie in a vertical plane. During discharge, flowing grain is in the passive state with vertical pressure being reduced in the region of flow. The major pressure lines are then oriented in a horizontal plane (Jenike and Johanson, 1968).

Differences between the active and passive pressure distributions were analyzed in a paper on bin loads by Jenike and Johanson (1968). The analysis suggested that as discharge is initiated, the state of pressure changes from the active to the passive state through a zone of transitional flow. The change starts at the discharge gate and progresses rapidly upward as more grain begins to flow. Jenike and Johanson suggested that the weight of the grain mass in the transition zone is supported by a large horizontal "switch" force located at the point of the bin where the transition zone intersects the wall. Nanninga in 1956 (as cited in Gaylord and Gaylord, 1977), showed that the switch force must occur between the boundaries of active and passive pressure as a requirement of static equilibrium.

The Jenike theory of flow pressure (Jenike and Johanson, 1968), is based on the minimization of recoverable strain energy. This strain energy is dissipated by means of the switch force. The switch can travel rapidly up the side of the bin wall and it may last for only a fraction of a second. It will not travel to the top of the grain mass, however, since the lower strain energy at this level is dissipated quicker in other ways (Jenike et al., 1973b).

In 1970, Lvin introduced a dynamic pressure theory which allowed for differences in  $k$  associated with active and passive pressures. As discussed by Moysey (1977), the theory proposed that  $k$  in passive pressure regions should be greater than  $k$  in active pressure regions to account for higher lateral passive pressures. Modeling the grain mass as a series of dimensionless rings, Lvin developed a set of pressure equations. A series of design charts created from dimensionless forms of these equations enabled the determination of  $k$ -passive. Singh and Moysey (1985) compared Lvin's method to those of Jenike and Janssen and concluded that Lvin's method provided the best fit to experimental data of Kovtun and Platonov (as cited in Turitzin, 1963) and Pieper (1969).

### 2.3.3 Type of Flow

Flow of granular bulk material occurs when the internal frictional strength of the material is exceeded and shear failure occurs (Jenike, 1954 as cited in Cook, 1961). Turitzin (1963) reported of two distinct flow patterns developing when grain was discharged from a bin. The two flow patterns were recognized by most authors, but this was initially unclear since the two flow types were identified by a variety of names.

Mass flow has also been termed dynamic flow (Taktamishev, 1939, as cited in Turitzin, 1963) and plug flow (Deutsch and Clyde, 1967). It is characterized by the entire mass of grain moving downward at a constant rate. Mass flow is desirable from a materials handling point of view since the first grain filled in the bin is also the first grain removed. In terms of grain pressures, however, mass flow is undesirable because large dynamic overpressures occur. Since the entire bulk is in motion, the material becomes fluid-like with a corresponding reduction in  $\mu'$  and an increase in  $k$ . This causes a significant change in lateral pressure as it approaches the hydrostatic condition. Smith and Lohnes (1980) suggested the lateral pressure increase was caused by grain dilation.

Funnel flow has been called non-dynamic flow (Taktamishev, 1939, as cited in Turitzin, 1963), pipe flow (Deutsch and Clyde, 1967), plug flow (Cook, 1961; Jenike, 1964), enveloping flow (Ross et al., 1980) and core flow (Paterson, 1980). With funnel flow, a narrow column of grain above the discharge outlet moves downward while the surrounding grain remains static. Flow progresses in a last in-first out pattern as the top layer of grain slides laterally into the column. Funnel flow is advantageous from a grain pressure point of view, as most of the grain remains static and only small overpressures occur. To induce funnel flow and thereby reduce overpressures in mass flow bins, a simple device called the anti-dynamic tube was developed by Reimbert and Reimbert (1963).

Although funnel flow pressures are lower than mass flow, they are more erratic and appear to show no repeatable pattern (Paterson, 1980; Ooms and Roberts, 1985). Mass flow pressures are usually well defined because the flow channel is constant (Gaylord and Gaylord, 1977).

Pure mass or funnel flow seldom occurs in grain bins and the actual flow pattern is usually a combination of the two. Funnel flow occurs in the bottom section of the bin and mass flow occurs in higher sections as the flowing column expands to include the entire cross-sectional area of the bin. The region between the fully developed primary flow zones is said to be a transition zone (Ross et al., 1980).

Jenike and Johanson are internationally recognized authorities on bin flow properties. One of their many contributions to the materials handling industry was the development of a design method which assured mass flow in bins. This was achieved by specifying a sufficiently steep hopper slope based on results from a device termed a flow factor tester. Using an empirical approach, design charts were developed to account for high lateral pressures associated with mass flow as well as the switch force discussed previously (Jenike, 1954; Jenike and Johanson, 1968 and 1969; Jenike et al., 1973a,b,c). McLean and Arnold (1976) developed a single bound approximation of the Jenike theory to provide a convenient equation for calculating peak cylinder flow pressures for mass flow.

An alarming deficiency in the Jenike approach is that it totally disregards the effects of wall friction under the assumption that the material stiffens the wall enough to handle the vertical friction load, claiming that "buckling of light shells under uniformly distributed loads is practically unknown." (Jenike, 1967). More surprising is that two advocates of the Jenike approach suggest that the main deficiency in silo design has been the "complete disregard of the effects of wall friction," (McLean and Arnold, 1984).

Sugden (1981) and Safarian and Harris (1985) extensively reviewed research studying flow patterns. Based on their findings, Safarian and Harris (1985) concluded that "it seems obvious that there is no unique flow pattern even for a particular material in a particular silo with a particular size of hopper and discharge opening." In light of this fact, it appears that bin designers should heed the advice of Colijn and Peschl (1981) and consider the various flow effects when designing bins.

#### 2.3.4 Pulsations and Oscillations

It was first noted by Kovtun and Platonov (1959 cited by Turitzin, 1963) that dynamic grain pressures exhibit a pulsating effect. This was later confirmed by other researchers (Collins, 1963; Pieper, 1969; Sugita, 1972; Jenike et al., 1973a; Kmita, 1985). The pulsations are caused by the formation and collapse of arches within the flowing grain mass (Theimer, 1969). As an arch is formed, due to either friction or cohesion of the particles, material underneath the arch continues to flow. This causes a void under the arch. When the arch collapses, the grain above it drops suddenly causing an impact loading on the wall.

Dubynin (1968) provided an excellent theoretical analysis of the pulsation effect and concluded that the amplitude and frequency of the pulsations depend on the orifice size and volumetric weight of the bulk solid. Richards (1977) measured oscillation frequencies up to 85 Hz with larger pulses occurring every four to six seconds.

High-speed instrumentation is required to measure the pressure pulsations and since many authors did not use such equipment, they did not observe the faster pulses. Moysey and Landine (1982) reporting on

previous work suggested the pulsations do not exist and that high-speed data acquisition was not required. It should be noted, however, that the pressure transducers used in their study were large and actually measured the average pressure over a given area of the wall.

Wlodarski and Pfeffer (1969) used a different approach and measured air pressure above the discharge orifice. They found that air pressure oscillations had a significant effect on the flow rate.

#### 2.3.5 Discharge Rate

Dynamic overpressures are assumed to be a quasi-static phenomenon that can be analyzed at a point in time using equations of statics since the momentum of flowing grain is considered to be negligible (Jenike and Johanson, 1968). It seems reasonable, however, as many authors suggest, that a grain bin discharged rapidly would experience greater loads than a similar bin discharged slowly. This opinion was supported by Griffith (1983) who reported of grain storage bins that gave 15 years of problem free service, but failed when the discharge rate was increased by 20%. Smith and Simmonds (1983) suggested the ability of dynamic overpressures to "lock-in" when discharge was stopped appeared to indicate that flow rate had no effect. Alternatively, if true "dynamic" effects such as acceleration and momentum of flowing grain are neglected, any dynamic overpressure should be able to lock-in since it is a quasi-static phenomenon.

There has been very little research devoted to the question of the effect of discharge rate. When results were reported, they often conflicted with those of other authors. The trend towards faster more

efficient bulk material handling will result in more, higher flow rate systems being constructed, so an answer to the question of the effects of such a move would be advantageous.

Reimbert (1955) was one of the first authors since Jamieson (1904) to note that different emptying and filling speeds could influence the magnitude of overpressure measurements. Prior to Reimbert's work, and even today, research papers simply stated that the bin was discharged, with no mention of the flow rate used.

Collins (1963) noted reports of dynamic pressure changes that were proportional to discharge rate. However, his own tests on paper models using sand as a fill material suggested there was no flow rate effect. The tests used 16 to 25 mm discharge orifice diameters which resulted in flow rates of less than  $0.01 \text{ m}^3/\text{min}$  in a 300 mm diameter bin.

Subsequent work by Pieper and Wenzel (1963, as cited in Safarian and Harris, 1985), Pieper (1969), Deutsch and Schmidt (1969), Richards (1977) and Manbeck et al. (1977) also concluded that flow rate had no effect on the magnitude of dynamic lateral grain pressures. Pieper's (1969) results indicated up to 14% variation over the ten fold range of discharge rates tested. Flow rates of  $0.09$  to  $0.27 \text{ m}^3/\text{min}$ , generated by outlets with diameters of 50 to 75 mm, were used by Deutsch and Schmidt (1969) in their 750 mm diameter model bin. Manbeck et al. (1977) used three model bin sizes with centric discharge outlets ranging in size from 38 to 102 mm. The larger 600 and 1200 mm diameter bins were filled with sand and the smaller 300 mm model was filled with iron ore filings. Richards (1977) varied discharge rate by a factor of six in 600 mm sand filled models, although actual discharge rates were not given.

Recent work at the University of Georgia (Thompson et al., 1982 and 1985; Thompson and Prather, 1984) indicated a statistically significant flow rate effect in most tests using wheat, corn and soybeans. The actual effect was marginal, however, showing only a 5 to 15% variation in one series of tests. Outlet diameters of 37 and 57 mm generated flow rates from 0.015 to 0.067 m<sup>3</sup>/min in a 910 mm diameter corrugated steel model bin. A 610 mm diameter smooth walled bin had 25 to 76 mm orifice diameters which resulted in flow rates of 0.007 to 0.09 m<sup>3</sup>/min.

Studies using the lamellar bin concept, first mentioned by Reimbert and Reimbert (1976), have been undertaken at the University of Manitoba. As pointed out in the first paper on the subject (Britton and Hawthorne, 1984), the Reimberts rejected using lamellar bins as storage structures since grain flowed out the sides of the slatted walls upon discharge. Britton and Hawthorne suggested that this very same phenomenon could be used as a research tool to study the effect of flow rate and location of discharge in dynamic grain studies. They suggested that the lateral flow rate of grain at a given point on the lamellar bin wall could be related qualitatively to the dynamic pressure increase at the same point on the wall of a solid walled bin during grain discharge. Four studies (Britton and Hawthorne, 1984; Rowley and Britton, 1985; Britton and Rowley, 1986; Towells and Britton, 1986) all indicated that there was an increase in the lateral flow rate of grain when a higher discharge rate (larger orifice) was used.

It is interesting to note that all the studies using agricultural grains showed some type of flow rate effect while those using isotropic materials such as sand and iron filings did not. One could speculate

the anisotropic nature of agricultural grains was a factor. Nielsen (1983, as cited in McLean and Bravin, 1985) found that the anisotropic behavior of grains did have a significant bearing on the loads they exerted on bin walls. Perhaps the reorientation of the grain kernels during discharge is much more pronounced at higher flows and this may cause a change in dynamic overpressures. More research to clarify this phenomenon is needed.

Flow rate may have an indirect effect on bin pressures by varying the flow pattern. A higher flow rate could increase or decrease the mass flow area or alter the location of the transition from mass to funnel flow. Sugden (1981) did an in-depth review of flow pattern studies and concluded that flow rate during discharge did not affect or relate to type of flow. This opinion was contradicted two years later when it was discovered there was a certain dependence of the observed flow pattern on the velocity, hence flow rate, of grain within the bin (Tuzun and Nedderman, 1983). No clear conclusions from these findings could be made.

#### 2.3.6 Location of the Discharge Outlet

In reviewing the literature, the location of the discharge outlet was seen to be one of the most important factors to affect the loading on grain bins. Discharging the bin from an outlet in the centre of the floor kept overpressures at a minimum, whereas using eccentric outlets generated pressures that were non-uniformly distributed resulting in the potential for severe buckling. Photographs of various bin failures (Theimer, 1969; Ravenet, 1983 and 1984) illustrated the common mode of

buckling failure in steel bins and vertical cracking in concrete silos when eccentric discharge problems arose.

Ketchum (1919) recognized the effect of using eccentric discharge outlets when he attributed Prante's high dynamic pressure measurements to the use of an outlet near or in fact in the side wall of the bin. Ketchum's opinion was probably influenced by Lufft's (1904) results which indicated an increase in lateral pressure on the wall opposite the discharge outlet with a corresponding lateral pressure decrease on the wall nearest the outlet.

Caughey et al. (1951) recorded a slight lateral pressure increase on the wall opposite the discharge outlet of their 457 mm diameter model bin. Because of this small diameter, however, the bin may not have accurately modeled the flow pattern of a full-sized bin. In model bin tests, Barre (1958) noted that the top of the flow funnel formed on the side opposite the discharge outlet and then gradually moved toward the outlet as grain height decreased. A distinct lateral flow of grain occurred in the slanted funnel. In full-sized bins, however, he noted that the funnel formed directly over the discharge outlet with grain flow in the vertical direction. These flow pattern differences would significantly affect the location of greatest pressure.

In his doctoral thesis research, Ravenet (1983) recorded dynamic overpressures of 95% of static lateral pressures on the wall opposite the discharge outlet. He also measured pressure reductions on the wall nearest the orifice. Sugita (1972) predicted the maximum lateral pressure would occur on the wall opposite the discharge outlet. He suggested this maximum pressure would occur at a location higher on the

wall than the location of maximum pressure for central discharge. This was due to a tilted collapse plane separating the mass and funnel flow regions. Sugita's theory of collapse planes was somewhat analogous to the Jenike concept of "switch" force.

Garg and Gopalakrishnan (1974) performed tests on a model bin and recorded lateral pressure increases on both opposite and near walls when using eccentric discharges although there was no consistency in the pressure measurements on the far wall. Pieper (1969) on the other hand, found the greatest overpressures on the near wall with smaller increases on the opposite wall for both full and semi-eccentric discharges.

The lamellar bin studies noted earlier also noted a relationship between lateral flow rates through the bin walls and the position of the discharge outlet. The greatest lateral flow rates were measured at the position of the wall nearest the orifice with flows decreasing as distance from the outlet increased (Britton and Hawthorne, 1984; Rowley and Britton, 1985; Britton and Rowley, 1986; Towells and Britton, 1986) If lateral flow rates relate to lateral pressures, then the greatest lateral pressures would occur nearest the discharge orifice.

Notwithstanding the increased lateral pressures associated with the use of eccentric discharge outlets, recent studies have shifted to an analysis of buckling and bending caused by the imbalance in load distribution. Moysey and Landine (1980) suggested that the unbalanced loading associated with the use of off-centre discharge may, in fact, be more critical than the actual pressure magnitude. Recent buckling failures of bins tend to support this opinion.

Jenkyn (1978) took a very basic approach in attributing the bending to the uneven height of grain around the bin wall. If this were in fact the case, compression buckles would appear on the wall opposite the discharge outlet. Tests with foil models showed that the buckles appeared predominantly on the wall near the orifice (Harms and Henry, 1976; Ross et al., 1980; Rennie, 1983). These reports suggested that the analysis of buckling loads on bins is more complex than Jenkyn suggested.

Most studies of lateral bin pressures during eccentric discharge focussed on the two extreme wall positions: the point nearest the discharge outlet and the point 180 degrees on the circumference (i.e. the point opposite the outlet). A recent study by Pieper and Stamou (1981) illustrated graphically that the lateral pressure distribution around the entire circumference of their bin during eccentric and semi-eccentric discharge was very erratic. The pressure distribution also varied with grain depth. Figures illustrating various pressure distributions showed no recurring pattern. Munch-Anderson and Nielsen (1986) suggested that the pressure distribution during discharge would often be unsymmetrical with respect to the geometry of the inlet and outlet, even for centric discharge.

A non-symmetrical pressure distribution causes unbalanced loading which is taken up through bending stresses. The buckling strength for a perfectly circular thin-walled bin can be calculated using Timoshenko's theory for cylindrical shells (Timoshenko and Gere, 1961). Owing to the relative thinness of steel bins, a certain degree of "out-of roundness" could be expected. An unbalanced lateral pressure distribution would

further add to circular imperfection. Bucklin et al. (1983) concluded from an analysis of shell theory that deviations from a perfect circular cross-section can reduce buckling strength to only 30% of that predicted using Timoshenko's equation for cylindrical shells. Haydl (1983) deemed the horizontal bending forces caused by unsymmetrical loading to be an important factor to be considered in the design of bins employing some form of eccentric discharge.

Bervig et al. (1977) developed a finite element program that could calculate actual bin wall loads using an unsymmetrical pressure distribution. They assumed a pressure equivalent to the static load on the far wall but used an overpressure factor of 2 on the near wall. As would be expected, the outlet wall showed an increase in the vertical compression force while there was a reduction on the far wall. This difference came as a result of the overturning moment generated by the lateral pressures. When asymmetric filling was added to the model, the bottom of the far wall was actually in vertical tension. They further suggested that the collapse of eccentric voids in the flowing grain mass could cause tension at higher elevations on the far wall.

Thompson et al. (1985) were among the few authors to report on vertical wall loads during eccentric discharge tests. Their results showed an increase in the vertical compression force on the near wall with a corresponding decrease on the far wall. Because of the nature of the test apparatus, which hung the bin, there was no way to record a tension on the far wall if it existed.

A report by McLean and Bravin (1985) was found to be one of the best overall studies into the effects of eccentric wall loads. They

suggested that eccentric discharge would not cause a problem when the flow zone did not intersect the bin wall. The effect would be more critical in shallow bins provided that in taller bins, the flow zone would intersect the wall opposite the outlet (i.e. the grain would be in a state of mass flow in the upper regions). The report noted that outlet dimension is critical to the flow zone in that a larger outlet diameter would cause the flow zone to intersect the far wall sooner.

Contrary to the quasi-static theory of centre discharge pressures, both Bravin (1983, as cited in McLean and Bravin, 1985) and Reimbert and Reimbert (1976) suggested that part of the eccentric effect is caused by the non-symmetric thrust of the flowing grain mass. Bravin noted the significance of discharge rate when using eccentric discharges due to the change in momentum (direction of flow) that occurs in the funnel of flowing grain as it reaches the narrower portions of the funnel. In order for grain flow to change direction, the bin wall must exert an additional horizontal thrust which would manifest itself as an increase in wall stress.

Using fully eccentric discharge outlets, Harms and Henry (1976) photographed the bin wall "sucking itself in" or buckling inward. The tests by Ross et al. (1980) using paper models noted the formation of buckles along the entire flow channel with a major buckle forming at the bottom. McLean and Arnold (1984) reported that inward buckling of silos was common in Australia.

There are documented cases of a 3 mm thick steel wall bin denting inwards (Jenike, 1967) and of concrete silos developing vertical cracks on the inside walls (Johnston, 1983). These failures were attributed

to the circumferential bending moments developed as a result of the unbalanced loading associated with eccentric discharge. Jenike (1967) developed a theory which explained the cause of the inward denting. It also predicted if and where a dent might occur. The theory was based on the assumption that lateral pressure inside a funnel of flowing grain would be smaller than the lateral pressure of the surrounding static material. The rationale for this assumption was based on Janssen's equation which suggested lateral pressures in a bin were proportional to the hydraulic radius. The flow channel was regarded as a small silo within a larger one and since it had a smaller hydraulic radius than the actual bin, the lateral pressures would also be smaller. Colijn and Peschl (1981) considered this assumption to be reasonable.

Jenike further suggested that the flow channel has a tendency to lean toward the bin wall since the smooth wall surface has a lower friction coefficient than the stationary grain mass (Jenike, 1967). Since the lateral pressure in the flow zone would be lower, symmetry of loading on the wall would be lost and the net effect would be a bending moment which has the same effect as a horizontal point force pushing inward at the position where the flow zone intersected the wall. The bin would dent inwards if its radius was greater than the critical radius, defined by an equation which was a function of the internal angle of friction, bulk density, lateral pressure and the ratio of the bin wall thickness to its diameter.

Various design procedures have been advanced to account for the increased loading of eccentric discharge. A common method uses the

imaginary bin concept (Theimer, 1969, Safarian and Harris, 1985), which calculates loads based on a larger bin radius equal to the distance from the centre of the discharge outlet to the far wall. Implicit in the approach is the assumption that pressure increases are proportional to the degree of eccentricity, with a fully eccentric discharge having the most severe effect.

This assumption was put in doubt by the results of two recent research papers. Using strain gages to give an indirect measure of lateral pressure, Pieper (1969) observed that semi-eccentric discharge tests gave higher strain readings than fully eccentric tests. Thompson et al. (1985) noted a similar effect in measuring the vertical wall loads on their corrugated model bin. With H/D ratios of 1.83 and 2.73, an eccentricity of 66% caused vertical load on the wall nearest the discharge outlet to be greater than with eccentricities of 33% or 88%. No explanation for this phenomenon was given. One might speculate, however, that the tendency for the flow channel to lean towards the wall in semi-eccentric discharge could result in a larger load imbalance or thrust than would occur with a fully eccentric discharge where the grain would flow straight down the bin wall. The critical eccentricity could also be a function of the H/D ratio.

It should be noted that both Pieper (1969) and Thompson et al. (1985) suspended their model bins from the top instead of mounting them firmly at the base as would be the case in a full size bin. There was speculation that this configuration may have influenced the results due to a lateral movement of the bottom of the bin wall nearest the discharge outlet.

## 2.4 MODEL TESTING

The variety of methods used by researchers to determine the loading of stored bulk grain are generally classified into two major categories: model tests and full-size tests. Although full-sized bin tests are preferable, economic considerations usually dictate the use of model bins. There is some question, however, as to whether model bin tests sufficiently duplicate the conditions found in full-sized bins. Until extensive full scale testing is undertaken, the answer to the question will never be known. Most authors, however, generally agree that model testing is appropriate within certain limits.

Lufft (1904) was one of the first to prove the validity of model testing. His conclusion was based on the fact that results from his full-sized bins agreed closely with Janssen's model experiments. For static pressure studies, this opinion is still held although Versavel (1985) suggested his tests may not have been valid for bin diameters less than 307 mm due to the relative grain size becoming too large.

Researchers have attempted to overcome the relative size problem by using smaller particles. Sugita (1972) used glass beads ranging in size from 177 to 250 microns in 1/45th scale model tests. The use of smaller particles, however, is not the perfect solution because material properties such as the friction coefficient, ratio of lateral to vertical pressure and bulk density may change, not to mention the stress-strain characteristics. Even if the same material is downsized, cohesion may begin to play a role. Nielsen and Kristiansen (1980) concluded that owing to this variation in material properties one model filling medium cannot be substituted for another.

When models are used for dynamic pressure and flow studies, the validity question becomes more complicated. Paterson (1980) suggested that as long as the flow properties and patterns were the same, model results should be able to be scaled up when free flowing, non-cohesive granular materials are used. Although they agreed that flow patterns are independent of bin size, Munch-Anderson and Nielsen (1986) offered that discharge pressures are bin size dependent, due to differences in the relative size of particles and the boundary layer of grain at the grain/wall interface occurring with mass flow. Paterson (1980) noted that discharge orifices should be at least 7 times the maximum particle size in order that flow patterns through the outlets not be altered.

An additional problem of model testing is that pressures and loads are generally very small with resulting errors in measurement being much higher than they would be in full scale testing. Strain gages were used on thin-walled model bins to record wall stresses, but sensitivity was quite low for the wall thicknesses used (Collins, 1963; Manbeck et al., 1977). Thinner materials allow larger strains but the low buckling resistance renders them unusable. Foil and paper models were used by Harms and Henry (1976) and Ross et al. (1980), but they generally only noted qualitative effects since the bins usually failed during testing.

Smith and Lohnes (1983) recommended the use of strain gages, since pressure transducers have to be too stiff to be effective. If they are not stiff, they record too low a pressure. The size of the pressure transducer can also become a factor as averaging begins to occur with larger pressure plates, but stress concentrations occur with too small a device.

Another alternative used in model testing made use of vertical frictional load measurement as opposed to lateral pressure measurement. Lenczer (1963) and Thompson et al. (1982, 1983 and 1985) supported their bin walls separately from the floor and could then determine what portion of the total grain load was carried by the wall and the distribution of that load around the wall.

## 2.5 INSTRUMENTATION

The instrumentation used by various authors in determining grain pressures varied as much as the authors themselves. As technology improved throughout the years, so did the quality of instrumentation. This increased the accuracy and precision of the measured results

In static tests, individual, periodic measurements were taken with no attention paid to the time interval between readings. When dynamic tests became popular, the time factor also became important. Analog chart recorders were used in some tests (Pieper, 1969; Sugita, 1972) while multi-channel data acquisition systems were employed in others (Garg and Gopalakrishnan, 1974; Moysey and Landine, 1980 and 1982). Chart recorders gave fairly precise results since pressure pulsations were often observed. Some researchers made use of computerized multi-channel data acquisition systems, although periods between successive readings were often greater than one or more seconds.

Moysey and Landine (1980, 1982) took two load readings per second in their model bin tests, but owing to the large size of the pressure plates, they could only measure average pressures. They suggested, nonetheless, that high-speed data acquisition was not required since

dynamic overpressure peaks lasted for a few seconds. This contradicted Collins' (1963) recommendation that multiple channel high-speed data acquisition be used to record the near instantaneous dynamic pressure changes. Reimbert and Reimbert (1976) supported Collins' position when they stated, "in a full-silo, an extremely small opening of the emptying gate involving flow of an insignificant amount of grain is sufficient to produce immediately in almost the entire ensiled mass, a descending movement which upsets the equilibrium of the latter and results in a considerable increase on the thrusts on the walls." Richards (1977) stated further, "It is clear that a fast measurement and recording system is needed to investigate wall pressures."

## 2.6 Summary

From the literature cited in this review, it is clear that the subject of grain bin loads and pressures is a complex matter. Although much research has been devoted to the subject, a precise fundamental bin design procedure which accounts for all loading situations has not yet been developed and unfortunately, such a procedure does not appear imminent. Bin design is still, as stated by Isaacson and Boyd (1965), a "hazardous task for the design engineer."

Many factors need to be considered when analyzing static loads, but as many of these factors are still little understood, their exact effect on static load has not been precisely defined. To simplify the problem, most design codes specify the use of a constant bulk density, a constant coefficient of friction and a constant ratio of lateral to vertical pressure with the equations of Janssen or Reimbert. It is

generally recognized, nonetheless, that these "constants" are, in fact, variables.

The additional analysis of dynamic loads further complicates the problem. The location of the discharge outlet appears to be one of the most critical variables affecting dynamic loads. Unfortunately, there are many differing opinions as to where the maximum effect of eccentric discharge manifests itself. Some authors suggest load peaks occur on the wall opposite the discharge outlet while others note load increases on the near wall. Although less critical than the effect of discharge location, the effect of discharge rate has also not been adequately determined. Many authors suggest the effect is negligible, yet there have been reports of bin failures when discharge rate was increased. Continued research into the effects of discharge rate and location, as well as other variables affecting grain loads is still much required.

CHAPTER III  
EXPERIMENTAL EQUIPMENT

3.1 TEST SYSTEM

The test system was originally designed and fabricated as part of the author's undergraduate thesis project (Pokrant, 1983). Details of the system were presented in a paper by Pokrant and Britton (1982) and a complete analysis, including the design criteria, were reported in the Bachelor's thesis. Modifications and additions required to make the system workable and suitable for this study were reported by Pokrant and Britton (1986). Figures 3.1 and 3.2 illustrate the basic setup as it was used in this study.

3.1.1 Main Frame and Base Table

A triangular steel frame supported 3300 mm above the floor by three steel pipes formed the outer support structure. A taller frame height was desired, but restrictions were imposed by the laboratory ceiling. The triangular pattern was chosen as it was the most basic stable shape that could provide support and it also simplified levelling of the system components.

Three steel rods suspended from the corners of the frame supported a base table which acted as a floor for a model bin. Each rod was cut near the top and a load transducer was placed in the break to measure

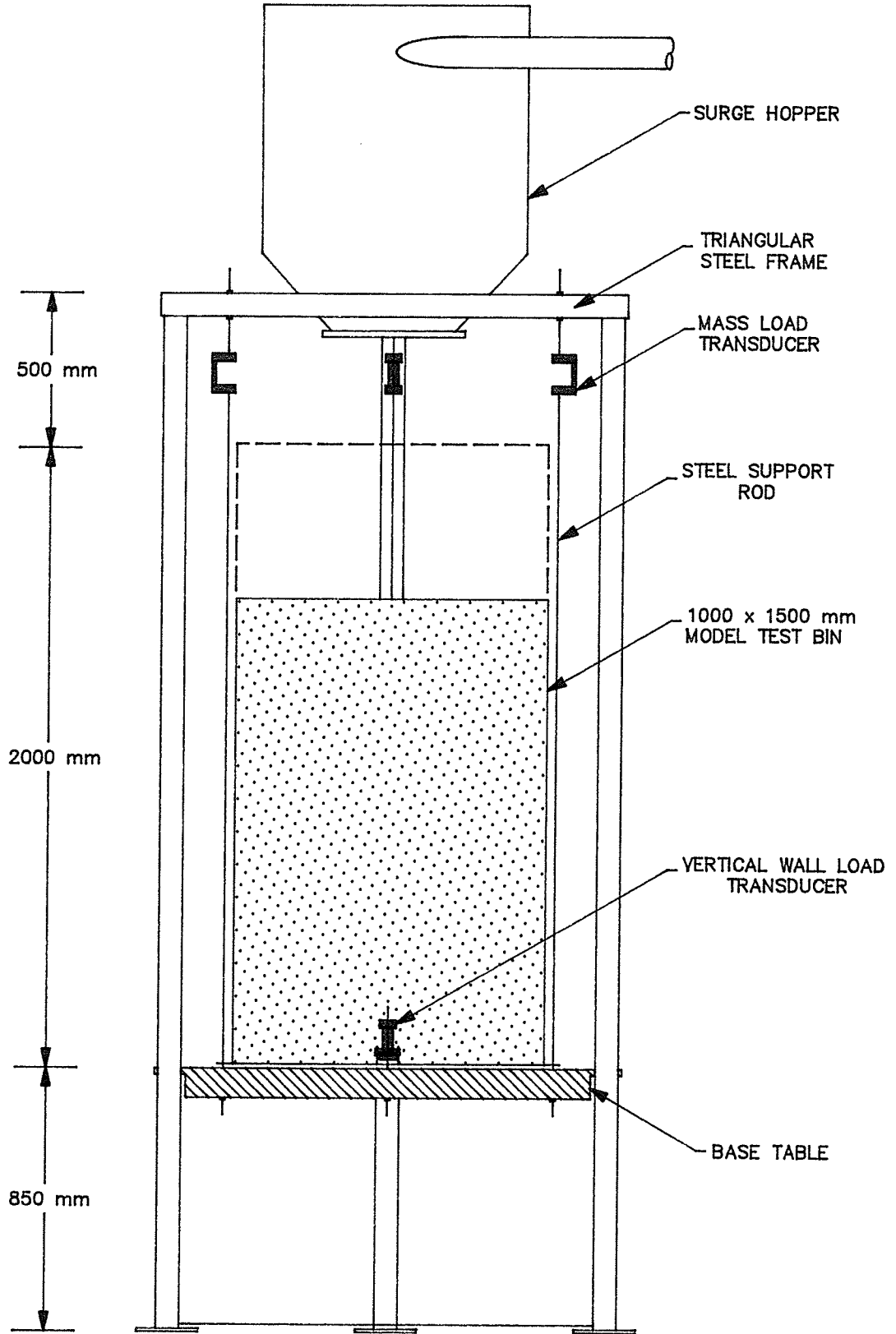


Figure 3.1 - Test system - front elevation

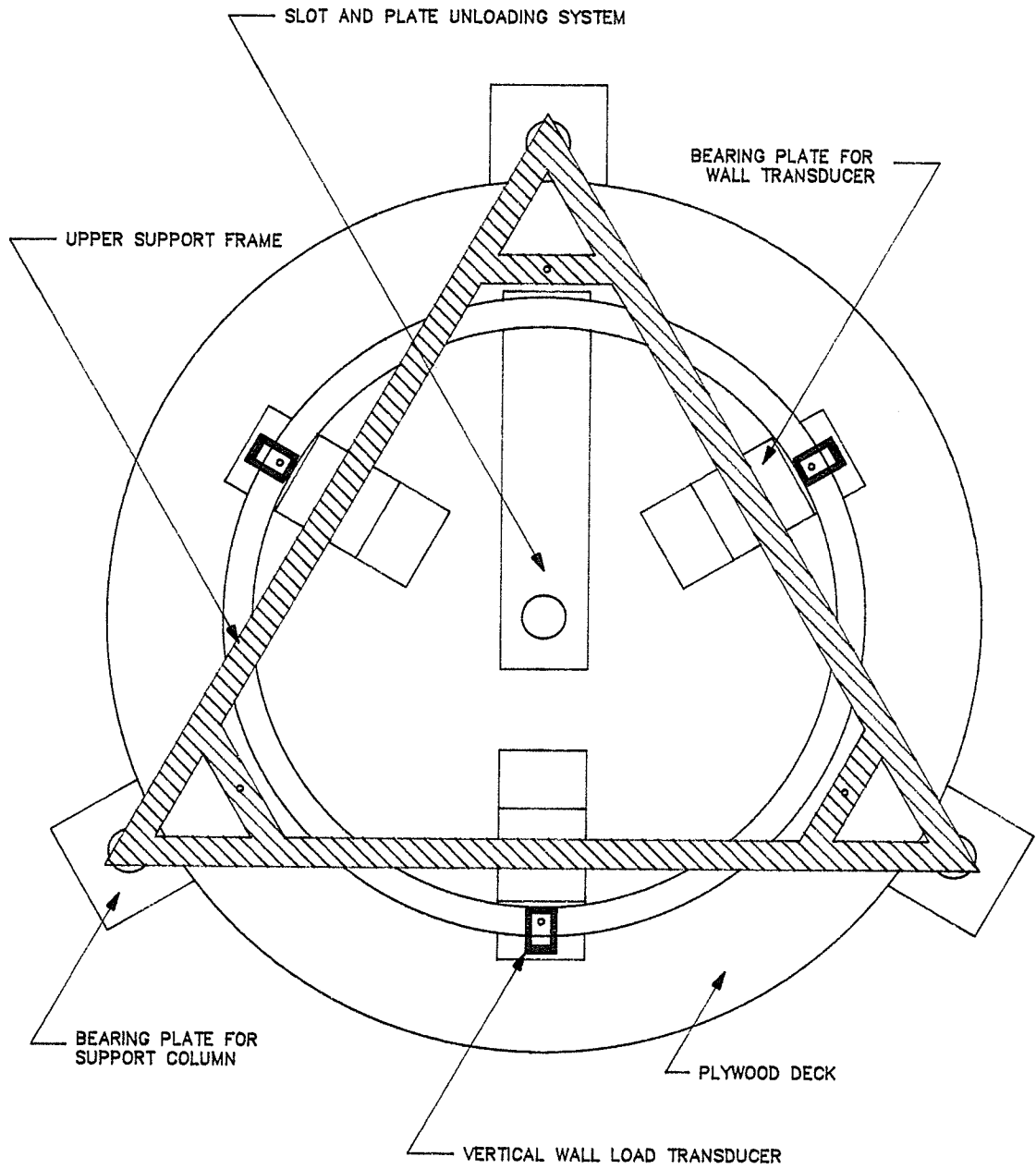


Figure 3.2 - Test system 3-point support - plan view

the entire mass of the bin/deck system. The base table consisted of a 1500 mm circular plywood deck mounted on top of a second triangular steel frame. This frame strengthened the deck and was designed to limit vertical deflection to 1 mm. The table could accommodate bins up to 1000 mm in diameter.

### 3.1.2 Model Bin

A 1500 mm tall bin with a nominal diameter of 1000 mm was made from 0.97 mm thick galvanized steel sheet. An angle iron ring was spot-welded to the outside bottom of the bin to facilitate mounting, but as the ring was rolled from straight stock, it did not form a perfect circle. This caused the inside diameter of the bin to vary from 996 to 1002 mm. The error was felt to be within acceptable limits. Of more concern was the fact that the bin wall was formed from three flat sheets joined together using vertical lap seams. Ease of bin fabrication dictated this design. The stresses in the wall caused by these seams resulted in the unloaded bin cross-section taking on a slightly non-circular shape.

The bin was supported approximately 5 mm above the deck by three load transducers placed 120 degrees apart (see Figure 3.2). These transducers sensed the vertical load, caused by grain friction, carried by the walls. The bin was mounted from the bottom so that the vertical force on the wall would manifest itself as a compressive loading. Some researchers suspended their model bins from the top and thus introduced tensile loading which did not accurately model the situation found in full-size structures. This was an important point since having the

wall in a state of vertical tension instead of compression could alter the stability of the bin wall, as well as possibly alter the state of stress in the grain mass.

To prevent grain leakage underneath the circular ring, a plastic skirt was taped to the bottom of the wall. The skirt made contact with the floor and was kept from bending by a thin steel band placed loosely between the skirt and the wall. Since the skirt was thin and flexible, it had no vertical strength and did not transfer any vertical load from the walls to the floor.

### 3.1.3 Discharge Outlets

The base table provided a variable discharge through the use of a slot and plate unloading system. A slot was machined into the deck and one of 16 equally sized plates was placed into the opening. Each plate had a circular hole cut somewhere along its longitudinal centre line to serve as the discharge outlet. The orifice had one of four diameters and was positioned at one of four locations on the plate, as shown in Figure 3.3. Flow rate and eccentricity were adjusted by simply changing the plate.

A pneumatic slide gate was installed below the plate and it could be positioned directly underneath the outlet, as shown in Figure 3.4. A solenoid valve used to control the slide gate could stop and start the discharge almost instantaneously. The pneumatic cylinder incorporated an air cushion to prevent it from impacting and causing vibrations. The opening inertia did cause the suspended base table/model bin system to sway slightly, however.



Figure 3.3 - Typical discharge plates

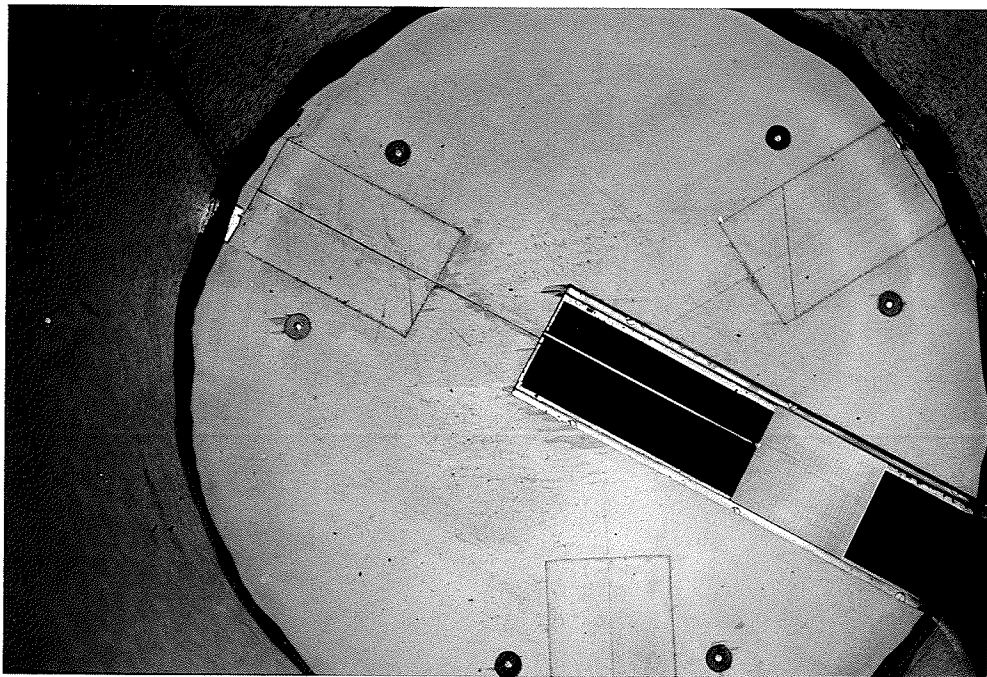


Figure 3.4 - Adjustable pneumatically controlled slide gate

Since one of the objectives of this thesis was to investigate the effect of flow rate, it was desired to use relatively high flow rates since previous work used lower rates. Paterson (1980) recommended a minimum discharge outlet diameter of no less than 7 times the maximum particle size. Assuming a maximum particle size of 6 mm using wheat as a fill material, the orifice diameter lower bound was 42 mm.

With these guidelines in mind, orifice diameters of 45, 60, 75 and 100 mm were chosen. This resulted in an approximate 9.5 fold variation in the discharge rate, which ranged from 0.48 to 4.58 kg/s (0.04 to 0.33 m<sup>3</sup>/min based on a measured bulk density of 825 kg/m<sup>3</sup>). Given the size of the test bin, discharge from the 100 mm orifice was felt to be relatively larger than any presently used in the grain industry.

To account for eccentric drawoff effects, four discharge locations were used. Offsets of 0, 150 and 300 mm from the centre of the bin to the centre of the outlet were used for the first three locations. The last position was defined by the outer edge of the outlet being located at the bin wall edge.

### 3.2 LOAD MEASUREMENT

To study the dynamic load effects of flow rate and eccentricity, it was necessary to obtain some indication of the lateral and vertical forces on the bin wall. The test system was designed to measure both total vertical grain load (mass) and total vertical wall load caused by friction. Total floor load was equal to the difference of the two values. By using a three-point support, an indication of the vertical load distribution around the bin circumference was also obtained.

In investigating lateral grain forces, most studies generally used some form of pressure transducer. Since small horizontal deflections of the measuring device could significantly alter the state of stress in the grain mass, accuracy of the results was often questioned unless very stiff transducers were used. This posed a sensitivity problem since bin pressures were small. Some authors used strain gages to measure stress on the bin wall, thus obtaining an indirect measure of grain pressures. This method was deemed to be satisfactory, provided the bin wall developed a sufficient degree of strain. For this reason, thin bin walls were recommended (Collins, 1963).

The strain gage approach was considered for this study. Rosettes were mounted at selected locations on the outside bin wall to determine the total state of wall stress at the chosen points. It was believed that mounting gages on the inside wall would significantly alter the grain/wall interface and thus distort the true state of grain pressure at the wall. For this reason gages on the inside surface were not used. Given the practical constraint of gage sensitivity and the apparent need for gages on the inside wall to account for bending, wall strain measurements had to be abandoned. A discussion of the selection of mounting locations and calibration of the gages is found in Appendix A.

### 3.2.1 Vertical Load Transducers

Six transducers in all were used. Three supported the base table and model bin and measured the total mass (weight) of grain in the bin. The other three suspended the model bin slightly above the deck and measured the total vertical frictional wall load.

The transducer design, construction and mounting was discussed by Pokrant (1983) in his Bachelor's thesis and only a brief description is given here. Six C-shaped transducers were designed for a maximum load of 5 kN. A strain gage was mounted to each side of the vertical member thereby maximizing sensitivity through bending. Initial calibration in 1983 indicated a sensitivity of approximately 1.9 N/microstrain with linear behaviour to the maximum design load. Mounting configurations for the transducers are illustrated in Figures 3.1, 3.2 and 3.5.

### 3.2.2 Transducer Calibration

Each transducer was connected to a variable gain instrumentation amplifier that incorporated Wheatstone bridge circuitry. A half bridge arrangement was used. The amplified signals were measured by a data acquisition system that had multi-channel capability, thus enabling a simultaneous calibration of all six transducers. Slight physical and electrical differences in the transducers and amplifiers required that each transducer had to be connected to the same amplifier, in order that proper calibration was maintained.

The transducers hung in a ladder type arrangement with a weight pan underneath, as shown in Figure 3.6. Mounting brackets allowed each transducer to rotate to a plumb position thus assuring that the applied load was vertical. In addition to the weights added to the weight pan, each transducer was also subjected to the weight of the transducers below it in the ladder arrangement, as well as the weight of the pan itself. This effect was compensated for in amplifier balancing as all outputs were zeroed for the "no load" (empty weight pan) condition.

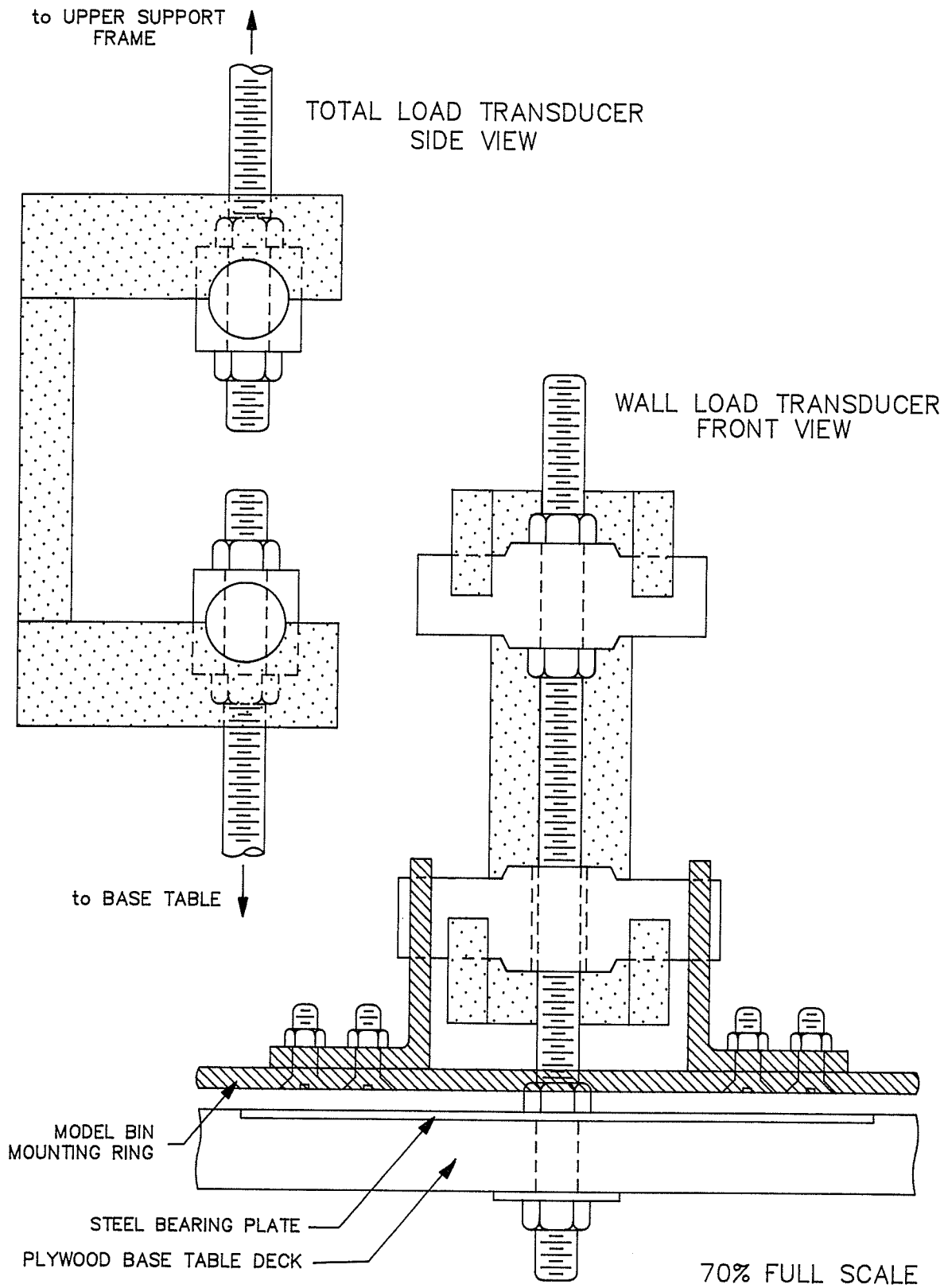


Figure 3.5 - Transducer mounting configurations



Figure 3.6 - Calibration setup arrangement

Before the calibration procedure could be initiated, the amplifier gains had to be set. The data acquisition unit read analog voltages in the range  $\pm 10$  volts and represented them with integer values from -2048 to +2047. If the amplifier gain was adjusted to a higher value, the sensitivity of the readings could be increased, but the output signal would reach the 10 volt saturation level at a lower transducer load. The approximate gain required to maximize the sensitivity of the transducer signals was between 600 and 900.

It was recognized that the wall transducers would be subjected to lower loads than the total load transducers, but as the exact dynamic effect on individual transducers was unknown, it was decided to assume the same maximum load for all six transducers. Further, since only a 1500 mm bin height was used, while the transducer design was based on a 2000 mm height, a lower maximum load could have been assumed. However, as this was the initial test series, the 5 kN design load was used.

To set the gain, the amplifier balance was adjusted to zero volts (represented by the integer value 0). The transducers were then loaded to 5 kN and the gain of each amplifier was adjusted so that the output signal was as near +10 volts (integer value +2047) as possible. There was an initial drift in the settings due to the extreme sensitivity of the amplifiers and so the gain adjustment procedure had to be repeated a number of times until the 0 reading at no load and the +2047 reading at full load were consistent.

Twenty-five, 20 kg suitcase weights were individually added to the pan to increment the load to the 4.9 kN (500 kg) maximum. As discussed later, in the Instrumentation section of this chapter, a micro-computer

was used to control the data acquisition unit. A BASIC computer program (CALBRAT6) was written to store the current load and the averages of 100 readings taken from each transducer as weight was added or removed. Four load-unload replications were performed and the data were pooled to give 102 points which a linear regression program, REGRESS6 used to generate calibration equations for each transducer. The calibration coefficients are given in Appendix B.

All six transducers had linearities less than 0.34% of full scale with R-squared values greater than 0.9999. The intercepts were unexpectedly non-zero, but this was attributed to the inaccuracy of the data acquisition unit near the 0 volt range. The intercepts were considered to be near enough to zero, however, to be insignificant and they were thus ignored in future load calculations.

### 3.3 INSTRUMENTATION

Two Taurus-One data acquisition units with T-3732 analog input modules and two IBM compatible Corona computers with 512 K of RAM were available for this study. Six instrumentation amplifiers with variable gains from 1 to 20,000 were designed and built for this project by the agricultural engineering electronics technician. They amplified the transducer signals and sent the voltages to the analog input modules on the Taurus-One units. The Taurus-One units in turn interfaced with the host computers via serial communication links. The electronic equipment was encased in a positively ventilated cabinet using a clean outside air supply. This prevented dust from contaminating any of the electronic components. The instrumentation setup is shown in Figure 3.7.



Figure 3.7 - Data acquisition instrumentation

It was initially intended that the transducers would be connected to one Taurus-One/computer system and the strain rosettes would be connected to the other. When the wall stress/strain measurements were abandoned, it was decided to connect the total load transducers to one data acquisition system and the vertical wall load transducers to the other, in order to maximize the efficiency of data collection.

The Taurus-One data acquisition units could take approximately 4000 readings per second with up to 64 single-ended channels. Although their internal memory was limited, data could be dumped to the host computer

while it was being taken. A memory overflow could still occur, however, if the period between each reading was too short. This then placed a limit on the number of readings that could be taken with a specified period. Both a period and scan time needed to be determined.

Since there was very little information in the literature as to when the maximum discharge pressure would occur after discharge began, the time required to measure the peak load was unknown. Collins (1963) concluded that the maximum overpressure occurred within a few seconds after discharge started. This was supported by reports of many grain bin failures taking place shortly after unloading began. A scan time of 120 s was arbitrarily chosen as a target for this study. This scan duration was believed to be conservative and most likely it would be modified for future studies, but as this was the first series of tests, it was felt to be appropriate. As a result of limitations outlined below, the 120 s window was later shortened to 109 s.

High-speed data acquisition has not been widely utilized by many researchers, except in cases where chart recorders giving a continuous analog signal were used. In rare cases, digital acquisition was used with periods as small as 500 ms. Harms and Henry's (1976) results with high-speed photography showed that fully developed dents could manifest themselves in less than 17 ms. A period smaller than 17 ms would be required to measure any rapidly occurring pressure effects. It was decided that a period of 10 ms would be desirable.

Given the memory constraints of the Taurus-One units, a scan time of 120 s and a period of 10 ms could only be accomplished with a maximum of 5 channels per unit. A period of 11 ms enabled 63 s of acquisition

time using six channels. This period/scan time combination was the initial choice. When wall strain measurements were abandoned, only three channels were required per Taurus-One unit. This enabled an even shorter period. A 6 ms period enabled infinite scan time, since data could be dumped as fast as it was read. A 5 ms period caused memory overflow after 109 s of data collection, but as 5 was an even fraction of 1000 ms (i.e. 1 s), it was chosen as the scan period and 109 s was accepted as an adequate scan time.

To eliminate human inconsistency, an electronic trigger was used to start data collection as soon as the discharge gate opened (solenoid was activated). As readings were being taken, each Taurus-One unit dumped the collected data to its host computer to be stored in random access files for later analysis.

### 3.2 MATERIALS HANDLING

The grain used in this study was Neepawa hard red spring wheat with an initial moisture content of 10% w.b. (using ASAE standard S352.1). There was some chaff present, but as this was felt to be representative of grain found in commercial bins, it was not removed. An initial sieve analysis indicated over 93% of the grain mass had a minimum dimension between 2 and 3.5 mm, with less than 0.5% smaller than 2 mm, based on round hole sieves. The remainder of the seeds had a minimum dimension larger than 3.5 mm. A total volume of approximately 2 m<sup>3</sup> was used with only 1.2 m<sup>3</sup> being required to fill the bin for each test. The excess grain was stored in a supply bin.

In order to facilitate materials handling and to allow for uniform filling of the test bin, a 0.6 m<sup>3</sup> surge hopper was mounted on top of the triangular support frame. The hopper forced centre filling of the bin, but the fill rate could be varied. In this study, the fill rate was obtained using a 70 mm orifice. Grain flow from the surge hopper was controlled by a pneumatically activated discharge gate. To catch the grain discharged from the model bin, a hopper cart was located directly below the deck.

Grain was circulated from a main supply bin using a pneumatic conveying system. Although not a direct part of this thesis project, the conveying system was manufactured and installed by the author and initially caused some unexpected problems. As grain moved along the PVC conveyance pipe, large static charges built up and resulted in a few "hair raising" experiences. As the grain discharged from the model bin, dust tended to collect on the under side of the frame, indicating that the grain was also building up a static charge. It was felt that the static charges would significantly influence the flow and load characteristics of the grain, so the pipes were all grounded and the laboratory humidity was increased to dissipate the charges. After a few initial setbacks, the problem was rectified.

## CHAPTER IV

### PROCEDURE

#### 4.1 EXPERIMENTAL DESIGN

The experiment was setup in a 4x4 factorial arrangement with flow rate and location (eccentricity) of discharge as the two independent variables. One replication of each of the sixteen combinations made up a single test series. Randomization of the testing order within each series was accomplished using the random number table found in Kennedy and Neville (1976). It was initially planned to run six test series, but as each test series required an extensive amount of time and as the data appeared to be quite similar between test series, the number of replications was reduced to three. Each series was completed before the next one was started, thereby enabling any effect of bin wall conditioning or mechanical grain damage to be accounted for.

#### 4.2 BIN WALL SURFACE CONDITIONING

Bin wall surface conditioning has a marked effect on the grain on bin wall friction coefficient. To negate this conditioning effect and to wear off any oils or rough spots caused by the galvanizing material, a number of fill-discharge sequences were run on the test system prior to the actual testing phase. The inside surface of the bin wall was also manually washed to remove any additional oil that remained.

#### 4.3 TESTING PROCEDURE

The series of tests were run during the three month period from December, 1986 to February, 1987. In total, 48 dynamic tests were run to investigate the effects of the two main variables of concern. Each of these tests used the procedure described below. To check the effect of a longer settling time between filling and emptying stages, three additional tests were conducted with the static grain allowed to equilibrate over an extended period. To verify that the transducer outputs did not drift during the static settling tests, a dead load test was performed using suitcase weights.

To control grain dust, the laboratory exhaust fan and intake air tempering unit were used. Because the winter air was very dry, a humidifier was used to maintain room humidity at a level above 75%. The evaporative cooling effect of this added moisture reduced the air temperature so an additional heating unit was also required. These air tempering systems were shut down at the end of each day of testing and they were restarted prior to the start of additional testing.

To ensure equilibrium of the laboratory airspace, the air control systems were allowed to run for at least one hour before any tests were conducted. The equilibration period allowed the room temperature to stabilize thereby ensuring no errors would be introduced into the data due to the lack of temperature compensation in the transducer signals. Since the dynamic tests used a scan time of less than two minutes, strain gage temperature compensation was not used as it was felt that room temperature would not change significantly in that time.

#### 4.3.1 Dynamic Tests

The entire dynamic test procedure was based on a computer program (COLLECT) used to control the operation of the data acquisition system. The program, described further in the next chapter, was written in BASIC and ran simultaneously on both computers, although the data download procedure was slightly different for the two versions (COLLECT1 and COLLECT2).

Before a test could be started, the discharge plate corresponding to the selected flow rate/eccentricity combination had to be inserted. The slide gate was positioned under the orifice and its operation was checked to make sure that it completely cleared the outlet when it was opened. The gate was then closed. A quick check was made of the space under the angle iron ring mounted to the bottom of the bin wall to make sure that no grain particles were stuck between the bin and the floor. These particles would have distorted the vertical wall load readings. Once these checks were made, the computer program was initiated.

The two computer screens displayed continuous readings of the six amplifier outputs. With the bin in the unloaded (empty) condition, the readings were zeroed by adjusting the balance control of each amplifier. This cancelled out the weight of the bin and deck thereby enabling the transducers to record only grain loads. After the balancing procedure was completed and the signals stabilized, a test name was entered. The test name was either seven or eight characters long and it indicated the outlet diameter in mm (D45, D60, D75 or D100), the location or position of the orifice (E0, E1, E2 or E3, with E3 indicating the fully eccentric position) and the replication or series number (S1, S2 or S3). A set

of empty bin readings was then made. If the displayed results were satisfactory (all zeros), the data were stored as record #1 in a random access static load file. The program went to a wait state displaying the current transducer outputs and the model bin was filled.

The surge hopper had 1/2 the capacity of the model bin, so filling was accomplished in two stages. The hopper could not be discharged and filled simultaneously since high internal air pressure generated by the pneumatic conveyor caused the grain to spray out, as opposed to flowing out in a steady stream. Approximately 15 min were required to fill the surge hopper while discharge took only 5 min. Once the model bin was completely filled, a second set of static readings were taken. These were stored as record #2 in the static file.

Using a tape measure, the height of the exposed inside bin wall was obtained at four points, spaced 90 degrees on the circumference. Grain depth was then obtained by subtracting the average of these four values from the total bin wall height. Filling angle of repose was measured using a protractor device, as shown in Figure 4.1. The device consisted of two wooden members hinged together at one end with a screw adjustment enabling rotation of one member relative to the other. By setting one member on the sloping grain surface and levelling the other, the angle of repose could be determined to the nearest degree. Although the bin was to be filled to its maximum capacity, few replications began with a "completely full" bin. The errors that would be caused by a variation in initial grain depth were recognized, but felt to be minimal. The problem, however, was corrected in later series by ensuring that the surge hopper was adequately filled at each loading stage.

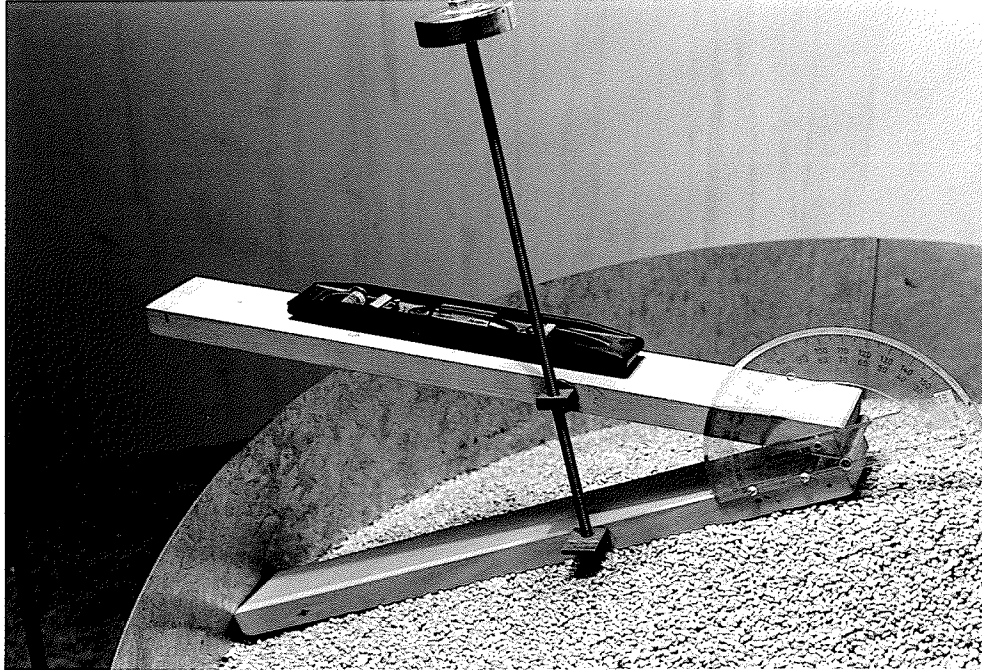


Figure 4.1 - Measurement of the filling angle of repose

At this point, the program went to another wait state to allow for settling time. The dynamic test series did not use a settling time and discharge was usually initiated within 5 min of filling. A third set of static readings was taken immediately prior to discharge to note any differences from the previous reading if a settling period was used. For these test series, the two static readings were usually identical, although minor variation did occur in some tests. After it set the trigger on the data acquisition system, the program then waited for the discharge gate to open. With the pneumatic grain conveying system activated to empty the hopper cart, the dynamic phase was ready to proceed.

When the discharge gate switch was activated via the hand held switch unit, two events occurred. First, dynamic data collection was

initiated with a 109 s scan duration and a 5 ms period, and secondly, the grain began to discharge. Since the electronics in the data acquisition system worked faster than the air cylinder controlling the discharge gate, the first few readings were actually taken before the slide gate opened with the grain still at rest in the static condition. This enabled any immediate load transfer occurring at the first movement of grain to be sensed.

The data transferred from the Taurus-One data acquisition units to the computers were stored in random access files created on RAM disks within the computers' internal memories. This format was used since RAM disk access was much faster than normal disk drive access, which resulted in a communication buffer overflow. Even using a RAM disk, a maximum sized 32 kbyte communication buffer had to be specified on one computer to prevent buffer overflow.

When data acquisition was finished, the program again went to a wait state to allow for complete emptying of the bin. To decrease test turnaround time, the first half of the discharged grain mass was conveyed directly back to the surge hopper, while the remainder was later transferred to the supply bin.

The grain handling system was very slow and only had a capacity of  $2.5 \text{ m}^3/\text{h}$ , which was approximately equivalent to the discharge through a 50 mm orifice. This resulted in the hopper cart filling faster than it could be emptied, with three out of the four discharge rates used. To prevent overflow, grain discharge from the test bin had to be stopped periodically to allow the grain conveying system to "catch up."

For the two lowest discharges, this caused no problem, but with the 75 mm outlet, the hopper cart became full at the 105 to 110 s mark. With the 100 mm orifice, the problem was much more severe and discharge had to be stopped after only 45 to 50 s of grain flow. Although this reduced the scan time of usable data, higher flow rates resulted in more grain discharging in a shorter time period thus the peak loads were believed to occur more quickly also. It was believed that 45 s of data with the 100 mm discharge was adequate.

As grain discharged from the model bin, periodic measurements were taken of the grain surface profile. Using a tape measure, grain depths at the centre of the flow funnel and at the two wall edges intersecting the line of discharge locations were obtained. This enabled a pseudo-determination of flow patterns that occurred using various flow rate/eccentricity combinations. The last profile measurement was taken when all the grain in the bin had freely discharged. The grain in this dead zone region was manually pushed to the discharge outlet, with the final emptying accomplished by climbing down into the bin and sweeping the floor clean with a broom and compressed air. The discharge plate was then removed and the plate for the next test was inserted.

Sweeping the bin floor caused grain to be pushed under the skirt and the angle iron mounting ring. This was removed using compressed air. After bin cleaning was completed, a fourth set of static readings was taken to ensure that the transducer outputs went back to zero. In most cases, readings were within Taurus numbers  $\pm 12$ . Errors were attributed to slight temperature variation or shift in the electronic balance of the amplifiers and were considered to be insignificant.

The data from the computer using COLLECT2 were downloaded to a floppy disk and then uploaded to the other computer, where all the readings were combined and downloaded onto a floppy disk. The static and dynamic data were stored in two separate random access files with extensions to the test name of .STA and .DYN, respectively. During the downloading procedure, which took approximately 8 min, the filters for the pneumatic grain handling system were cleaned and the conveying pipes were moved into place for the next test. When downloading was complete, the program went back to the balancing sequence. Then the diskettes were replaced and the system was ready for the next test. The entire test procedure took approximately 1.5 h.

#### 4.3.2 Settling Tests

After some preliminary analysis of the earlier test series, the effect of settling time was questioned. Although it was not a primary variable to be considered in this study, settling time was a factor which affected comparison of dynamic/static ratios (DSR) since the static wall load was believed to decrease with settling of the grain. Since the severity of the effect was unknown, a brief investigation was undertaken. Tests were conducted over three consecutive weekends when dynamic tests were not being performed.

The tests were identical in procedure to the dynamic tests except for a settling period between the filling and discharge stages. The length of this period was 35 h in one test and 85 h in the other two. These times were chosen arbitrarily based on the time available from the start of the test till the end of the weekend.

The computer program was modified and given the new name ACQUIRE. Once the bin was filled and the first static load readings were taken, the computer created a new file with the .DAT extension. One reading from each transducer was taken every minute during the entire time of settling. After the settling period, the program made a final reading of the static bin loads, the trigger was set and the discharge phase continued as previously described.

The discharge location was arbitrarily chosen as the one 150 mm from the bin centre (i.e. E1). Three discharge rates were used: those corresponding to the 45, 60 and 75 mm outlets (i.e. D45, D60 and D75). The test series was given the number S0. The air control system could not be left unattended during the weekend, so the humidifier and the heater were not used for these tests.

#### 4.2.3 Dead Weight Test

Preliminary analysis of the settling tests indicated that the wall transducer outputs held relatively constant for a number of hours, but then dropped suddenly by up to 6% within a one minute interval. This discovery was puzzling since all three wall transducers indicated drops during the same intervals. It was speculated that the phenomenon might be related to voltage spikes or electrical noise in the instrumentation to which the transducers were connected. A static dead weight test was conducted to determine if any instrumentation problem existed. By using dead weights to simulate floor and wall loads, any change in load recorded by the transducers could be attributed to the instrumentation since the weights themselves would not change.

ACQUIRE, the program used for the static tests, was again used exactly as it had been before. The only change for this test was that instead of filling the bin with grain, eighteen 20 kg suitcase weights were placed on the deck to simulate a floor load and seven weights were placed on wood beams laying across the top of the bin wall, to simulate vertical wall loads. The magnitude of the wall load was similar to that of the static grain wall load, although there were insufficient weights to simulate the floor load. After the static data were collected, the test was complete.

#### 4.4 GRAIN QUALITY CONTROL

It was anticipated before testing started that the grain might damage mechanically as a result of a surge hopper manufacturing flaw. The pressure side of the pneumatic conveyor charged grain into the surge hopper horizontally tangent to the circular wall. This enabled the surge hopper to act as a cyclone separator with the grain spinning in a clockwise direction. When the hopper was constructed, the cylindrical wall was rolled from one piece of sheet metal, with a single overlapping seam. The seam was inadvertently overlapped such that the spinning grain caught the exposed edge thus increasing the tendency for the grain to shatter. As major reconstruction of the surge hopper was required to rectify the problem, no alterations were made. In addition, since approximately 60% of the total grain supply was used for each test, the grain was subjected to much handling. This further advanced grain damage.

To monitor grain quality, periodic moisture content determinations (ASAE standard S352.1) and sieve analyses were made using representative grain samples. The initial set of these quality control tests was taken prior to the start of the first test series. Additional quality control tests were conducted after each test series was completed.

Results of the tests indicated that average grain size was slowly decreasing, but not to any significant degree. Visual inspection of grain samples made during testing indicated increases in the number of cracked and shattered wheat kernels as well, although these kernels never made up more than approximately 1% of the total grain mass. The moisture content of the grain remained around 9% w.b. Since the blower fan driving the pneumatic grain conveyor heated the air, the relative humidity in the pipes was only around 25 to 30% even though the ambient air in the laboratory was in the range of 75 to 80%. Short of spraying water directly into the intake line, there was no way of maintaining a higher grain moisture level, thereby reducing mechanical grain damage.

#### 4.5 DISCUSSION

Test procedures and computer programs written for data collection worked well, although the testing phase was very time consuming due to the low capacity of the pneumatic grain conveyor. If time constraints do not pose a major concern in future tests, one test per day could be conducted. After the bin is filled, the grain could be given 23 h to settle (since little load shift occurs after one day of settling) and then one hour would be allowed for the discharge phase, with filling for the next test occurring immediately after.

During pre-test filling/discharge sequences, it was noticed that the full bin distorted in the cross-section to a more circular shape. To prevent binding as this distortion occurred, clearance between the walkways setup around the test system and the bin wall was increased slightly. The level of the frame, base table and test bin were also checked. Manufacturing flaws in the bin made "levelling" somewhat of an arbitrary procedure as the bin was always "out of level" somewhere. After a few tries, a satisfactory mounting position was obtained.

As mentioned previously, the number of cracked kernels and fines in the grain mass increased with testing. It was not believed that the friction characteristics of the grain changed significantly, but a slight increase in the bulk density was noticed. The mechanically damaged grain mass did add to one problem, however. A small clearance was allowed between the discharge plate and the slide gate to provide ease of opening when the bin was filled. With large grain particles this clearance was satisfactory, but as more small particles and fines developed, they tended to lodge into this clearance causing the slide gate to stick when the discharge switch was activated. Because of the trigger set on the data acquisition system, data collection proceeded even though the discharge gate would not open. A restart feature was incorporated into the program which allowed the user to return to the trigger setup and pre-discharge wait state without losing the static load data. This restart feature was used often throughout the testing especially in the final series.

The discharge gate could usually be loosened by manually prying it open slightly making sure that the outlet still remained covered. In

three tests, a small number of grains were discharged. The data were still considered valid although some interesting observations from these tests were made as discussed in the Chapter 6. In many of the tests from the final series, particularly those using 75 mm outlets, the gate could not be loosened and it had to be manually pulled open when the data acquisition was initiated. This caused some swinging of the base table which could usually be damped out, although some of the tests recorded the oscillatory load shift caused by this vibration.

## CHAPTER V

### DATA ACQUISITION AND ANALYSIS PROGRAMS

#### 5.1 INTRODUCTION

Microcomputers were used in both the data collection and analysis stages of this study. The data files were stored in compressed random access format, but the storage requirement was still large. In order that any or all of the data be immediately accessible to the analysis programs, 12 Mbytes of memory was required. Examination of actual data values indicated that, although rapid load changes occurred, they could still be accurately represented using only every second reading. This then reduced data storage requirements to 6 Mbytes.

#### 5.2 COMPUTER PROGRAMS

Several computer programs were written by the author to control the Taurus-One acquisition units during data collection. Additional programs were used to process information generated by the tests. All programs were written in GWBASIC using an MS-DOS disk operating system. The major programs are outlined in the following pages:

##### 5.2.1 CALBRAT6

This program was used to collect and store data simultaneously from the six transducers during a calibration cycle. A Taurus-One scan table

was set up to include the six channels to which the transducer/amplifier pairs were connected. With each load increment, 100 scans of the table were taken with an 11 ms period between each scan. The 11 ms delay was chosen, since at the time of calibration, this was the scan period that was going to be used in the tests (the test scan period was shortened to 5 ms as explained in section 3.3). If the standard deviations of the 100 readings for each channel was less than one Taurus number, the six average readings, as well as the load used to generate the readings were stored in a random access file (86TRANS6.DAT) for later use by the calibration linear regression program.

#### 5.2.2 REGRESS6

Using the data from the file 86TRANS6.DAT, REGRESS6 simultaneously generated linear regression equations for the six force transducers. Slope, intercept, R-squared and linearity were calculated with the results being used to convert the Taurus numbers corresponding to the transducer signal outputs back to actual force (load) values.

#### 5.2.3 COLLECT

The basic outline of this program was given in section 4.3.1. Two versions of the program were written: COLLECT1 was used on the computer reading vertical wall load transducers #1 to #3, while COLLECT2 acquired data from total load transducers #4 to #6 and allowed for data transfer to the other computer so that all the readings could be merged into one large file. A listing of COLLECT1 is given in Appendix G.

The COLLECT programs necessitated some changes in the computer setup procedure. Computer #1 required a RAM disk of 264 kbytes while computer #2 required a RAM disk of 132 kbytes. In loading GWBASIC, the extension /s:5232 needed to be specified because of the large record size that was used in downloading the files. The maximum communication buffer size (extension /c:32767) was also required since an overflow condition would result with a smaller buffer due to the high-speed data transfer from the Taurus units. To maximize the acquisition abilities of the Taurus-One, a maximum baud rate of 9600 was used.

Data were transferred to the computers during the 5 ms delay between channel scans. The program further transferred these data from the buffers to RAM disk files during the communication sequence in 240 byte blocks. One reading occupied 2 bytes, with one scan of the three channels taking up 6 bytes. Although the filenames were the same, COLLECT1 used the extension .123 and COLLECT2 used .456. After the discharge sequence was complete, data from computer #2 were downloaded to a diskette file, transferred to computer #1 and then uploaded to the RAM disk. A final download sequence merged the two files together and created separate static (.STA) and dynamic (.DYN) files on the disk in drive B. Six bytes were alternately taken from each RAM disk file to combine the six transducer readings measured at the same point in time.

#### 5.2.4 ACQUIRE1

This program was used together with COLLECT2 and was identical to COLLECT1 except for one subroutine used at line 1410 during the wait state between the filling and discharge sequences. As explained in

section 4.3.2, the added subroutine took readings of all six transducers at one minute intervals until the operator signalled that discharge was ready to begin. This subroutine was used to monitor the static load as the grain settled over the weekend that the test was run.

A slight hardware adjustment was required to run this program. The multiple connector serial cable connecting computer #1 to channel A of Taurus-One unit #1 also had to be connected to channel A of Taurus-One unit #2. To prevent communication errors, COLLECT2 had to be initiated before ACQUIRE1.

#### 5.2.5 NOISE

In graphing the results from the first series of tests, it was observed that there were a number of "spikes" that appeared to occur randomly throughout individual tests. Both the magnitude of these spikes and their individual occurrence (data points on either side of the spike were normal), indicated that the probable cause was due to the presence of random electrical noise in the instrumentation, as opposed to load surges. Further examination of the spikes indicated that the Taurus numbers recorded usually represented a 5 or 10 volt reading, which was probably picked up from the 5 volt power supplies on the Taurus boards.

A program was written to scan the data to search for any possible occurrences of noise. When the data for one channel over a one second interval had a range greater than 40 Taurus numbers, corresponding to a load of approximately 100 N, that particular section of data for the transducer in question was flagged for later analysis. The range of 40

was chosen so that small noise levels would be ignored while medium to large spikes would be flagged.

#### 5.2.6 CHANGES

This program was used specifically for checking the data flagged by the NOISE program and making changes as required. The 200 data points for the one second of readings in question were displayed with the maximum and minimum values highlighted for easy location. If a number was deemed by the user to be abnormally out of range due to a noise spike, it was manually changed to a new value. The new value was calculated as the average of the two adjacent readings, which were, in most cases, identical.

#### 5.2.7 CONVERTS

The readings to this point were still in the raw form of Taurus numbers. In order to be of any use, the numbers needed to be converted to transducer force values using the calibration equations developed by the program REGRESS6. As these six readings corresponded to the three total loads and three vertical wall loads measured by the transducers, a further transformation was required to obtain actual bin loads. The equations of statics were used to create this transformation matrix. Manufacturing and assembly errors of the test system were taken into account in the development of these equations thus the coefficients for loads B and C were not identical even though the loads appeared to be symmetric. The equations are outlined in Appendix C.

Assumptions regarding the nature of the bin loads were required. First, since a triangular support was used, three uniform vertical wall loads were assumed to act over three 120 degree sections of the wall circumference, with each section including the 60 degrees on either side of the respective transducer. Wall section A was opposite the discharge outlet while sections B and C were directly adjacent, as shown in Figure 5.1. Since the loads were assumed to be uniform, they were modeled as point loads acting at the centroids of each section.

The floor loads were also assumed to be uniformly distributed over three, 120 degree, pie-shaped sections located geometrically similar to the wall sections. As per the wall loads, the floor loads were modeled as point loads acting at the centroids of the pie-shaped floor sections.

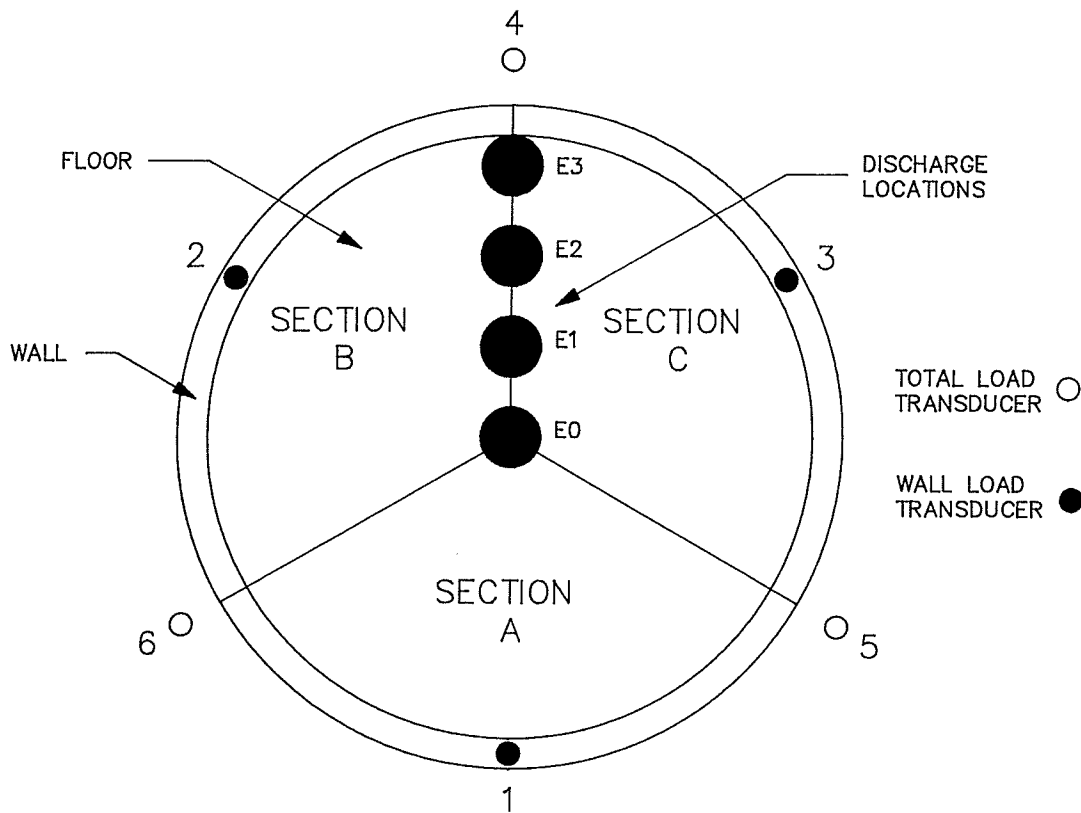


Figure 5.1 - Model bin floor and wall sections

The assumption of uniformly distributed loads was made arbitrarily. As no loading model seemed more justified than any other, the most basic one was chosen. A linear variation of the load from the near wall to the opposite wall may have more accurately represented actual loading, but as only three vertical wall load transducers were used, there was no way of confirming this hypothesis. Since obtaining general load trends, as opposed to exact quantitative results was the main objective of this study, the model used was felt to be satisfactory.

Using the original raw dynamic data files (.DYN), CONVERTS created two new files. The first (.TRA) stored the converted transducer loads which were used in some preliminary analysis and the other file (.BIN) stored the converted and transformed wall and floor loads. Although data readings were taken every 5 ms, preliminary analysis indicated that no major pulsations or rapid surges were recorded. This was due to the fact that the transducers recorded average bin loads. In order to reduce storage and data analysis requirements, the .TRA and .BIN files were created using only every second reading from the .DYN file. The last nine seconds of acquisition was also discarded, thus recording 100 readings per channel for 100 s. This data reduction enabled three test files to be stored on one 360 kbyte floppy diskette.

#### 5.2.8 STATICS

In addition to the dynamic data, static readings from each test were also analyzed. The program STATICS converted the raw static data to transducer loads and bin loads as per CONVERTS and the new values were simply appended to the existing data file. The static results for

the three test series were then printed out, in addition to bin loads and percentages of total loads for the readings taken immediately after the bin was filled. A listing of the output is shown in Appendix E.

#### 5.2.9 STATDYNA

As indicated in the discussion of instrumentation in section 3.3, the first few readings from the dynamic acquisition actually measured grain loads during the static condition prior to discharge. Comparison of these values to the static readings taken after the bin was filled should have indicated no differences. Large differences, however, were apparent in selected cases.

The program STATDYNA was written to compare the six static and dynamic (pre-flow static) bin loads for all forty-eight test cases. One set of static and one set of dynamic bin loads were listed as well as the differences between the two. The static values used were the ones taken immediately after the bin was filled. These values were chosen over the ones taken prior to discharge since the settling time in each case was not the same, although it was never greater than ten minutes. By using the first set of static readings, some degree of uniformity could be obtained. The dynamic values used were the first ones taken.

#### 5.2.10 FLOWBULK

The program FLOWBULK was written to calculate the initial bulk density of the grain and the discharge rate for each test. Grain volume was first calculated by entering the grain height as measured

during testing and assuming an angle of repose of 27 degrees. This value was then divided into the weight of grain, obtained by summing the static readings from transducers #4 to #6. Dividing further by the gravitational acceleration, bulk density was defined in  $\text{kg/m}^3$ .

The discharge rate was obtained by performing a linear regression of the total grain load measured at two second intervals throughout the discharge test. To account for the delay in the opening of the slide gate, the first reading was taken at the 10 s interval. Readings were only taken up to the 40 s interval for tests using the 100 mm discharge outlet, since discharge had to be stopped early.

The slope of the regression represented the discharge rate which was expressed in both  $\text{kg/s}$  and  $\text{m}^3/\text{min}$ . The latter value was obtained by dividing by the previously calculated bulk density.

#### 5.2.11 GRAPHS

GRAPHS was a program used to plot load vs. time curves for the various dynamic tests using a Hewlett Packard 7440A Colorpro plotter. Both vertical and horizontal scales and ranges as well as titles and labels could be inputted by the user and from one to six channels could be plotted thus making the program as adaptable as possible.

Graphing reduced the large volume of data to a form that could be easily analyzed visually. This enabled quick preliminary analysis which aided the author in establishing procedures for more in-depth analysis. Graphed results from test series #1 are shown in Appendix D.

#### 5.2.12 SEARCH and RESULTS

With centre unloading, the plotted data indicated rapid increases in wall loads at the initiation of discharge. For all the eccentric discharge tests, load increases were apparent on wall sections B and C with decreases occurring on wall section A. Although the loads changed very rapidly at the beginning of each test, they tended to be much more stable after a few seconds of flow and then they gradually decreased. The maximum loads often occurred during the initial period of rapid change, but this was not always the case.

A program was written to scan the dynamic data files to search for various load peaks in each test. The floor loads were greater than the vertical wall loads, but they generally reflected a mirror image of the wall loads. For this reason, only the wall loads were analyzed.

For centre discharge tests, the program searched for peak loads on wall sections A, B and C as well as the peak average load on sections B and C combined. During eccentric discharge tests, however, a peak load on wall section A was of little concern since the load on that section was decreasing. Many researchers indicated that eccentric discharge load imbalance was critical, so with the eccentric discharge tests, the peak load on wall section A was replaced with a search for the peak difference between the load on wall section A and the average load on wall sections B and C. This load difference was termed "delta."

At each peak, the complete bin loading condition was noted. Load totals were calculated as well as percentages of the respective total load for the wall and floor sections. Dynamic/static ratios were

obtained using the static value recorded immediately after the bin was filled. The start of discharge was arbitrarily defined as the point at which the load on wall section B differed from its initial value by more than 15 N. The time of each peak was noted in seconds after discharge started. These peak load results were stored in the file RESULTS.DYN and the program RESULTS printed a hardcopy as shown in Appendix F.

#### 5.2.13 PEAKS

This program was written to take out selected critical peak values from the previously generated data file RESULTS.DYN. These peaks were stored in a new file called PEAKS.DYN, for later use in an analysis of variance program, ANOVA. The file had twenty-one records and 48 values in each record.

The first four records stored the static loads on wall sections A, B and C and the total wall load. Records #5 to #8 stored the peak dynamic loads on wall sections A, B and C as well as the peak average load on wall sections B and C combined. Record #9 corresponded to the peak delta values, which were peak load differences between wall section A and the average of wall sections B and C. Records #10 to #13 stored dynamic-to-static ratios corresponding to the peak wall loads in records #5 to #8. Records #14 to #17 were the times required to reach the peak loads of records #6 to #9, while the last four records stored the weight of grain that had discharged at the same peak loads.

#### 5.2.14 ANOVA

As implied by the name, the program performed analyses of variance on the test results for the particular peak load conditions defined in the last section. A 4x4 factorial model with 3 replications was used in all tests except those for the dynamic load peaks on wall section A and the peak delta results. For these analyses, 4x1 and 4x3 factorial models, respectively, were used. The program printed a summary table of the data as well as an ANOVA table.

#### 5.2.15 SAS

The ANOVA indicated no interaction between the effects of flow rate and eccentricity, so a regression analysis was performed using the university's main frame computer and the Statistical Analysis System (Anonymous, 1982) multiple regression procedure (PROC STEPWISE). The peak average dynamic load on wall sections B and C were inputted together with the discharge rates and eccentricities used, in order to calculate an empirical equation that could be used to predict the peak wall load.

One discharge rate was used for each outlet size. This rate was the average rate obtained from all the tests using the outlet size in question. Eccentricity was defined as the ratio of the distance between the centre of the bin and the centre of the orifice, and the bin radius. Linear, quadratic and cubic terms were allowed in the model and the program calculated the best fit equation using each of one to six variables in the model.

CHAPTER VI  
RESULTS AND DISCUSSION

6.1 STATIC LOADS

6.1.2 Dynamic Tests

The results of the static measurements were very much as expected. After the bin was filled, the total weight of grain sensed by the three total load transducers ranged from 8756 to 10284 N throughout all 48 tests with an average grain load of 9451, 9865 and 10182 N for series #1, #2 and #3, respectively. Variation in the results was caused by two factors. In early tests, two surge hopper fill/discharge sequences did not completely fill the model bin, but as test time was a factor to be considered, the tests were run with the level of fill obtained. As the operator became more familiar with the test equipment, the surge hopper was filled more completely, thus the average depth of fill and average grain load increased with each test series. Bulk density also increased over the test period from 826 to 838 kg/m<sup>3</sup>. This was probably a direct result of mechanical damage to the grain caused by material handling. This change in bulk density, however, was less than 1.5% overall and was felt to be negligible as far as any other measurements were concerned.

As the bin was being filled, the transducers recorded no vertical load until the grain depth at the walls reached approximately 100 mm. This same phenomenon was also observed by Thompson et al. (1982), who

reported no measurable wall load at grain depths less than 250 to 300 mm in continuous circulation dynamic tests.

Once the bin was filled, the wall supported, on average, 17% of the total vertical grain load, although the average percentage was 19% in series #1 and it decreased to 15% in series #3. Analysis of variance of the static loads on each of the three wall sections as well as the total static wall load indicated a significant block (series) effect in all cases at the 1% level ( $\alpha=0.01$ ). Since the average total load and bulk density increased with additional testing, the results could only be explained by a change in the grain properties  $k$  and  $\mu'$ .

The increase of fine particles in the grain mass with additional testing may have caused a denser packing arrangement which increased the internal friction and lowered the value of  $k$ , since  $k$  is usually defined as a function of the internal friction angle  $\phi$  (equation [2.3]). It was assumed that variation in  $\mu'$  was more probable however, due to increased surface conditioning. As more tests were performed, both the bin wall and grain became more polished with friction between the two decreasing. This reduced friction caused less vertical load to be supported by the wall with a corresponding increase in the floor load percentage.

The decreasing static wall load effect was not totally unexpected, although the bin wall surface was believed to be well conditioned prior to testing. Janssen's equation was used to determine the values of  $\mu'$  required to obtain the average total wall load from each test series. The average bulk density from all the tests was approximately  $835 \text{ kg/m}^3$  and assuming an internal friction angle of 27 degrees, a constant value of  $k=0.38$  was used. Resulting coefficients of friction were 0.17 for

series #1, 0.15 for series #2 and 0.14 for series #3. The magnitude of change was slight, but the percentage of difference was large because of the small initial value. These friction coefficients were reasonable values for 9% moisture wheat on smooth galvanized steel (NRCC, 1977).

The wall and floor loads on sections A, B and C were approximately one third of the respective total loads, as expected, due to symmetry of loading. Slight variation in the average percentages occurred as a result of manufacturing and mounting geometry flaws. Wall section A, on average, supported 34.7% of the vertical wall load while section B supported 32.3% and section C supported 33.0%. Average loads on floor sections A, B and C were 33.9%, 32.5% and 33.6% of the total vertical floor load respectively.

The second set of static readings taken immediately prior to bin discharge generally agreed with the initial readings taken just after the bin had been filled. Some tests recorded a slight decrease in wall load indicating that settling of the grain mass occurred even during the short time the full bin was sitting static before being discharged. The decreases, however, were slight and considered to be negligible.

#### 6.1.2 Settling Tests

The static bin loads measured during the settling tests noted a decrease in wall loads and a corresponding increase in floor loads over the settling period. A similar pattern was observed by Versavel (1985) in tests using smooth walled model bins. Decreases up to 33% of the initial static load were noted after 85 h of settling with most of the load shift occurring within the first 24 to 30 h.

The pattern of load shift was not continuous as initially expected but rather took the form of a step function with load shifts occurring within the one minute interval between successive readings as shown in Figure 6.1. A number of small decreases in wall load occurred during the first five to ten hours with only four or five major steps noted over the remainder of the settling time. No load change was recorded between these major steps with up to 30 h between steps.

It was initially believed that the step function response may have been due to an electrical problem in either the amplifiers or the data acquisition system. The dead weight tests, however, confirmed the accuracy of the readings since all measured loads were constant over the 120 h of continuous monitoring. A slight shift in load from wall section C to section B was observed, but this was attributed to creep in the wood planking used to support the suitcase weights.

As there was no instrumentation problem, the step function nature of the wall loads was attributed to the sudden collapse of arches within the grain mass as settling occurred. Although the overall grain depth at the bin wall did not measurably change, it was believed that a slight compaction may have occurred. Downward settling of the entire grain mass caused by microscopic reorientation of the particles was resisted by vertical friction at the grain/bin wall interface. Once the full frictional strength was exceeded, the arches held together by the grain's internal friction collapsed and a sudden slight vertical movement took place causing the material to compact somewhat. The increased strength of the compacted grain applied less load on the walls and more was taken up by the floor. As grain kernels continued

60 mm ORIFICE DIAMETER - 30% ECCENTRIC DISCHARGE

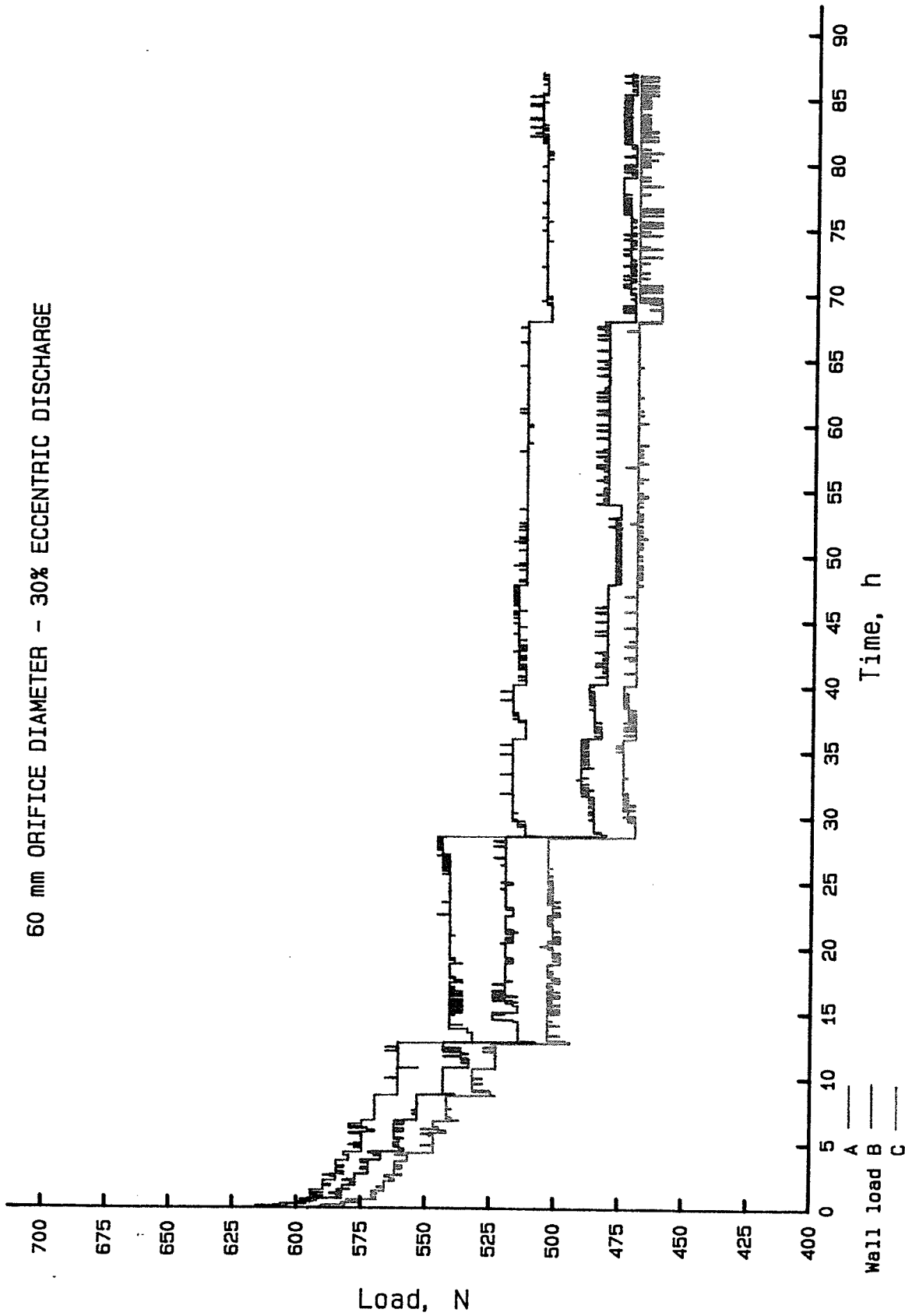


FIGURE 6.1 - WALL TRANSDUCER LOADS VS. SETTLING TIME - test D60E1S0

to reorient to a more stable position, the cycle of load would repeat itself. With increased settling, the rate of reorientation decreased and arch collapses occurred less frequently, although they were more severe.

Two of the three tests measured decreases in static wall load to the same limiting value, even though they began with slightly different initial loads. The third test measured lower initial loads and a lower limiting value, even though the bin was filled similar to the previous two cases. The reason for the difference in the third test was unclear. A possible explanation was that the grain mass was in a more compacted state, since fewer load shifts occurred at the beginning of the settling period for this test.

### 6.1.3 Pre-flow Static Load Comparison

A comparison of static load readings taken during the two phases of testing generally showed the two loads to be similar, as expected. Ten of the forty-eight tests indicated some settling had taken place, since the static wall loads were as much as 10% lower when read as part of the dynamic test.

Three tests, all with the discharge outlet at the wall, showed noticeable decreases (up to 24%) in the load on wall section A with increases as high as 78% of static on sections B and C. The opposite effect was noted in the floor loads. These three tests were the ones that accidentally allowed a small amount of grain to discharge when an attempt was being made to dislodge the slide gate, which had become stuck. Only a very small amount of grain was discharged, but it was

sufficient to cause the load shift. This supported Reimbert and Reimbert's (1976) observation that slight discharges of insignificant amounts of grain can cause significant wall load increases. The fact that these discharge load increases were "locked-in" once the discharge gate was closed tended to support the view that dynamic loads are, at least in part, a quasi-static phenomenon caused by reorientation of the grain mass.

One series #1 test, using a 75 mm orifice and a 60% eccentricity (i.e. test D75E2S1), noted 44% and 29% increases in static load on wall sections A and C, respectively, with a 2% reduction on wall section B. The slide gate also became stuck during this test but no premature grain spillage occurred upon loosening of the gate. The pattern of load shift noted above did not correspond to that occurring with eccentric discharge, thus the only explanation was that vibrations created as the slide gate was being loosened caused an unexpected random load shift.

Although the above noted pre-flow static load differences were undesirable, they were not considered serious. Larger shifts and peak loads were observed once the actual discharge phase of each test was initiated and dynamic data were collected. As the major focus of this study was concerned with analyzing peak loads, the tests in question were not repeated.

## 6.2 GRAIN FLOW OBSERVATIONS

### 6.2.1 Flow Rate

Plots of total grain load vs. discharge time had constant slopes over the test scan duration, since grain flow is independent of head (depth). Typical results for the four orifice diameters are shown in Figure 6.2. Reimbert and Reimbert (1976) suggested that a higher flow rate would occur with eccentric drawoff as opposed to centre unloading for the same orifice size, but the results of this study indicated no apparent relationship between discharge rate and outlet location.

Regression analysis of the grain load vs. time data yielded average grain discharge rates of 0.48, 1.13, 2.10 and 4.58 kg/s for the 45, 60, 75 and 100 mm orifices respectively. Variation in the flow rate using a particular outlet diameter was less than 7% for all sizes except the smallest one. The 14% variation of flow rate with the 45 mm orifice was probably the result of the larger relative particle size becoming a factor. This pointed to a possible model scale error when using smaller discharge outlets.

Using the discharge rates obtained from each test, a regression analysis was used to develop a prediction equation of the form  $Y=aX^b$  which defined flow rate as a function of orifice diameter (for the 12 mm plywood plates). The equation obtained was as follows:

$$Q = (1.073 \times 10^{-5}) D^{2.819} \quad [6.1]$$

where Q = discharge rate, kg/s  
D = orifice diameter, mm

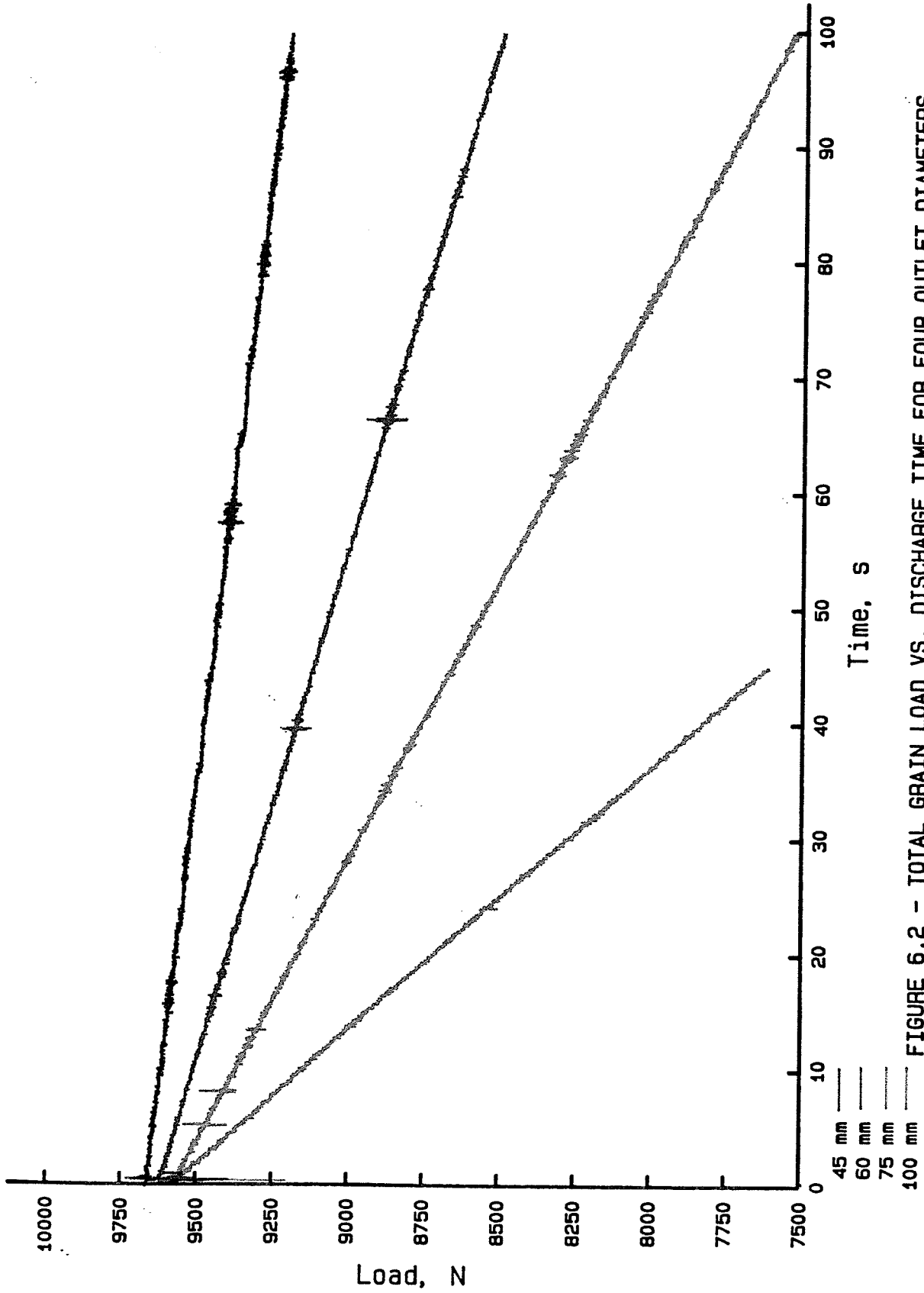


FIGURE 6.2 - TOTAL GRAIN LOAD VS. DISCHARGE TIME FOR FOUR OUTLET DIAMETERS

When plotted on a larger scale, total grain load vs. discharge time data for the 45 mm central outlet appeared more as a step function than a straight line, as illustrated in Figure 6.3. The steps had periods of approximately three to five seconds and magnitudes of 15 to 30 N (5 to 10 N per transducer). Because of the small step magnitudes, it was not certain whether the pattern observed was the true total load condition or simply an error introduced by the instrumentation.

Observations of the flow patterns on the top of the grain surface indicated pulsations both in the horizontal and vertical direction with periods similar to those observed on the flow graphs. Dubynin (1968) suggested that flow of bulk granular media manifests itself through the continuous formation and collapse of domes over the discharge orifice, thus it would be reasonable to assume that the total vertical grain load could exhibit pulsating or step function characteristics.

Alternatively, the data acquisition system would often represent a uniformly increasing or decreasing voltage as a sudden jump of two or three Taurus numbers, due to a lack of sensitivity in the analog-to-digital converter. Since a 5 N change of load on a given transducer was represented by a shift of approximately only two Taurus numbers, the step function nature of the curve may have, in fact, been a misrepresentation of the true load vs. time condition. No firm conclusions about the pulsating nature of the discharge could therefore be made.

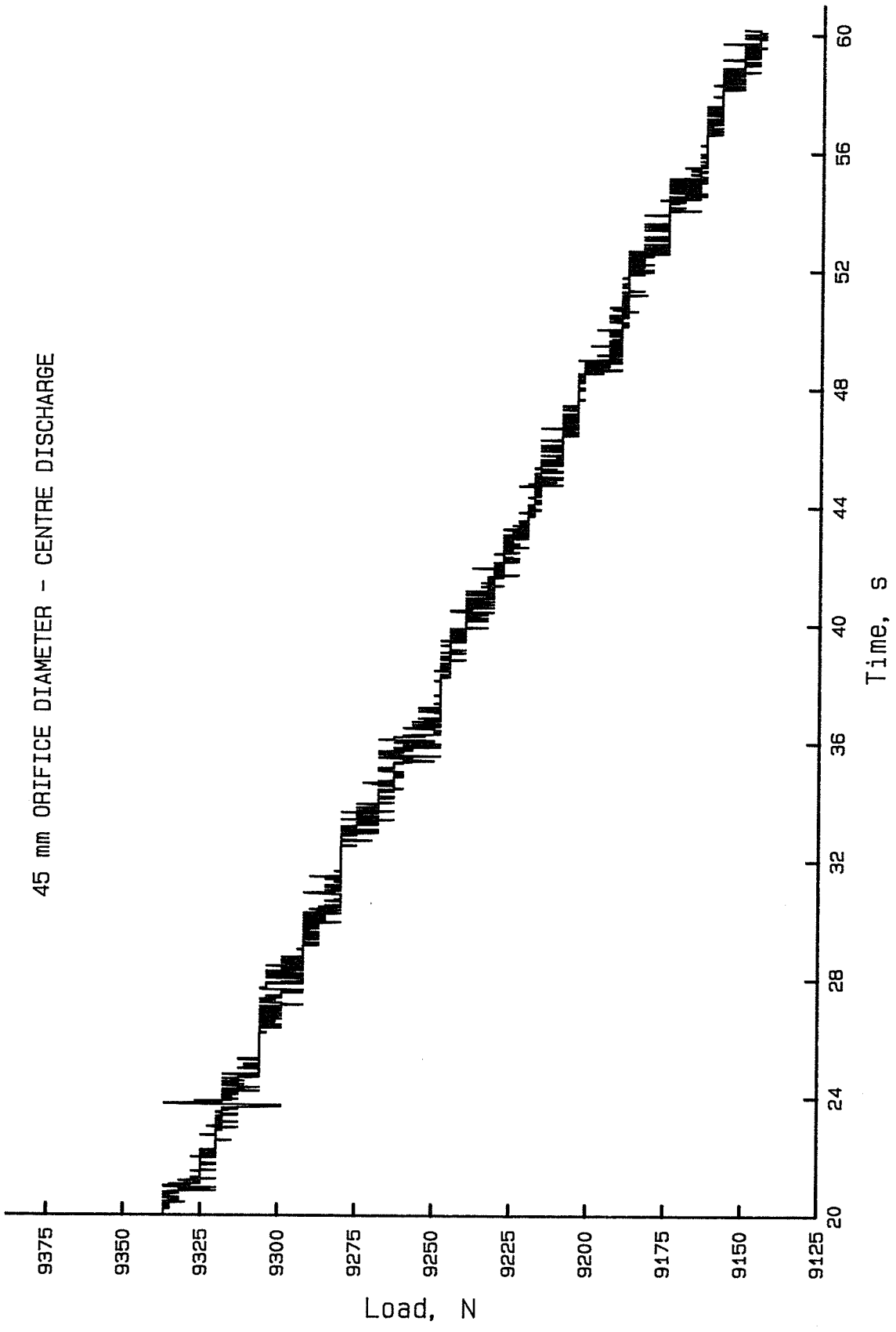


FIGURE 6.3 - TOTAL GRAIN LOAD VS. DISCHARGE TIME - MAGNIFIED SCALE - test D45E0S1

### 6.2.2 Flow Patterns

Figure 6.4 illustrates the four main patterns of flow that occurred during testing. Although it was impossible to observe the flowing grain within the bulk mass, it was believed that profile measurements of the top surface of the grain mass taken at various stages of emptying gave a fairly accurate description of the nature of the flow. As measurements from each test were plotted, it was discovered that the flow pattern was independent of flow rate and a function only of discharge location.

In centre unload (E0) tests, the flow pattern was axisymmetrical, as expected. The upward sloping cone of surcharge yielded to a downward sloping cone, via funnel flow, with the ring of grain nearest the top of the bin wall in a state of mass flow. As grain depth decreased, the mass flow region diminished and the funnel expanded until it intersected the bin wall. The zone of transition flow corresponded to that observed by Ross et al. (1980) in tests with paper models. The angle of repose during fully developed funnel flow was approximately 22 degrees.

In the E1 series tests, the centre of the flow channel was offset from the bin centre, but to a greater degree than the discharge outlet. In other words, the centre of the flow channel leaned towards the wall. Jenike (1967) made the same observation with eccentric discharge and he rationalized the phenomenon on the basis of flowing grain following the path of least resistance. The friction on a smooth-walled bin is less than grain's internal friction, thus the grain tries to flow along the wall. A transitional flow zone occurred at the top of the grain mass at the start of discharge, but fully developed funnel flow occurred much sooner than in the centre unload tests.

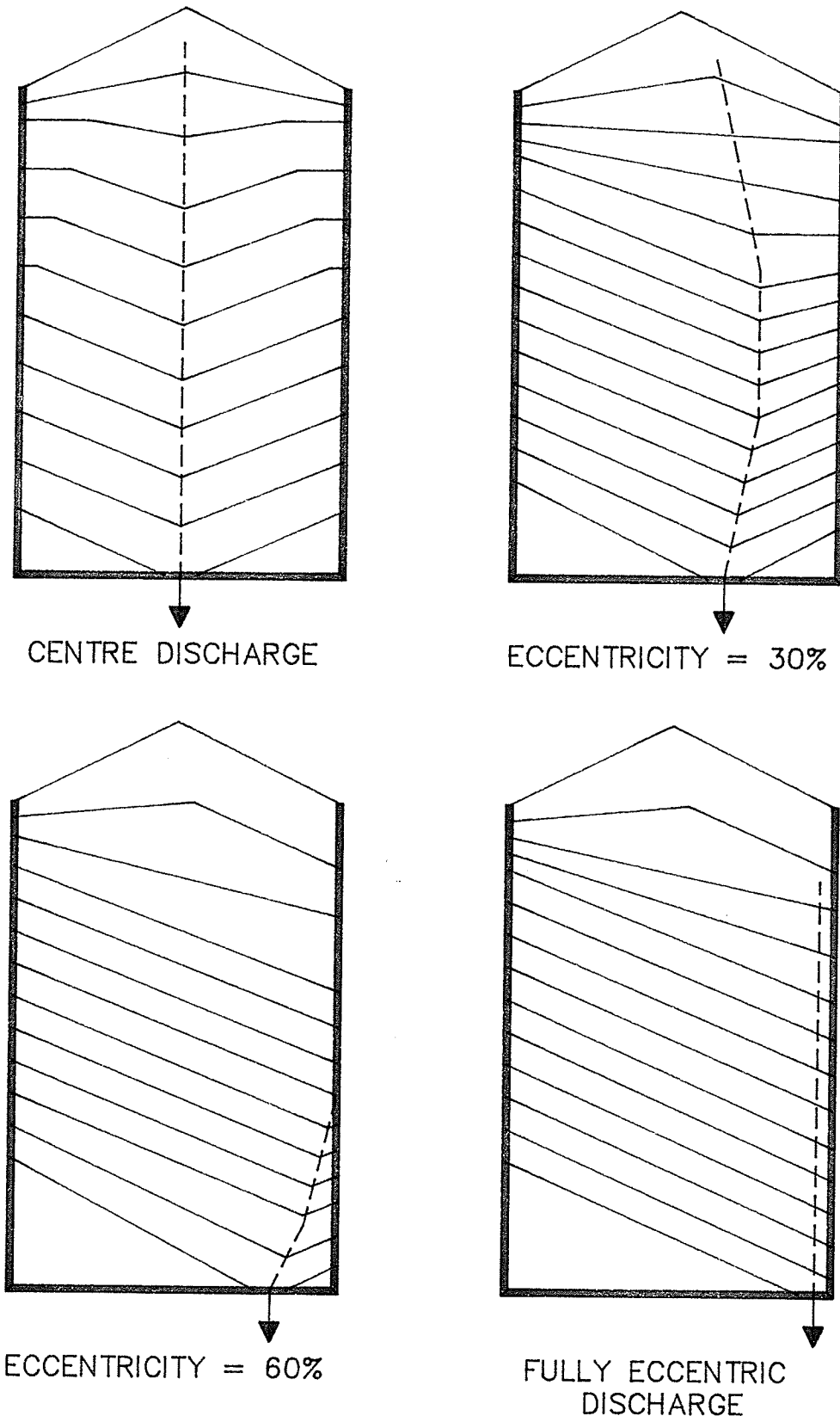


Figure 6.4 - Grain surface profiles for four discharge eccentricities

Offset flow channels were again apparent when the discharge outlet was located 300 mm from the bin centre (location E2). In these tests, however, the centre of the flow channel intersected the bin wall almost immediately and there was no zone of transitional flow. The centre of the funnel remained along the wall until it reached the 600 mm level at which point it moved inward and approached the discharge orifice. The angle of repose during flow was 22 degrees although it increased to 25 degrees in the dead zone region once free flow of grain ceased.

Using the fully eccentric discharge location (E3), funnel flow was apparent from the initiation of discharge. The flow channel developed directly above the outlet and rose vertically to the top of the grain mass directly along the wall. The angle of repose was somewhat higher at 24 degrees. This could have been caused by the greater width of one funnel side giving a larger mass of static grain to support the funnel.

### 6.3 DYNAMIC LOADS

#### 6.3.1 Load vs. Time Graphs

A series of graphs were made of the transducer loads vs. discharge time. Transducers #4 to #6 recorded total grain load and plots of the data generally took the form of downward sloping straight lines with constant slopes. Similar curves were illustrated earlier in Figure 6.2. With the 45 mm opening, signals were slightly noisier than with the larger orifices, but this was felt to be a result of the larger relative grain size vs. outlet diameter and was not considered to be a problem for this study.

Although the discharge gate incorporated an air cushion mechanism, a slight impact load was still measured by the total load transducers when the gate was opened. When the gate was closed, a larger impulse was recorded as a simple harmonic damped vibration. Series #3 tests had a number of cases where the discharge gate became stuck and had to be manually opened. If the suspended base table was not stopped from swinging after the gate was loosened, the effect was recorded on the total load measurements as an oscillatory wave with a frequency of approximately 20 Hz. This was probably the natural frequency of the system when the bin was loaded.

Figures 6.5 to 6.8 illustrate typical plots of the wall transducer loads for the 60 mm orifice at the four discharge locations. With a central discharge, each wall transducer recorded a sudden load increase at the start of grain flow. The loads then decreased uniformly along a slope similar to that of the total load vs. time curves. The maximum loads usually occurred within the first two seconds of discharge.

For the eccentric discharge tests, transducer #1, measuring the vertical load over wall section A, recorded an initial rapid rate of decrease in load. The rate soon decreased and the load then tended toward a nearly constant value. Wall transducers #2 and #3, on the other hand, recorded initial near instantaneous load increases. The loads increased further for a time and then decreased along a slope similar to that of the total load vs. discharge time curves.

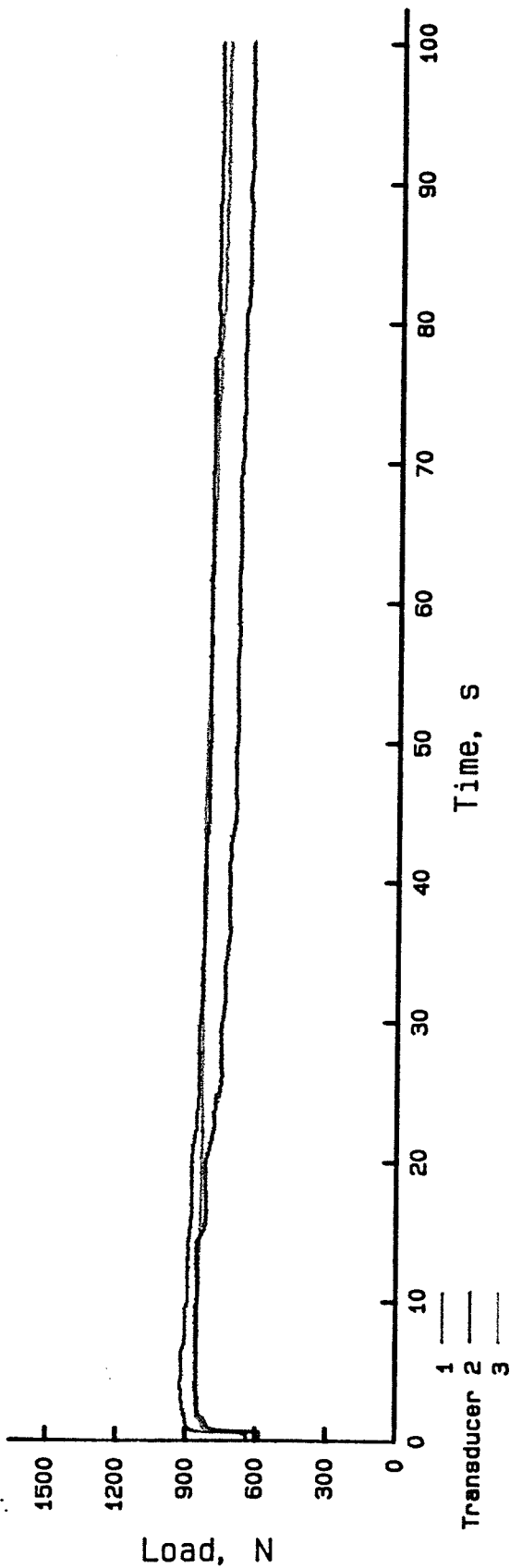


FIGURE 6.5 - WALL TRANSDUCER LOADS VS. DISCHARGE TIME - test D60E0S2

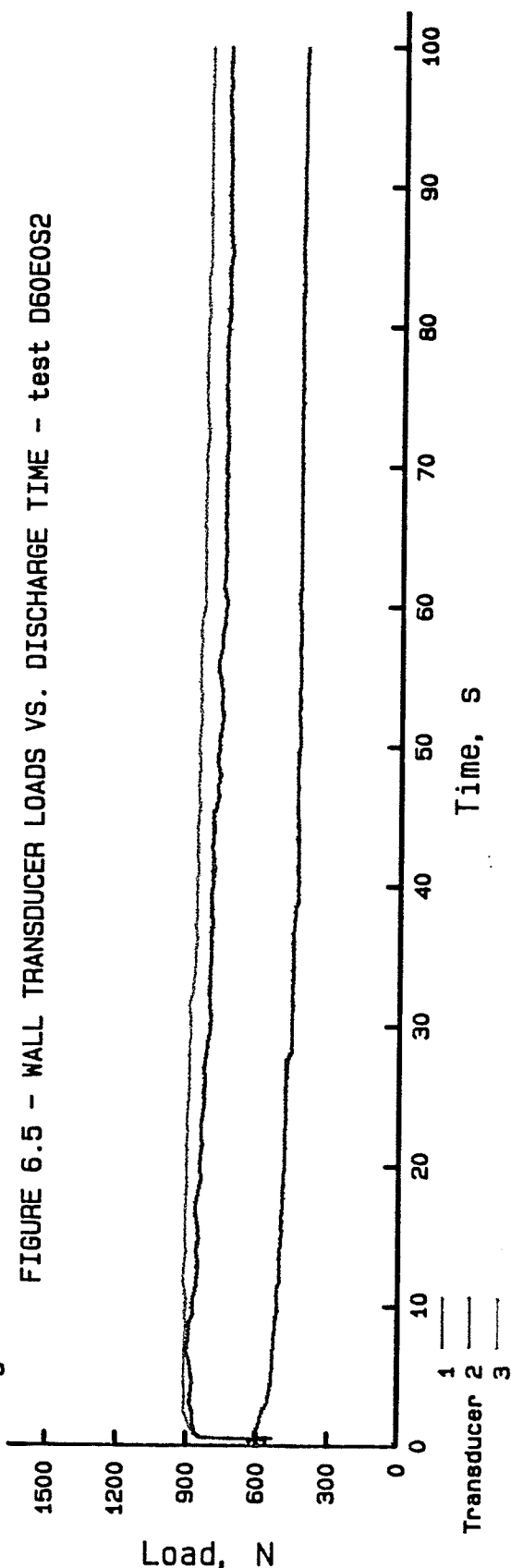


FIGURE 6.6 - WALL TRANSDUCER LOADS VS. DISCHARGE TIME - test D60E1S2

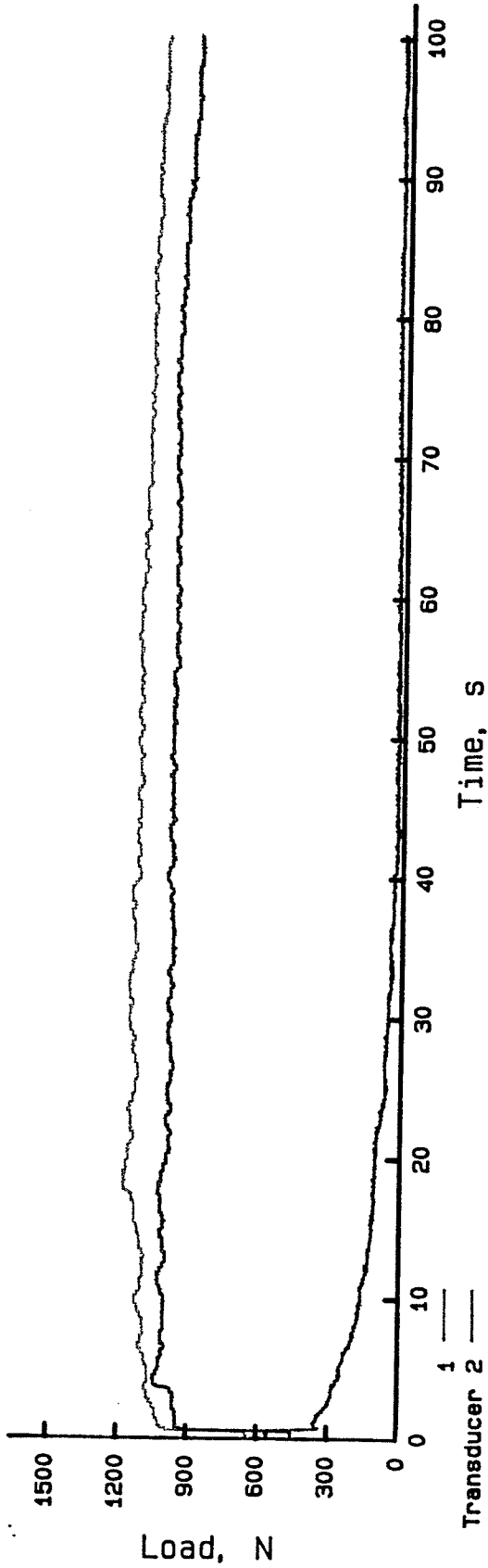


FIGURE 6.7 - WALL TRANSDUCER LOADS VS. DISCHARGE TIME - test D60E2S2

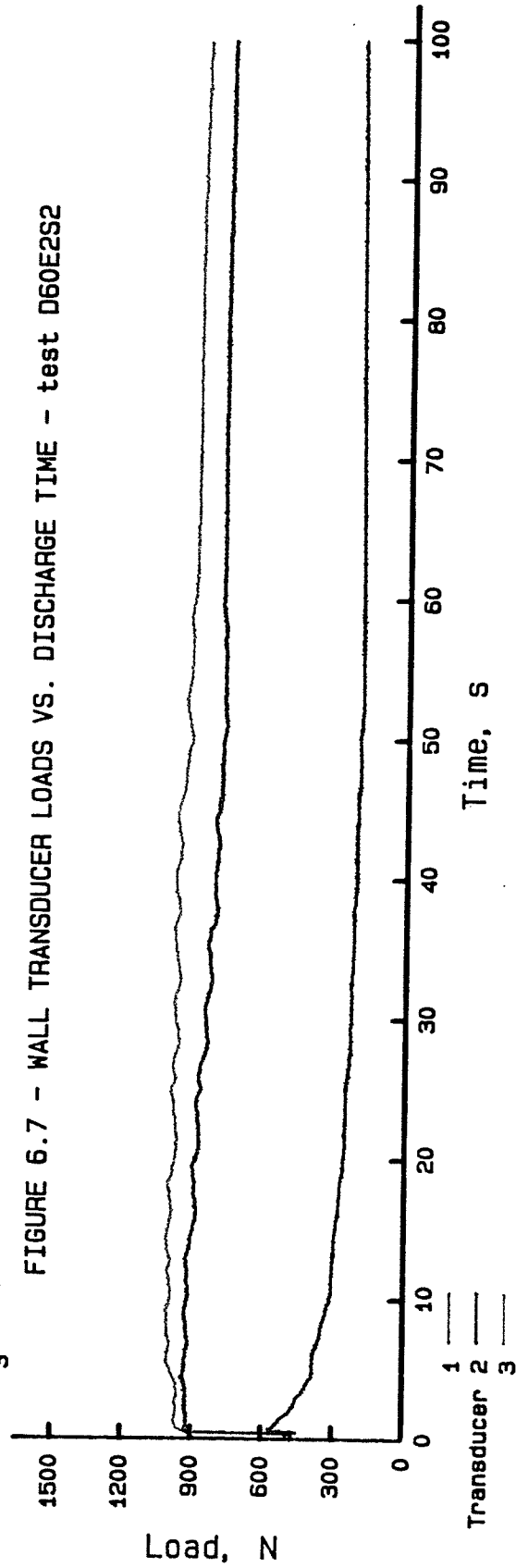


FIGURE 6.8 - WALL TRANSDUCER LOADS VS. DISCHARGE TIME - test D60E3S2

As expected, graphs of bin wall loads vs. time yielded patterns similar to the wall transducer loads. The only difference was that the magnitudes of the loads were more extreme, since the transducers tended to average load effects from the three wall sections. With eccentric discharge, wall section B and C loads were greater than corresponding transducer loads. Wall section A load was correspondingly lower.

The floor loads were calculated as functions of the six transducer loads using the transformation matrix developed earlier. The result was essentially the difference between total load and wall load. Total load vs. discharge time plotted as a straight line, thus the floor loads were basically mirror images of wall loads, with slightly higher magnitudes. Typical wall and floor load vs. discharge time curves for a 60 mm outlet at the four discharge locations are shown in Figures 6.9 to 6.12.

Each transducer reading had error and variation associated with it which was magnified six fold for each floor load. This caused the floor load curves to appear to be much noisier than the wall loads, which were functions of only three transducer values. Floor loads were plotted for each test, but as they offered little information beyond which could be obtained from wall loads, no further analysis of floor loads was done. Wall loads then became the sole focus for the remainder of the study.

In all tests, load on wall section C was about 6% higher than on wall section B. The difference was attributed to bin geometry and/or transducer location errors. As load trends were of more concern than absolute load magnitudes the effect was deemed to be negligible. The data thus confirmed the assumption of load symmetry on wall sections B and C, which were symmetrical relative to the discharge orifice.

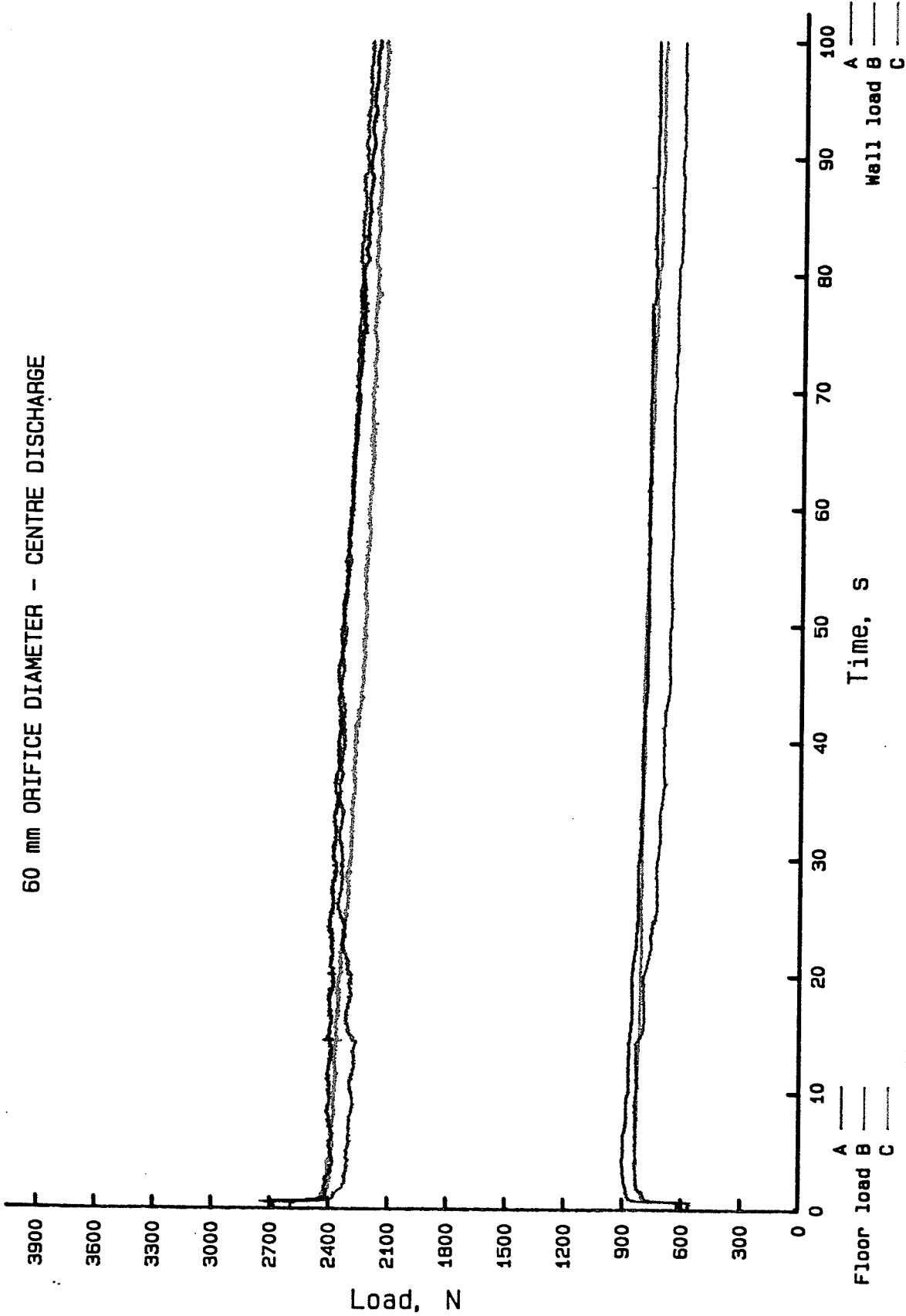


FIGURE 6.9 - FLOOR AND WALL LOADS VS. DISCHARGE TIME - test D60E0S2

60 mm ORIFICE DIAMETER - 30% ECCENTRIC DISCHARGE

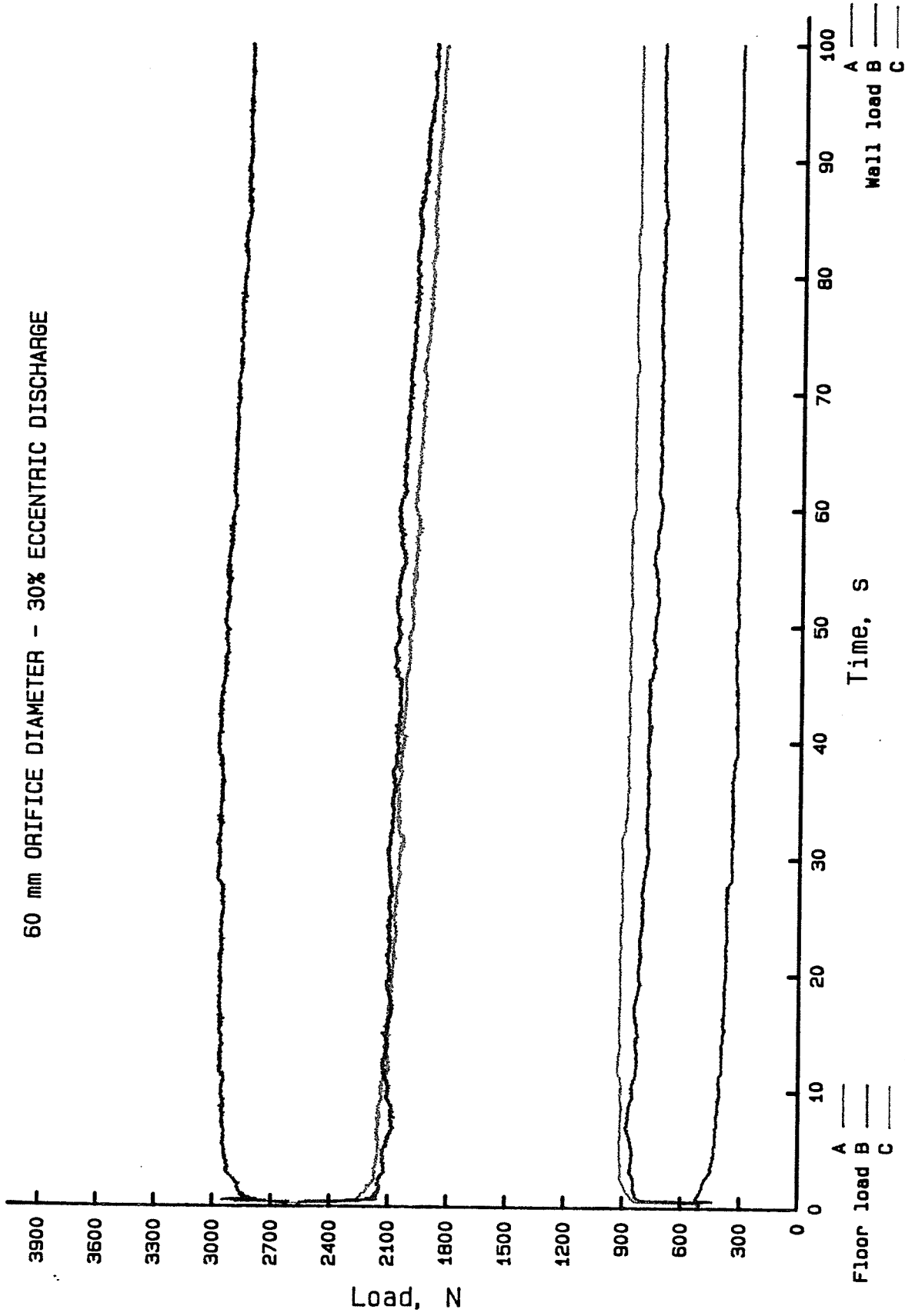


FIGURE 6.10 - FLOOR AND WALL LOADS VS. DISCHARGE TIME - test D60E1S2

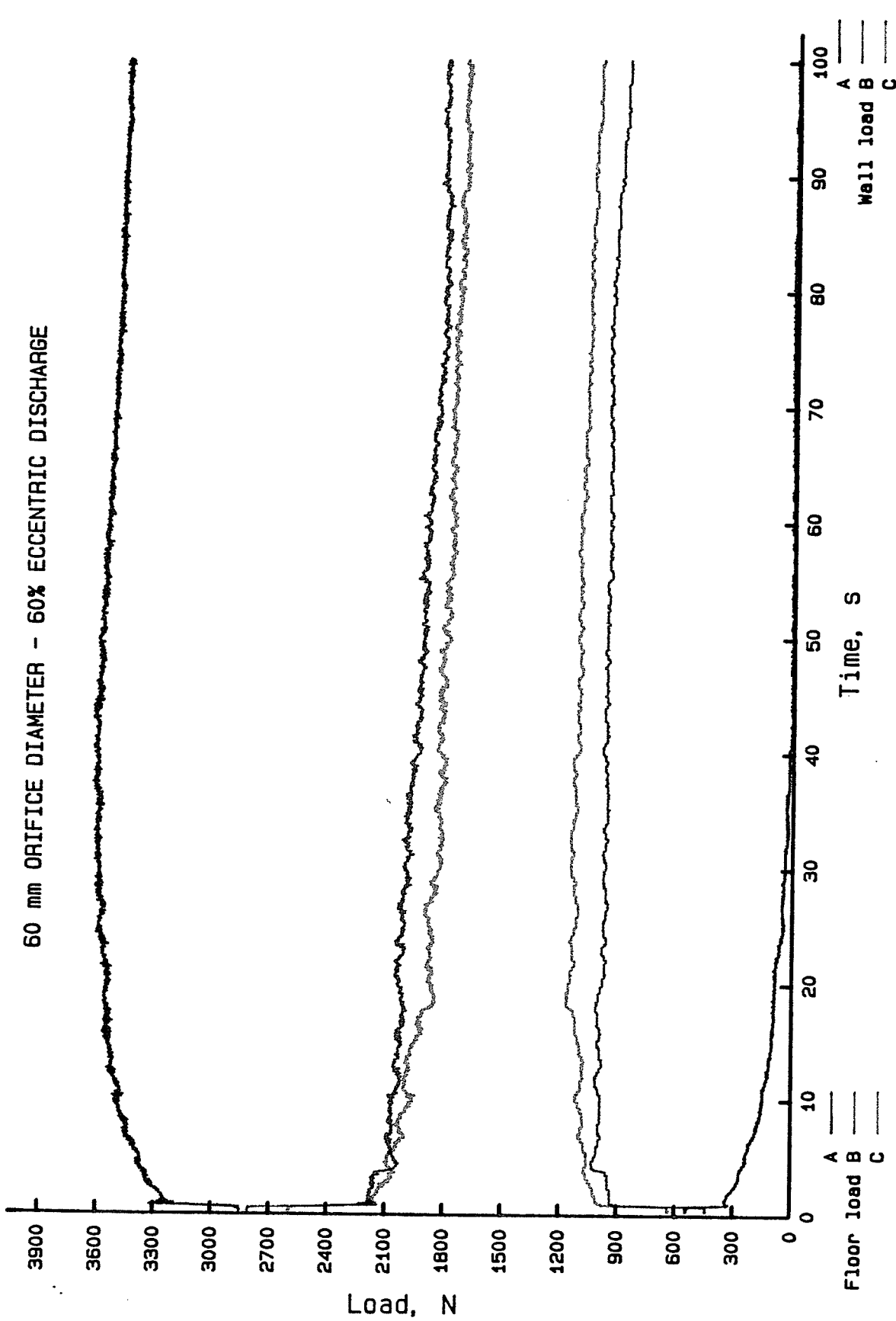


FIGURE 6.11 - FLOOR AND WALL LOADS VS. DISCHARGE TIME - test D60E2S2

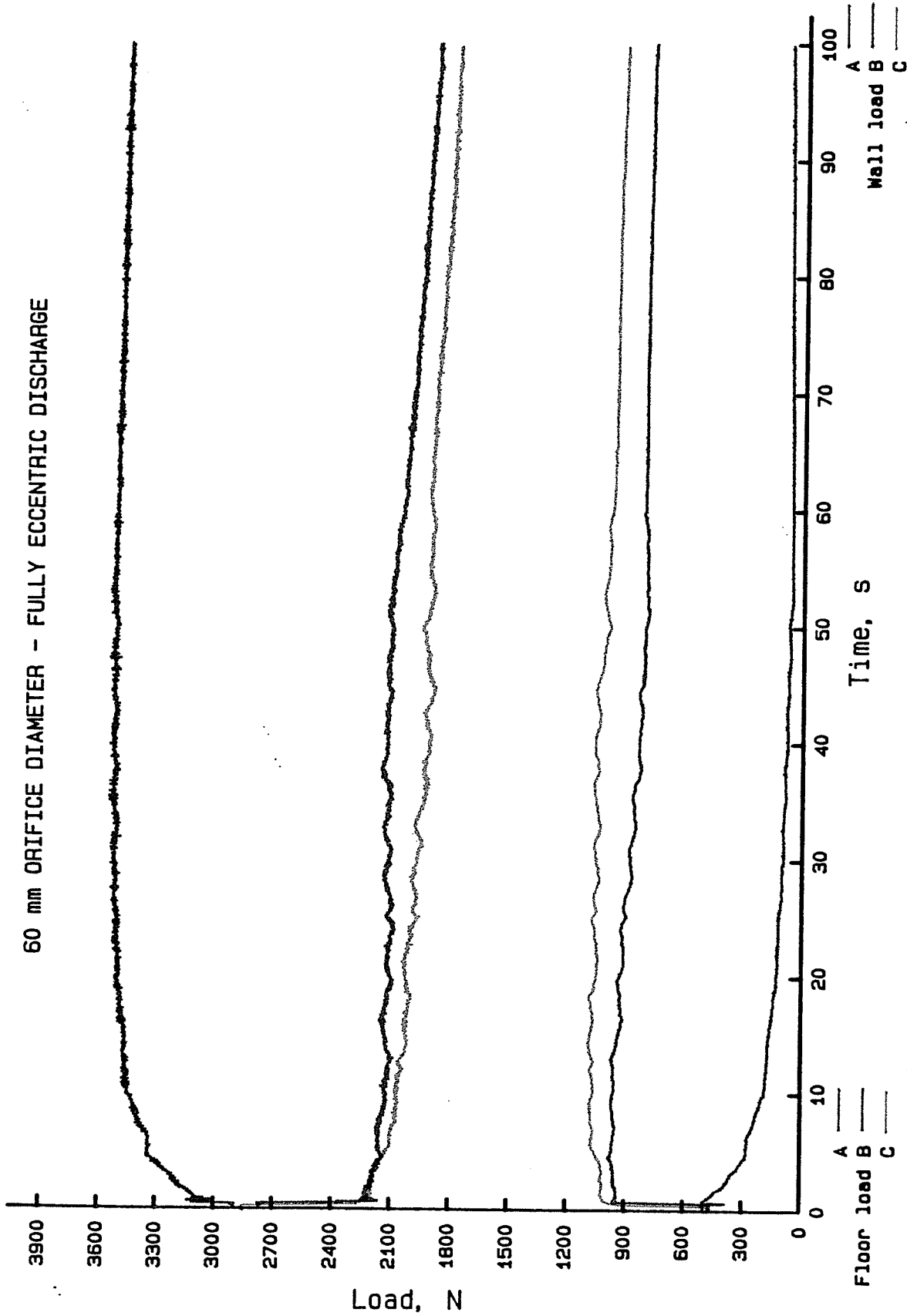


FIGURE 6.12 - FLOOR AND WALL LOADS VS. DISCHARGE TIME - test D60E3S2

The curves for the same discharge condition from all three test series showed excellent repeatability, although there appeared to be more noise and vibration in many of the series #3 tests. This was a direct result of the undamped vibration created in the system in trying to loosen the discharge gate which became stuck more frequently due to the increase in grain fines. After the discharge gate was loosened, an attempt was made to stop the base table/model bin system from swaying so that any abnormal vibrations and oscillations would be removed. Obviously, all vibrations were not removed. Although many of the load curves for test series #3 showed minor oscillations, general patterns were similar to the other series. For this reason, it was felt that the results were still usable and the tests were not repeated.

The first major analysis of the data with respect to the effects of flow rate and discharge location took the form of visual comparison of the load curves representing the sixteen test combinations. It was immediately obvious that there was a definite eccentricity effect which caused an increase in vertical load on wall sections B and C (hereafter referred to as the near wall) and a decrease in load on wall section A (hereafter referred to as the far wall).

The imbalance in the loading increased with higher eccentricity, but only to a point, since the effect was not as great with E3 tests (maximum eccentricity) as it was with E2 tests (60% eccentricity). The effect of the fully eccentric discharge was, however, greater than the effect of location E1 (30% eccentricity). This pattern repeated itself for all four flow rates with the overall magnitude of load increasing slightly with increased flow rate.

6.3.2 Peak Loads

Since the wall transducers sensed the average load over one-third sections of the bin wall circumference, no sudden pulsations or switch forces could be measured. It appeared that each wall load tended to a peak value and then decreased. This visual inspection of the data led to the computer search for the critical peak load on each wall for all sixteen test conditions and the peak delta, or load imbalance between the near and far wall when an eccentric discharge was used.

Near wall effects: Summaries of peak loads on wall sections B and C, as well as the peak average load on these two wall sections combined are listed below in Tables 6.1 to 6.3:

Table 6.1 - Peak Dynamic Load on Wall Section B, N

Distance of outlet from centre, mm	Series number	Outlet diameter, mm				Location means		
		45	60	75	100			
0	1	827	743	788	980	817		
	2	701	855	829	857			
	3	<u>753</u>	<u>786</u>	<u>798</u>	<u>892</u>			
	mean	760	795	805	910			
150	1	997	912	1042	1093	982		
	2	976	920	958	961			
	3	<u>918</u>	<u>980</u>	<u>981</u>	<u>1045</u>			
	mean	964	937	994	1033			
300	1	984	934	1085	1142	1066	Series	
	2	1038	1051	1113	1173		means	
	3	<u>1012</u>	<u>1054</u>	<u>1065</u>	<u>1143</u>		1	975
	mean	1011	1013	1088	1153		2	966
wall edge	1	859	1044	1043	1133	1035	3	984
	2	884	978	1090	1072			
	3	<u>992</u>	<u>1020</u>	<u>1088</u>	<u>1155</u>			
	mean	912	1020	1088	1120			
Flow rate means		912	941	994	1054	975		

Table 6.2 - Peak Dynamic Load on Wall Section C, N

Distance of outlet from centre, mm	Series number	Outlet diameter, mm				Location means	
		45	60	75	100		
0	1	743	792	799	903		
	2	830	853	731	809		
	3	<u>682</u>	<u>798</u>	<u>811</u>	<u>905</u>		
	mean	752	814	780	872	805	
150	1	985	1030	982	1160		
	2	997	952	1080	997		
	3	<u>1020</u>	<u>1064</u>	<u>1043</u>	<u>1077</u>		
	mean	1001	1015	1038	1078	1033	Series means
300	1	1116	1047	1204	1220		1 1019
	2	1179	1175	1206	1270		2 1029
	3	<u>1179</u>	<u>1194</u>	<u>1250</u>	<u>1231</u>		3 1057
	mean	1158	1139	1220	1240	1189	
wall edge	1	973	1104	1150	1088		
	2	1022	1089	1112	1154		
	3	<u>1147</u>	<u>1101</u>	<u>1198</u>	<u>1209</u>		
	mean	1047	1098	1153	1150	1112	
Flow rate means		989	1017	1048	1085	1035	

Table 6.3 - Peak Average Dynamic Load on Wall Sections B and C, N

Distance of outlet from centre, mm	Series number	Outlet diameter, mm				Location means	
		45	60	75	100		
0	1	762	767	786	936		
	2	747	850	778	824		
	3	<u>712</u>	<u>789</u>	<u>804</u>	<u>888</u>		
	mean	740	802	789	883	804	
150	1	974	963	1001	1123		
	2	975	928	1003	972		
	3	<u>953</u>	<u>990</u>	<u>1000</u>	<u>1046</u>		
	mean	967	960	1001	1047	994	Series Means
300	1	1049	987	1132	1177		1 989
	2	1085	1097	1152	1207		2 985
	3	<u>1086</u>	<u>1118</u>	<u>1144</u>	<u>1177</u>		3 1009
	mean	1073	1067	1143	1187	1118	
wall edge	1	909	1057	1094	1105		
	2	948	1021	1075	1099		
	3	<u>1062</u>	<u>1054</u>	<u>1140</u>	<u>1179</u>		
	mean	973	1044	1103	1128	1062	
Flow rate means		939	968	1009	1061	994	

An analysis of variance of the peak loads indicated both flow rate and eccentricity (location) effects at the 1% level of significance for all three peak load conditions. The F value for the location effect was approximately one order of magnitude greater than the F value for flow rate which indicated that although both effects were significant, the location effect was much more pronounced. The lack of any significant interaction between the main effects, even at the 5% level, was somewhat surprising, but this indicated the independence of the effects of flow rate and discharge location with respect to determination of the peak wall load.

A comparison of the mean peak values for the four outlet locations indicated that the load on the near wall increased in going from central discharge (E0) to partially eccentric discharge (E2), but then decreased slightly when the discharge outlet was located directly at the bin wall. On average, the increase of the dynamic load on wall sections B and C using an eccentric discharge as compared to a central discharge was 24% with E1 tests, 39% with E2 tests and 32% with the E3 tests. This trend agreed with the findings of Pieper (1969) and Thompson et al. (1985) who noted that semi or partially eccentric discharge outlets produced the greatest loads on the wall nearest the outlet.

The reasoning for this phenomenon was unclear but it was speculated that the overturning moment caused by the unsymmetrical flow pattern would be greater for partially eccentric discharge tests because of the tendency of the flow channel to lean towards the wall and then move inward again towards the discharge outlet. The change of direction of the flowing grain would manifest itself as a lateral force higher up the

bin wall and this could only be resisted by an increased vertical wall load. With a fully eccentric discharge outlet, the flow channel would locate itself directly at the wall. The flowing grain would not change direction since it could flow straight down to the outlet. This would reduce the lateral load and the overturning moment exerted on the near wall. The critical outlet location resulting in the greatest load might then be related to the flow pattern with respect to how and where it intersects the bin wall. Further study would be required to confirm or deny this hypothesis.

In comparing mean peak values for the four flow rates used, one could see that the load magnitude increased with flow rate. Although the effect was significant at the 1% level, the actual change in load was not that large. With a flow rate of 4.58 kg/s using the 100 mm orifice, the average peak load on wall sections B and C was only 12% larger than that obtained with a flow rate of 0.48 kg/s using the 45 mm orifice. This indicated that although the majority of the dynamic wall load was probably a quasi-static phenomenon caused by particle reorientation, there was also a true "dynamic" contribution probably caused by the momentum of the flowing grain mass. This dynamic force would be proportional to the flow rate since a higher flow rate would result in an increased momentum in the flow channel. Extrapolating the flow rate effect to full scale bins would appear reasonable since the relative momentum of the flowing grain would be similar. However, the preliminary nature of this study did not justify this conclusion.

Since there was no interaction term in the analysis of variance, a SAS (Anonymous, 1982) multiple regression procedure (PROC STEPWISE) was

performed using linear, squared and cubic terms in the model to generate an equation that could predict the peak average dynamic load on wall sections B and C as a function of flow rate and eccentricity. The best fit equation was a three variable model containing first order terms for flow rate and eccentricity and a third order term for eccentricity. The equation had an  $R^2$  value of 0.912 and was as follows:

$$P = 746 + 695 * E - 479 * E^3 + 27.2 * F \quad [6.2]$$

where P = peak average vertical load on wall sections B and C, N  
E = eccentricity,  $0 < E < 1$   
F = flow rate, kg/s

The equation suggested that even with a negligible flow rate and a central discharge, the dynamic load would be greater than the static load, which averaged 550 N immediately after the bin was filled. This 35% increase was the quasi-static effect caused by grain reorientation. The contribution by flow rate would be the true "dynamic" effect as discussed earlier. The location effect would become evident once the flow pattern developed.

This empirical equation was only valid for the model bin and grain used in the study and it should not be regarded as a prediction equation for bin design. It did, however, illustrate a fundamental relationship between flow rate, discharge location and the peak vertical load on the section of wall nearest the discharge outlet. The equation predicted that the maximum peak load would occur at an eccentricity of 70% for any flow rate. This highlighted, once more, the fact that fully eccentric discharge does not result in the greatest wall load as most design codes have suggested. The critical discharge location would probably vary with grain characteristics and the bin H/D ratio.

Imbalance effects: With the centre unloading tests, peak loads on wall section A were similar to those on walls B and C, as expected, due to symmetry. In the eccentric discharge tests, wall load A decreased, so a peak load analysis was of little concern. In a few tests (D45E2S2, D60E2S2 and all E2 tests in series #3) the far wall load decreased to below zero indicating that the wall was actually in a state of tension. This effect was predicted by Bervig et al. (1977) using a finite element analysis and its cause was explained by the large overturning moment created by the imbalance in loading between the near and the far walls. Delta, the magnitude of this imbalance, was calculated as the difference between the average vertical load on wall sections B and C, and the load on wall section A. A summary of the peak deltas is listed in Table 6.4. Analysis of variance of the deltas indicated location and series effects at the 1% level of significance, but no flow rate effect was apparent.

Table 6.4 - Peak Dynamic Load Imbalance Between the Near and Far Wall Sections, N

Distance of outlet from centre, mm	Series number	Outlet diameter, mm				Location means		
		45	60	75	100			
150	1	535	554	576	565	593	Series means	
	2	636	514	635	507			
	3	618	657	661	662			
	mean	596	575	624	578			
300	1	900	720	901	907	996	1	722
	2	1047	1051	1008	1032		2	825
	3	1087	1075	1151	1069		3	905
	mean	1011	949	1020	1003			
wall edge	1	621	704	849	763	863		
	2	825	888	885	874			
	3	954	880	975	1076			
	mean	800	846	903	904			
Flow rate means		803	790	849	828	817		

As discussed previously, the flow rate effect on wall sections B and C was independent of the eccentricity effect and it appeared to be associated with the momentum of flowing grain. Since the entire grain mass was affected by the discharge condition, a reasonable assumption could be made that this "dynamic" effect occurred evenly around the bin circumference. Since delta was a measure of the difference between the loads on the near and far walls, any increased loading associated with higher flow rates would be cancelled out and flow rate would thus be insignificant as far as the load imbalance was concerned.

A flow rate effect did seem apparent, however, when a settling time was allowed. Test D60E1S0 had a delta 13% greater than test D45E1S0 even though the static load condition was identical prior to discharge. Test D75E1S0 had an even greater 37% increase compared to the test using the 45 mm opening. Although this effect appeared quite pronounced, no firm conclusions about its existence could be made since only three settling tests were performed.

The significant location effect on delta was anticipated in light of the previous analysis on the near wall. By extrapolating regression equation [6.2] using pseudo-eccentricity values in the range  $-1 < E < 0$ , loads on the far wall could possibly be predicted. This suggested that far wall load decrease was simply the mirror image of near wall load increase. Although the extrapolation assumed a one-to-one correlation, a less restrictive assumption suggested that pattern of load change as opposed to the exact magnitude might be inversely proportional between opposite walls. This led to a hypothesis that altering the location of the discharge outlet might simply cause redistribution of the total

dynamic wall load as opposed to increasing it. Examination of the ratios of total wall load to total floor load at the peak delta conditions confirmed this hypothesis since for a given flow rate, the wall/floor load ratios were constant for all discharge locations used. This trend was in fact observed for all peak load conditions.

The discovery of a block effect was somewhat perplexing since it was not found to be significant in the analysis of variance of near wall loads only. It was concluded, therefore, that variation between series must have been contributed to by far wall loads. The increasing mean delta between series indicated that average load on wall section A must have been decreasing with each test series. Visual inspection of the graphed data and investigation of actual wall loads used to calculate delta confirmed that load on wall section A decreased while average loads on wall sections B and C remained fairly consistent between replications.

A decrease in wall load with each test series was the same trend observed with the static data. Since the funnel flow pattern with the eccentric tests resulted in grain against wall section A being in the static part of the funnel, it would be reasonable to assume that the majority of the vertical load on wall section A would be generated by static friction and thus proportional to the friction coefficient  $\mu'$ . As discussed in the static load section,  $\mu'$  decreased during testing due to surface conditioning of the bin wall. This, then would account for the decrease in load on wall section A.

Although the quasi-static effect would also occur on the near wall sections not in contact with the flowing grain, a dynamic friction load

would occur on the portions of the wall intersecting the flow channel. An outward lateral force would also have to be resisted as the flow channel leaned toward the near wall section. These dynamic factors contributing to the overturning moment would be independent of surface conditioning effects and thus the load on the near wall would be much more constant.

This hypothesis was further supported by results from the settling tests. Although dynamic load patterns on near wall sections indicated no effect of grain settlement with respect to load magnitude, dynamic load on the far wall section was lower than that for the identical condition in the main test series which allowed no settling time. The graphs in Figures 6.13 and 6.14 clearly illustrate this pattern.

A change in shape of the load vs. time curve for wall section A was also observed in the settling test results. Once discharge was initiated, load on wall section A decreased almost instantaneously to a minimum and then recovered slightly, whereas in the dynamic test series it decreased relatively more gradually over a number of seconds to its limiting value. This may have been the result of a greater degree of grain reorientation in going from a no-flow to a flow condition, since the grain mass had settled to a much more stable position after the settling period. Again, as only three settling tests were undertaken this explanation was only speculative. It appeared then that for eccentric discharge tests, the dynamic load on the far wall was very much affected by static load influences whereas the dynamic load on the near wall was only dependent on dynamic flow considerations.

60 mm ORIFICE DIAMETER - 30% ECCENTRIC DISCHARGE

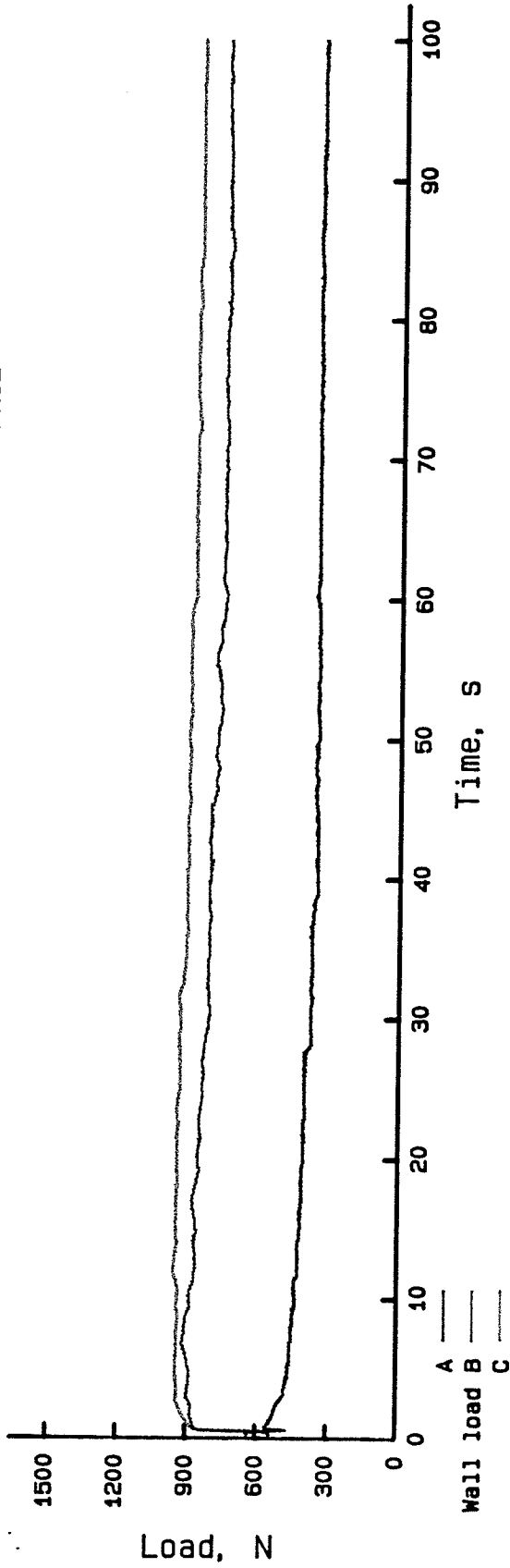


FIGURE 6.13 - WALL LOADS VS. DISCHARGE TIME - dynamic test D60E1S2

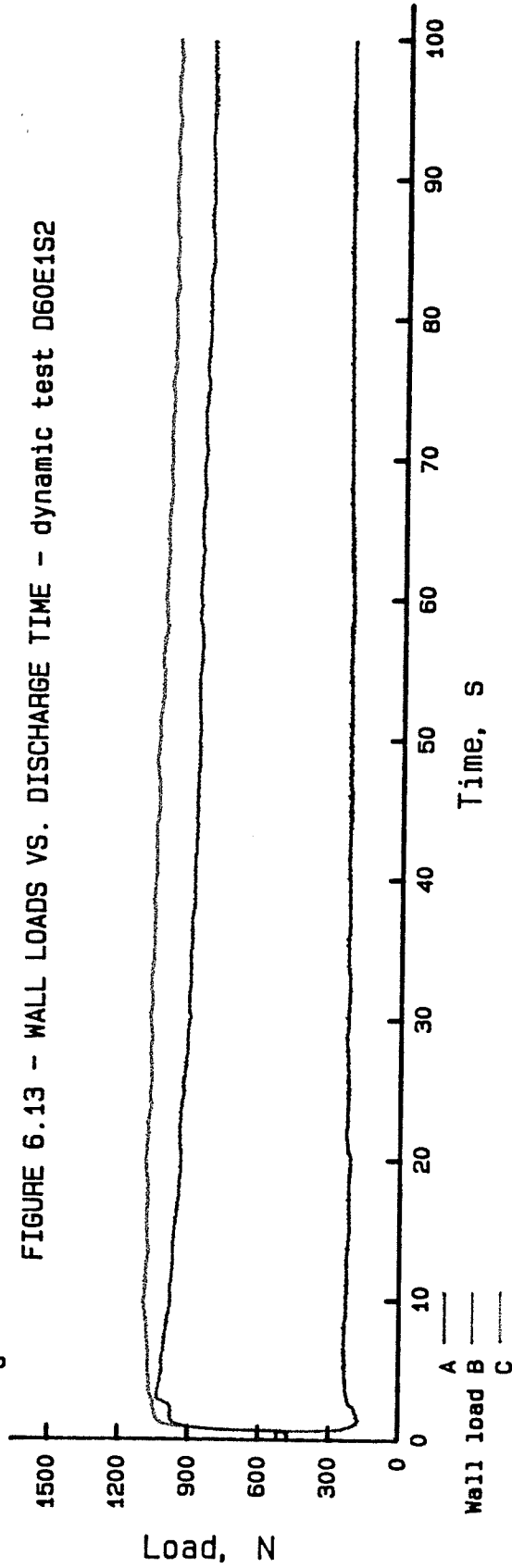


FIGURE 6.14 - WALL LOADS VS. DISCHARGE TIME - settling test D60E1S0

### 6.3.3 Dynamic/Static Ratios (DSR)

In much of the literature, the increased bin loads associated with grain discharge were reported in terms of a ratio of dynamic load to static load. This technique allowed results obtained using various model sizes to be compared, in addition to giving an indication of the magnitude of the dynamic effects relative to the static forces. An analysis of DSR's was undertaken and a summary of the results for the peak average ratio for wall sections B and C is listed in Table 6.5.

Table 6.5 - Peak Average Dynamic/Static Ratio on Wall Sections B and C

Distance of outlet from centre, mm	Series number	Outlet diameter, mm				Location means	
		45	60	75	100		
0	1	1.18	1.31	1.25	1.55		
	2	1.52	1.49	1.60	1.77		
	3	<u>1.25</u>	<u>1.49</u>	<u>1.63</u>	<u>1.66</u>		
	mean	1.32	1.43	1.49	1.66	1.47	
150	1	1.72	1.79	1.88	1.73		
	2	1.53	1.69	1.76	1.75		
	3	<u>1.97</u>	<u>2.15</u>	<u>1.84</u>	<u>1.94</u>		
	mean	1.74	1.88	1.82	1.81	1.81	Series means
300	1	1.88	1.66	2.26	1.93		1 1.68
	2	2.21	2.01	2.05	2.27		2 1.88
	3	<u>2.19</u>	<u>2.29</u>	<u>1.99</u>	<u>1.99</u>		3 1.97
	mean	2.09	1.99	2.08	2.07	2.06	
wall edge	1	1.40	1.80	1.72	1.74		
	2	1.91	2.20	2.21	2.12		
	3	<u>2.14</u>	<u>1.85</u>	<u>2.52</u>	<u>2.72</u>		
	mean	1.82	1.95	2.15	2.19	2.03	
Flow rate means		1.74	1.81	1.89	1.93	1.84	

Analysis of variance of the results indicated a significant block effect at the 1% level of significance. The average DSR was 1.68 for series #1, but this increased to 1.97 in series #3. The increase was

reasonable and basically highlighted the fact that static loads were decreasing with each series due to surface conditioning of the wall.

As far as treatments were concerned, only the location effect was significant at the 1% level. A flow rate effect was undetectable, due to an increase in the experimental error, which accounted for 25% of the total variation in the DSR analysis, but only 6%, on average, in the analysis of peak loads. By using two sets of readings to generate the DSR values, the errors associated with both the dynamic and static readings were pooled. This caused F values in the ANOVA table to be reduced and consequently, the ANOVA test had less ability to detect significant treatment effects. The ratios between F values for flow rate and location were, however, relatively the same as those generated in the analysis of peak loads so the relative significance of the two effects was still apparent.

Since the static readings were taken immediately after the bin had been filled, the grain was at a random level of reorientation. If a settling time of 24 h or more was allowed before static readings were taken, a much more uniform state of settling would have been obtained among the various tests. With proper surface conditioning and grain quality control, experimental error could be reduced and DSR analysis would have a more powerful comparison ability.

#### 6.3.4 Time of Peak Load

Visual observation of the graphed data and inspection of the peak load results suggested there might be a relationship between the two major test variables, flow rate and eccentricity, and the time required

to reach the peak loads. A summary of the time values for the peak average load on wall sections B and C, listed in Table 6.6, indicated that there was considerable variation in the data between replicates. Analysis of variance of these results, however, indicated significant flow rate, location and interaction effects, all at the 1% level.

Table 6.6 - Time of Peak Average Dynamic Load on Wall Sections B and C, seconds after start of discharge

Distance of outlet from centre, mm	Series number	Outlet diameter, mm				Location means	
		45	60	75	100		
0	1	11.49	4.17	2.64	0.39		
	2	2.31	2.65	1.75	0.83		
	3	<u>5.86</u>	<u>9.47</u>	<u>1.71</u>	<u>1.25</u>		
	mean	6.55	5.43	2.03	0.82	3.71	
150	1	7.91	5.86	2.07	1.56		
	2	8.13	6.33	1.17	1.05		
	3	<u>7.57</u>	<u>2.51</u>	<u>4.46</u>	<u>0.97</u>		
	mean	7.87	4.90	2.57	1.19	4.13	Series means
300	1	29.47	9.72	5.71	1.90		1 7.47
	2	27.51	17.33	8.38	5.04		2 7.37
	3	<u>45.27</u>	<u>14.00</u>	<u>10.54</u>	<u>1.15</u>		3 9.30
	mean	34.08	13.68	8.21	2.70	14.67	
wall edge	1	27.04	2.08	6.76	0.78		
	2	17.99	8.92	7.48	1.10		
	3	<u>33.24</u>	<u>8.60</u>	<u>1.24</u>	<u>0.88</u>		
	mean	26.09	6.53	5.16	0.92	9.68	
Flow rate means		18.65	7.64	4.49	1.41	8.05	

The location effect could be seen in observing the mean times for the four locations, which followed a pattern similar to that for the peak loads. On average, the peak loads were reached the fastest with centre unload, with the time required increasing with eccentricity to location E2 and then decreasing slightly again with a fully eccentric discharge. The reason for this was unclear, but a possible explanation

could be made based on the development of the flow patterns. It was reasoned earlier that overturning moments could be generated by unsymmetrical flow patterns which tended to lean towards the near wall. The flow patterns resulting in larger overturning moments might have required more grain to discharge and thus, they took a longer time to develop.

The flow rate effect was logical since one would expect the peak load to be reached sooner with a higher rate of grain discharge. This was clearly indicated by the decreasing mean time for each increasing flow rate. The significance of the interaction term highlighted the fact that a change in flow rate affected the time more so at higher eccentricities than at lower ones. The reasoning for this trend was again unclear.

An analysis of the time required to reach the peak deltas was also made. There was considerable variation in the time results, however, so only the flow rate effect was noted as being significant, although the pattern of the location effect appeared to be similar to that observed for the peak load times. The high degree of variability in the results made it difficult to make any definite conclusions. One interesting observation to be made was that it took much longer to reach the peak delta than it did to reach the peak load on the near wall; on average, three to four times as long. This was due to the relatively slow decrease in the load on wall section A. With settling, the load on wall section A was shown to change nearly instantaneously, so the time to reach the peak delta would most likely decrease as well.

6.3.5 Weight of Discharge at Peak Load

To account for the flow rate effect in the previous time analysis, an analysis was made of the weight of grain discharged at the peak load conditions. Results for weight of discharge at the peak average dynamic load on wall sections B and C are listed in Table 6.7.

Table 6.7 - Discharge Weight at Peak Average Dynamic Load on Wall Sections B and C, N

Distance of outlet from centre, mm	Series number	Outlet diameter, mm				Location means		
		45	60	75	100			
0	1	52	43	64	20	40		
	2	14	29	34	31			
	3	<u>22</u>	<u>107</u>	<u>18</u>	<u>50</u>			
	mean	29	60	39	34			
150	1	23	56	40	0	44		
	2	44	74	17	39			
	3	<u>35</u>	<u>53</u>	<u>94</u>	<u>51</u>			
	mean	34	61	50	30			
300	1	97	105	46	79	144	1	60
	2	126	197	180	237		2	87
	3	<u>219</u>	<u>158</u>	<u>223</u>	<u>59</u>		3	87
	mean	147	153	150	125			
wall edge	1	130	14	150	40	84		
	2	86	101	144	44			
	3	<u>146</u>	<u>92</u>	<u>29</u>	<u>33</u>			
	mean	121	69	108	39			
Flow rate means		83	86	87	57	78		

Analysis of variance of the weight of discharge results indicated only a location effect. At the peak average load on wall section B and C, the weight of discharge mean was very nearly equal, for the four flow rates used. There was more random variation among the mean results at the separate peak loads on the two wall sections. In all cases however,

the discharge weight means were within the same order of magnitude, even though the flow rates varied almost 10 fold. This appeared to indicate that the peak loads occurred when a set amount of grain discharged from the bin, regardless of the rate at which it discharged. Although this conclusion was based on data with a high degree of variability, it seemed reasonable, since the flow pattern was independent of flow rate. Once the given amount of grain had discharged, the flow pattern would be such that the maximum load condition would be obtained. Since a flow rate effect was observed in the analysis of peak loads, it could be suggested that although the maximum load was reached after the same volume of grain discharged, an increase in rate added to the magnitude of the load due to the increased momentum of the faster moving grain.

## CHAPTER VII

### CONCLUSIONS

For a smooth steel wall model grain bin of the type used in these tests, the following conclusions can be drawn:

1. Static vertical wall load decreases over time to an apparent limiting value with most of the decrease occurring within the first 24 h after filling. Load shift occurs as a series of sudden step changes interspersed between periods of constant load.
2. Significant load transfer from the floor to the walls is achieved with discharge of only a small amount of grain from the bin. The fact that this effect can be "locked-in" once discharge is stopped supports the view that dynamic load increase is, at least in part, a quasi-static phenomenon caused by particle reorientation.
3. With partially eccentric discharge, the centre of the flow channel leans towards the near wall and can intersect the wall even though the discharge orifice is located away from the wall edge.
4. Eccentric discharge causes redistribution of wall loads but it does not alter the total dynamic wall load. As the discharge orifice is moved away from the bin centre, the load on the near wall increases and load on the far wall correspondingly decreases. With some eccentricities, the far wall can actually be in tension.

5. Partially eccentric discharge is more critical than fully eccentric discharge. With the model bin used in this study, the maximum load shift condition was predicted to occur at an eccentricity of 70%.
6. Discharge rate is a power function of orifice diameter and it is unaffected by the eccentricity of the discharge location.
7. Vertical wall load increases linearly with discharge rate and the effect appears to be a true "dynamic" phenomenon over and above the quasi-static effect of particle reorientation. A 9.5 fold increase in flow rate increased the total wall load by approximately 12%.
8. Dynamic load on the far wall is more affected by grain settling and surface conditioning than is dynamic load on the near wall.
9. For a given eccentricity, peak dynamic load on the near wall appears to occur when a given amount of grain has discharged, regardless of the rate at which it discharges.

CHAPTER VIII  
RECOMMENDATIONS

1. A full series of tests should be performed allowing for at least a 24 h settling time between filling and discharge stages, as this probably better represents the true grain storage condition.
2. Additional test series should be performed using a corrugated bin, H/D ratios greater than 1.5, and other grains such as flax and canola to increase the knowledge of flow rate and eccentricity effects and pave the way toward eventual full-scale testing.
3. The use of piezo-electric film as a pressure sensing medium should be investigated as an alternative to strain gages.
4. If strain gages are used to measure bin wall stress/strain, it is recommended that a wall thickness no greater than 0.5 mm be used with gages mounted to both the inside and outside surface of the wall to account for bending effects.
5. Particular attention should be paid to the test bin manufacturing details to ensure sufficient cross-sectional roundness. The use of one vertical welded seam is recommended.
6. Slide gate modifications should be made to prevent it from binding.
7. To minimize the effects of mechanically damaged grain, a larger supply of grain should be used.

## LIST OF REFERENCES

- American Concrete Institute. 1968. Bin wall design and construction. ACI Journal. Proceedings. 65(7):499-506.
- American Concrete Institute. 1969. Discussion of "Bin wall design and construction." ACI Journal. Proceedings. 66(3):211-218.
- American Concrete Institute. 1975. Recommended Practice for Design and Construction of Concrete Bins, Silos, and Bunkers for Storing Granular Materials (ACI 313-77) and Commentary. American Concrete Institute. Detroit, Michigan. 40pp.
- Anonymous. 1982. SAS User's Guide: Statistics. SAS Institute Inc. Box 8000. Cary, North Carolina. 27511.
- Barre, H. 1958. Flow of bulk granular materials. Agric. Eng. 39:534-539.
- Bervig, D., A. Wiley and T. Sutton. 1977. Influence of static and dynamic asymmetric loading conditions on silo design. Proc. ASME Design Eng. Tech. Conference. September 26-30. Chicago, Illinois. Paper No. 77-DET-145. 8pp.
- Bickert, W.G. and F.W. Bakker-Arkema. 1968. Inconsistencies among friction data for grains. Quarterly Bulletin of the Michigan Agricultural Experiment Station. 50(4):591-598.
- Bickert, W.G. and F.H. Buelow. 1966. Kinetic friction of grains on surfaces. Trans. ASAE. 9(1):129-134.
- Bishara, A.G., S.F. Ayoub and A.S. Mahdy. 1983. Static pressures in concrete circular silos storing granular materials. ACI Journal. Title No. 80-21. May-June:56-62.
- Bovey, H.T. 1904. Experiments on grain pressures in deep bins and the strength of wooden bins. Eng. News. 52(2):32-34.
- Britton, M.G. 1977. State of the art - predicting static pressure in grain bins. Paper presented at the 1977 ASAE Winter Meeting. Chicago, Illinois. December. Paper No. 77-4501. 8pp.
- Britton, M.G. and C.R. Hawthorne. 1984. Dynamic behavior of wheat in a lamellar bin. Paper presented at the 1984 ASAE North Central Region Meeting. Morris, Minnesota. October. Paper No. NCR 84-501. 10pp.
- Britton, M.G. and R.B. Rowley. 1986. Dynamic load research using lamellar bins. Paper presented at the 1986 ASAE Summer Meeting. San Luis Obispo, California. June. Paper No. 86-4072. 9pp.

- Britton, M.G. and P.A. Versavel. 1985. Bin wall configuration - bulk wheat interaction. Paper presented at the 1985 ASAE Summer Meeting East Lansing, Michigan. June. Paper No. 85-4001. 14pp.
- Brubaker, J. and J. Pos. 1965. Determining the static coefficient of friction of grain on structural surfaces. Trans. ASAE. 8(1):53-55.
- Bucklin, R.A., I.J. Ross and G.M. White. 1983. Influence of grain pressure on the buckling loads of thin walled bins. Paper presented at the 1983 ASAE Summer Meeting. Bozeman, Montana. June. Paper No. 83-4005. 37pp.
- Caughey, R.A., C.W. Toolles and A.C. Scheer. 1951. Lateral and vertical pressure of granular material in deep bins. Iowa Eng. Expt. Station Bulletin No. 172. 22pp.
- Colijn, H. and I.A. Peschl. 1981. Non symmetrical bin flow problems. Bulk Solids Handling. 1(3):377-384.
- Collins, R.V. 1963. Determining pressures in cylindrical storage structures. Trans. ASAE. 6(2):98-101,103.
- Cook, A. 1961. Flow of granular material in bins. Paper presented at the 1961 ASAE Winter Meeting. Chicago, Illinois. Paper No. 61-905. 8pp.
- Cowin, S.C. 1977. The theory of static loads in bins. Trans. ASME. J. App. Mech. (E). 44(3):409-412.
- Deutsch, G.P. and D.H. Clyde. 1967. Flow and pressures of granular materials in silos. ASCE. J. Eng. Mech. Proceedings Paper 5660. 93(EM6):103-125.
- Deutsch, G.P. and L.C. Schmidt. 1969. Pressures on silo walls. Trans. ASME. J. Eng. Ind. (B). 91(1):450-455 with discussion 455-459.
- Dubynin, N.G. 1968. Kinematics and dynamics of bulk solids during discharge from orifices. Paper presented at the Symposium on Flow of Solids. October 20-23. Boston, Massachusetts. ASME publication No. 68-MH-27. 5pp.
- Fankhauser, C.D. 1977. Analysis and design of corrugated grain tanks. Paper presented at the 1977 ASAE Winter Meeting. Chicago, Illinois. December. Paper No. 77-4502. 15pp.
- Garg, R. and S. Gopalakrishnan. 1974. An experimental investigation of wall loads in wheat silos. Indian Concrete Journal. 48:308-313.
- Gaylord, E.H. and C.N. Gaylord. 1984. Design of Steel Bins for Storage of Bulk Solids. Prentice-Hall. New Jersey. 468pp.
- Griffith, J. 1983. Analysis of a silo failure. Proc. 2nd Int. Conf. Design of Silos for Strength and Flow. November 7-9. Stratford-on-Avon Hilton. Powder Advisory Centre. pp14-23.

- Haaker, G. and O. Scott. 1983. Wall loads on corrugated steel silos. Proc. 2nd Int. Conf. Design of Silos for Strength and Flow. November 7-9. Stratford-Upon Avon Hilton. Powder Advisory Centre. pp480-503.
- Harms, H.P. and G.M. Henry. 1976. Model studies of the effect of off centre unloading of grain bins. Paper presented at the 1976 CSAE Annual Meeting. Halifax, Nova Scotia. Paper No. 76-216. 13pp.
- Haydl, H.M. 1983. Additional forces in circular silo walls due to eccentric discharge. Proc. Inst. Civ. Eng. (London). 75(2):307-310.
- Isaacson, J.D. and J.S. Boyd. 1965. Mathematical analysis of lateral pressures in flat-bottomed deep grain bins. Trans. ASAE. 8:358-360,364.
- Jenike, A.W. 1954. Better design for bulk handling. Chem. Eng. 61:175-180.
- Jenike, A.W. 1967. Denting of circular bins with eccentric drawpoints. J. Str. Div. ASCE. Proc. Paper No. 5087. 93(ST1):27-35.
- Jenike, A.W. and J.R. Johanson. 1968. Bin loads. J. Str. Div. ASCE. Proc. Paper 5916. 94(ST4):1011-1041.
- Jenike, A.W. and J.R. Johanson. 1969. On the theory of bin loads. Trans. ASME. J. Eng. Ind. (B). 91(2):339-344.
- Jenike, A.W., J.R. Johanson and J.W. Carson. 1973a. Bin loads - part 2: Concepts. Trans. ASME. J. Eng. Ind. (B). 95(1):1-5.
- Jenike, A.W., J.R. Johanson and J.W. Carson. 1973b. Bin loads - part 3: Mass-flow bins. Trans. ASME. J. Eng. Ind. (B). 95(1):6-12.
- Jenike, A.W., J.R. Johanson and J.W. Carson. 1973c. Bin loads - part 4: Funnel-flow bins. Trans. ASME. J. Eng. Ind. (B). 95(1):13-16.
- Jenkyn, R.T. 1978. Calculation of material pressures for the design of silos. Proc. Inst. Civ. Eng. (London). 65(2):821-838.
- Jofriet, J.C., B. LeLievre and T.F. Fwa. 1977. Friction model for finite element analysis of silos. Trans. ASAE. 20(4):735.
- Johnston, F.T. 1983. Solutions for silo asymmetric flow problems. Proc. 2nd Int. Conf. Design of Silos for Strength and Flow. November. Stratford-Upon-Avon Hilton. Powder Advisory Centre. pp1-13.
- Kennedy, J.B. and A.M. Neville. 1976. Basic Statistical Methods for Engineers and Scientists. 2nd ed. Harper & Row, Publishers, Inc. New York. 490pp.
- Ketchum, M.S. 1919. The Design of Walls, Bins and Grain Elevators. McGraw-Hill Book Company, Inc. New York. 556pp.

- Kmita, J. 1985. Silo as a system of self-induced vibration. ASCE. J. Struc. Eng. 111(1):190-204.
- Kramer, H.A. 1944. Factors influencing design of bulk storage bins for rough rice. Agric. Eng. 25:463-466.
- Lenczer, D. 1963. An investigation into the behaviour of sand in a model silo. Struc. Eng. 41:389-398.
- Lufft, E. 1904. Tests of grain pressure in deep bins at Buenos Aires, Argentina. Engineering News. 52(24):531-532.
- McLean, A.G. and P.C. Arnold. 1976. Prediction of cylinder flow pressures in mass flow bins using minimum strain energy. Trans. ASME. J. Eng. Ind. (B). 98(4):1370-1374.
- McLean, A.G. and P.C. Arnold. 1984. Wall loads on agricultural silos. Agric. Eng. Aust. 13(1):10-18.
- McLean, A.G., P.C. Arnold and D.J. Martin. 1983. Simplified mass-flow bin wall load predictions. Bulk Solids Handling. 3(4):787-793.
- McLean, A.G. and B. Bravin. 1985. Wall loads in eccentric discharge silos. Int. J. Bulk Solids Storage in Silos. 1(1):12-24
- Manbeck, H.B., M.G. Goyal, G.L. Nelson and M.G. Singh. 1977. Dynamic over pressures in model bins during emptying. Paper presented at the 1977 ASAE Winter Meeting. Chicago, Illinois. December. Paper No. 77-4505. 26pp.
- Moriyama, R. and G. Jimbo. 1985. The effect of filling methods on the wall pressure near the transition in a bin. Bulk Solids Handling. 5(3):603-609.
- Moysey, E.B. 1977. Prediction of pressures in deep bins during emptying and filling. Paper presented at the 1977 ASAE Winter Meeting. Chicago, Illinois. December. Paper No. 77-4506. 13pp.
- Moysey, E.B. 1984. The effect of grain spreaders on grain friction and bin wall pressures. J. Agric. Eng. Res. 30:149-156.
- Moysey, E.B. and P.G. Landine. 1980. Transient pressures in deep grain bins. Paper presented at the 60th Annual AIC Conference. CSAE. Edmonton, Alberta. August. Paper No. 80-205. 14pp.
- Moysey, E.B. and P.G. Landine. 1982. Effect of changes in bin cross-section on wall pressures. Paper presented at the 1982 ASAE Summer Meeting. Madison, Wisconsin. June. Paper No. 82-4073. 12pp.
- Munch-Anderson, J. 1986. The boundary layer in rough grain silos. Proc. Conf. Bulk Materials, Storage, Handling and Transportation. Wollongong, Australia. July 7-9.

- National Research Council of Canada. 1977. Canadian Farm Building Code. NRCC No. 15564. Associate Committee on the National Building Code. NRCC. Ottawa, Ontario. 215pp.
- National Research Council of Canada. 1983. Canadian Farm Building Code. NRCC No. 21312. Associate Committee on the National Building Code. NRCC. Ottawa, Ontario.
- Nielsen, J. and N. Kristiansen. 1980. Related measurements of pressure conditions in full-scale barley silo and in model silo. Proc. Int. Conf. Design of Silos for Strength and Flow. September 2-4. University of Lancaster. Powder Advisory Centre. 24pp.
- Ooms, M. and A.W. Roberts. 1985. The reduction and control of flow pressures in cracked grain silos. Bulk Solids Handling. 5(5): 1009-1016.
- Otis, C. and J. Pomroy. 1961. Tower silo design. Agric. Eng. 2(7):356.
- Paterson, W.S. 1980. Measurement of pressures in hoppers and silos. Proc. Int. Conf. Design of Silos for Strength and Flow. September 2-4. University of Lancaster. Powder Advisory Centre. 25pp.
- Pieper, K. 1969. Investigation of silo loads in measuring models. Trans ASME. J. Eng. Ind. (B). 91(1):365-372.
- Pokrant, D.G. 1983. A Test System for Grain Pressure Studies. Unpublished B.Sc. thesis. University of Manitoba. Winnipeg, Manitoba. 70pp.
- Pokrant, D.G. and M.G. Britton. 1982. A test system for grain pressure studies. Paper presented at 1982 ASAE North Central Region Meeting Brookings, South Dakota. October. Paper No. NCR 82-103. 17pp.
- Pokrant, D.G. and M.G. Britton. 1986. An investigation into the effects of eccentric drawoff and flow rate in model grain bin studies. paper presented at the 1986 ASAE Summer Meeting. San Luis Obispo, California. June. Paper No. 86-4076. 10pp.
- Ravenet, J. 1983. The development of industrial silos throughout the world during the last 100 years. Bulk Solids Handling. 1(1): 127-140.
- Ravenet, J. 1984. Grain and meal silos in Latin America: part I. Bulk Solids Handling. 4(2):363-372.
- Reimbert, M. 1955. Design of silos. Conc. Const. Eng. 50:170-172.
- Reimbert, M. and A. Reimbert. 1976. Silos: Theory and Practice. Trans Tech Publications. Clausthal-Zellerfeld, Germany. 250pp.
- Reisner, W. and R.M. von Eisenhart Rothe. 1971. Bins and Bunkers for Handling Bulk Materials - Practical Design and Techniques. Trans-Tech Publications. Clausthal-Zellerfeld, Germany. 280pp.

- Rennie, R.E. 1983. Foil model grain bin failure. Unpublished B.Sc. Thesis. University of Manitoba. Winnipeg, Manitoba. 53pp.
- Richards, P.C. 1977. Bunker design - part 1: Bunker outlet design and initial measurements of wall pressures. Trans. ASME. J. Eng. Ind. (B). 99:809-813.
- Ross, I.J., T.C. Bridges, O.J.Loewer and J.N. Walker. 1979. Grain bin loads as affected by grain moisture content and vertical pressure. Trans. ASAE. 25(5):1344-1348.
- Ross, I.J., D.W.Moore, O.J.Loewer and G.M. White. 1980. Model studies of grain bin failures. Paper presented at the 1980 ASAE Winter Meeting. Chicago, Illinois. December. Paper No. 80-4504.
- Ross, I.J., T.C. Bridges and C.V. Schwab. 1986. Vertical wall loads on conical grain bins. Paper presented at the 1986 ASAE Summer Meeting. San Luis Obispo, California. June. Paper 86-4074. 25pp.
- Rowley, R.B. and M.G. Britton. 1985. Grain flow variation from a lamellar bin wall. Paper presented at the 1985 ASAE North Central Region Meeting. Bismarck, North Dakota. October. Paper No. NCR 85-508. 10pp.
- Safarian, S.S. and E.C. Harris. 1985. Design and Construction of Silos and Bunkers. Van Nostrand Reinhold Co. New York. 468pp.
- Saul, R.A. 1953. Measurement of grain pressures on bin walls and floors. Agric. Eng. 34(4):231-234.
- Schott, R.W. and M.G. Britton. 1984. Plane strain behavior of bulk grain. Paper presented at 1984 ASAE North Central Region Meeting. Morris, Minnesota. October. Paper No. NCR 84-503. 14pp.
- Schott, R.W. and M.G. Britton. 1985. Plain strain of wheat with various moisture contents. Paper presented at the 1985 ASAE North Central Region Meeting. Bismarck, North Dakota. October. Paper No. NCR 85-505. 14pp.
- Schwedes, J. 1983. Evolution of bulk solids technology since 1974. Bulk Solids Handling. 3(1):143-147.
- Singh, D. and E.B. Moysey. 1985. Grain bin wall pressures: theoretical and experimental. Can. Agric. Eng. 27(1):43-48
- Smith, D.L.O. and R.A. Lohnes. 1980. Grain silo overpressures induced by dilatancy upon unloading. Paper presented at 1980 ASAE Summer Meeting. San Antonio, Texas. June. Paper No. 80-3013. 8pp.
- Smith, A.B.B. and S.H. Simmonds. 1983. Lateral coal pressures in a mass flow silo. University of Alberta Department of Civil Engineering Structural Report. No. 113. November. 308pp.

- Snyder, L.H., W.L. Roller and G.E. Hall. 1967. Coefficients of kinetic friction of wheat on various metal surfaces. Trans. ASAE. 10(3):pp411-413,419.
- Sokol, L. 1986. Wall loads in vertical silos. Int. J. Bulk Solids Storage in Silos. 1(1):1-11.
- Sugden, M.B. 1981. Effect of initial density on flow patterns in circular flat-bottomed silos. J. Powder Bulk Solids Technology. 5(1):21-32.
- Sugita, M. 1972. Flow and pressures of non-cohesive granular materials in funnel-flow bins. Paper presented at the 2nd Symposium on Storage and Flow of Solids. Chicago, Illinois. September. Paper No. 72-MH-20. 8pp
- Sundaram, V. and S.C. Cowin. 1979. A reassessment of static in bin pressure experiments. Powder Technology. 22:23-32.
- Suzuki, M., T. Akashi and K. Matsumoto. 1985. Flow behaviour and stress conditions in small and medium silos. Bulk Solids Handling. 5(3):611-620.
- Theimer, O.F. 1969. Failures of reinforced concrete grain silos. Trans. ASME. J. Eng. Ind. (B). 91(2):460-477.
- Thompson, S.A. and T.G. Prather. 1984. Dynamic wall loads in a corrugated walled model grain bin. Trans. ASAE. 27(3):875-878.
- Thompson, S.A., I.J. Ross, J.N. Walker and L.G. Wells. 1982. Vertical wall loads in a model grain bin. Trans. ASAE. 25(5):1344-1348.
- Thompson, S.A., J.L. Usry and J.A. Legg. 1985. Wall loads as a function of discharge rate in a corrugated model grain bin. Paper presented at the 1985 ASAE Summer Meeting. East Lansing, Michigan. June. Paper No. 85-4003. 25pp.
- Timoshenko, S.P. and J.M. Gere. 1961. Theory of Elastic Stability. 2nd ed. McGraw-Hill Book Co. Inc. Chapter 11: Buckling of Shells pp457-519.
- Towells, D.B. and M.G. Britton. 1986. Flow variations with height of a lamellar bin wall. Paper presented at the 1986 ASAE-NCR/CSAE Annual Meeting. Winnipeg, Manitoba. September. Paper No. NCR-86-606. 5pp.
- Trahair, N.S. 1985. Structural design criteria for steel bins and silos. Int. J. Bulk Solids Storage in Silos. 1(2):11-20.
- Turitzin, A.M. 1963. Dynamic pressure of granular material in deep bins. ASCE. J. Str. Div. Proc. Paper No. 3479. 89(ST2):49-73.
- Tuzun, U. and R.M. Nedderman. 1983. Gravity flow of granular materials round obstacles. Bulk Solids Handling. 3(3):507-517.

- Versavel, P.A. 1985. Examination of the interaction of bulk wheat with bin wall configuration in model bins. Unpublished M.Sc. thesis. University of Manitoba. Winnipeg, Manitoba. 104pp.
- Walters, J.K. 1973. A theoretical analysis in silos with vertical walls. Chem. Eng. Sci. 28:13-21.
- Wlodarski, A. and A. Pfeffer. 1969. Air pressure in the bulk of granular solid discharged from a bin. Trans. ASME. J. Eng. Ind. (B). 91(1):373-381.

## APPENDIX A

### WALL STRAIN GAGE LOCATIONS AND CALIBRATION

#### Selection of Strain Gage Locations

In addition to the six transducers, instrumentation constraints only allowed for six channels of strain to be measured with any given test. For this reason, it was decided to limit the area of interest to the vertical strip of the wall that intersected the radial line joining the centres of the discharge locations. This was commonly the area of greatest failure when eccentric discharge was used. Since there was little information as to location of the height of greatest bin wall stress, gage locations were chosen somewhat arbitrarily based on the location of the pseudo-hopper-to-wall transition described below.

After complete discharge took place from the flat-bottomed bin, a funnel-shaped grain mass still remained. The approximate shape of this funnel was defined by the material's angle of repose. The intersection of the top of the stationary grain mass and the wall formed a pseudo-hopper-to-wall-transition which Jenike and Johanson (1968) noted as being a potential location for large switch forces. The height of this transition along the bin circumference was inversely proportional to the distance from the outlet, with the extreme case occurring with a fully-eccentric discharge. In this situation, there was no transition at the point where the bin wall and outlet intersected.

The angle iron ring attached to the bottom of the bin added to the rigidity of the wall and a fixed end had to be assumed. End moment and shear distorted the state of stress near the bottom thus in order to get an accurate indication of the effect of the grain pressure, the first rosette had to be located some distance away. St. Venant stated that the effect of a stress discontinuity should be negligible at a distance of 10 times the material thickness, but use of this principle did not account for the cylindrical shape of the bin. Timoshenko's analysis of cylindrical shells suggested that the effect of end moment and shear for 1 mm thick, 1000 mm diameter steel bins would be reduced to less than 1% at a distance of 80 mm from the fixed end (Timoshenko and Gere, 1961). An additional 50 mm was added to Timoshenko's 80 mm value to account for the height of the steel ring and thus measurements made 130 mm from the bin bottom were considered to be free from any fixed end effects.

Four strain rosette locations were thus selected at points 130 mm above the pseudo-hopper-to-wall transitions that theoretically resulted with the four discharge locations used. Assuming an angle of repose of 28 degrees, a gage spacing of 80 mm was required. The bottom rosette was mounted at the 130 mm level, since there was no transition, and the other three were mounted at heights of 210, 290 and 370 mm. A fifth rosette was located 80 mm above the last one at a height of 450 mm from the bin bottom. Figure A.1 shows the strain gages as they were mounted on the bin wall.



Figure A.1 - Strain rosettes mounted to the bin wall

Two rosettes (six gages) could be measured for each test. The 450 mm rosette was always monitored so as to compare the flow rate and eccentricity effects at the same bin wall location. The wall strains at the bottom location would be measured when the fully-eccentric location was used. The rosette second from the bottom would be chosen when the location 300 mm from the bin centre was used and so on. By choosing the second rosettes in this manner, allowance could be made for the varying location of the pseudo-hopper-to-wall transition.

#### Strain Gage Calibration

Just as the transducers were calibrated, it was felt necessary to initiate some form of calibration of the strain gages on the bin wall. After considering other alternatives, it was decided that pressurizing

the inside of the bin with a uniform lateral pressure afforded the best opportunity to correlate wall strain readings and bin pressures.

An air pressure cylinder was constructed as shown in Figure A.2, using two rigid plywood discs for the ends with a flexible plastic side wall made from vapour barrier. The 990 mm diameter plywood discs were held firmly in place, 750 mm apart using threaded rods. A flat double layer of plastic was taped together at the ends to form a cylinder and this sleeve was placed over the two plywood discs. To minimize air leakage, the plastic was clamped to the edge of the wooden discs with steel banding and small holes were plugged with tape and silicon seal. An air line was inserted through one of the wooden discs and when pressurized, the bladder expanded laterally.

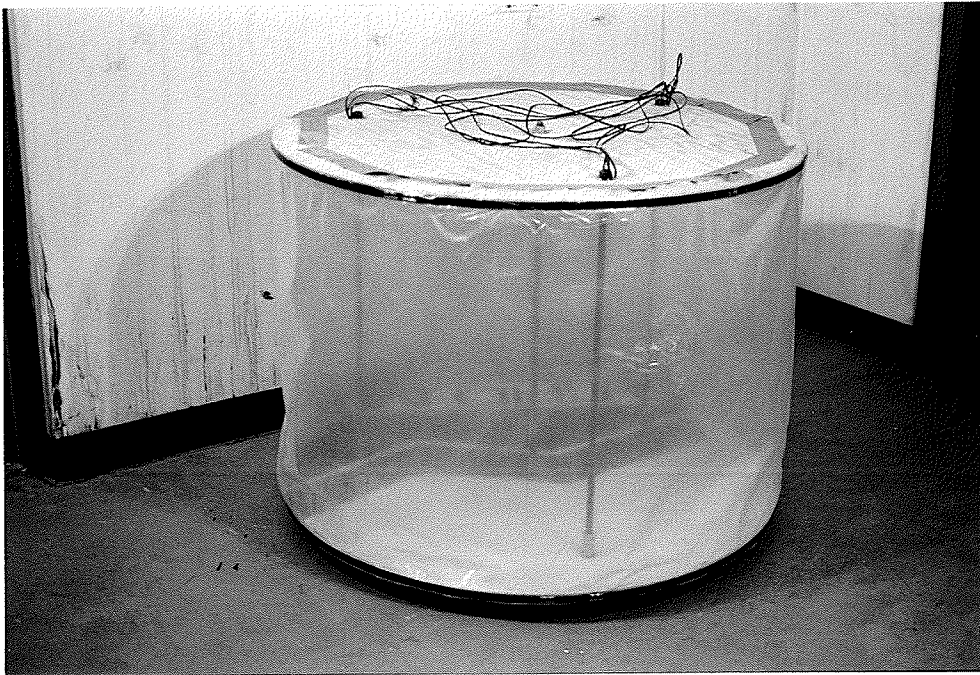


Figure A.2 - Air pressure cylinder used in strain gage calibration

Unconstrained, a very small pressure could have blown the cylinder side walls apart, but when placed inside the bin, the air pressure could build. The threaded rods held the plywood discs together and accounted for the vertical force, while the bin wall constrained the plastic liner and absorbed the uniform lateral pressure. A needle valve controlled air flow (pressure) to and from the cylinder while a U-tube mercury manometer measured the air pressure.

Strain readings were taken from a number of gages at various air pressure levels. It was initially anticipated that the readings would show linear correlation since lateral cylinder stress was proportional to the applied inside pressure. The results of the readings, however, were totally erratic and showed no discernible pattern. Some gages showed decreases followed by later increases in strain. The maximum pressure level used was 50 mm of mercury or approximately 6.6 kPa. This was calculated to be the maximum lateral pressure that would be exerted by the grain mass when the bin was full.

After some "head scratching" it was discovered that the strains being recorded were not so much from the stretching of the wall caused by internal pressure, but rather from the bending of the wall to a more cylindrical shape. As discussed earlier, the test bin was manufactured in three sections and had a somewhat non-circular cross-section when unloaded. As pressure was applied, the cross-section tended toward a more circular shape, although the vertical seams still maintained a certain degree of non-circularity. Had additional gages been used on the inside wall surface, this bending could have been accounted for. With only outside gages, however, the results were meaningless.

Owing to bin design flaws, low sensitivities and time constraints, the decision was made to abandon the wall strain measurements. It was felt that this would not jeopardize the objective of the study since the major loads of concern causing the most damage in thin-walled structures appeared to be the vertical floor and wall loads. The importance, however, of using both inside and outside strain gages relative to the effects of altering the wall surface characteristics was made clear through this calibration procedure.

APPENDIX B

TRANSDUCER CALIBRATION RESULTS

TABLE B.1 - Load Transducer Regression Analysis Summary

Transducer	Slope	Intercept	R <sup>2</sup>	Linearity
1	2.423	-9.05	> 0.9999	0.212%
2	2.430	-11.38	> 0.9999	0.249%
3	2.427	-11.51	> 0.9999	0.235%
4	2.412	-10.01	> 0.9999	0.253%
5	2.435	-9.79	> 0.9999	0.332%
6	2.412	-11.48	> 0.9999	0.303%

where: Slope has units of N/unit Taurus number  
 Intercept has units of N  
 Linearity expressed as percentage of full scale load

Note: regression was based on 102 data points

APPENDIX C

TRANSDUCER-TO-BIN LOAD CONVERSION EQUATIONS

The bin floor was divided into three equivalent pie-shaped sections as shown in Figure C.1. Each section was assumed to be acted upon by a uniform vertical load, represented as a point load at the centroid of the section. Equations of statics were sufficient to define these floor loads as functions of the six transducer loads. Transducer mounting geometry relative to the bin centre was as shown in Figure C.2. A mean bin radius of 499 mm was used, with actual values shown in Figure C.3.

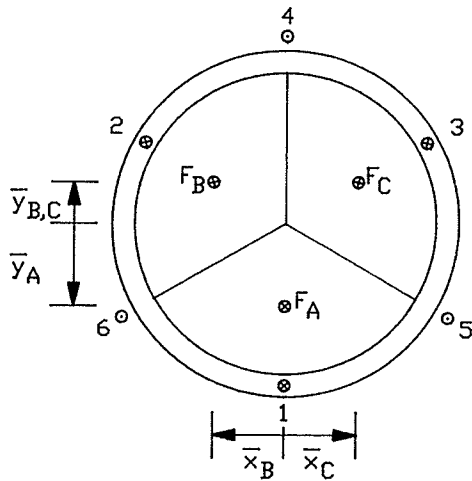


Figure C.1  
Floor sections A, B and C

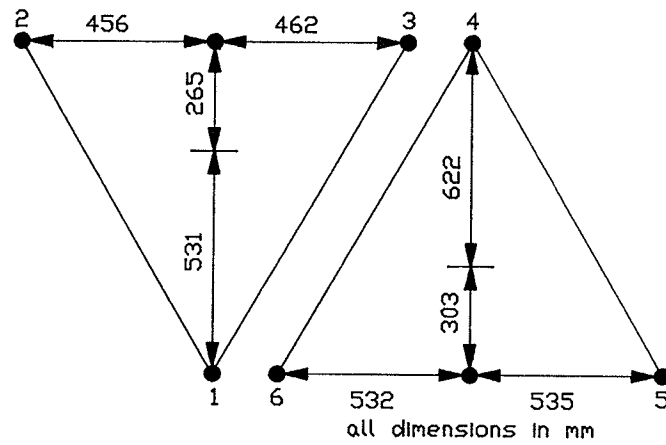


Figure C.2  
Transducer mounting geometry

Equations defining the centroids of the circular sectors:

$$\bar{y}_A = \frac{2 r \sin \theta}{3 \theta} = \frac{2*499*\sin(\pi/3)}{3*(\pi/3)} = 275 \text{ mm}$$

$$\bar{y}_{B,C} = \bar{y}_A \cos \theta = 275 \cos(\pi/3) = 138 \text{ mm}$$

$$\bar{x}_{B,C} = \bar{y}_A \sin \theta = 275 \sin(\pi/3) = 238 \text{ mm}$$

$\Sigma M_x = 0$  about line BC

$$(531+138)T_1 - (265-138)(T_2+T_3) + (622-138)T_4 - (303+138)(T_5+T_6) + (413)F_A = 0$$

$$F_A = \frac{-669*T_1 + 127*(T_2+T_3) - 484*T_4 + 441*(T_5+T_6)}{413}$$

$$F_A = -1.620*T_1 + 0.308*T_2 + 0.308*T_3 - 1.172*T_4 + 1.068*T_5 + 1.068*T_6 \quad [1]$$

$\Sigma M_y = 0$  about line 4A1

$$456*T_2 - 462*T_3 + 535*T_5 - 532*T_6 + 238*(F_B+F_C) = 0$$

$\Sigma F_z = 0$

$$T_1 + T_2 + T_3 - T_4 - T_5 - T_6 + F_A + F_B + F_C = 0$$

Solving for  $F_B$  and substituting for  $F_A$  gives:

$$F_B = -1.916*T_2 + 1.941*T_3 - 2.248*T_5 + 2.235*T_6 + F_C \quad [2]$$

$$F_B = 0.620*T_1 - 1.308*(T_2+T_3) + 2.172*T_4 + 2.068*(T_5+T_6) - F_C \quad [3]$$

Equating [2] and [3] and solving for  $F_C$  gives:

$$F_C = 0.310*T_1 + 0.304*T_2 - 1.624*T_3 + 1.086*T_4 + 1.090*T_5 - 1.152*T_6 \quad [4]$$

Substituting for  $F_C$  in [2] and solving for  $F_B$  gives:

$$F_B = 0.310*T_1 - 1.612*T_2 + 0.317*T_3 + 1.086*T_4 - 1.158*T_5 + 1.084*T_6 \quad [5]$$

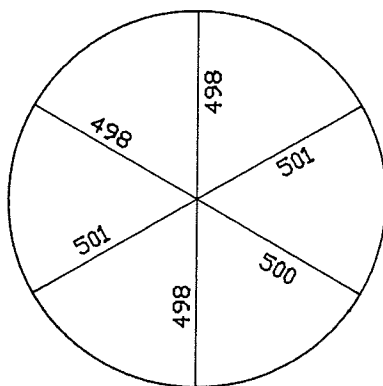


Figure C.3  
Actual bin radii

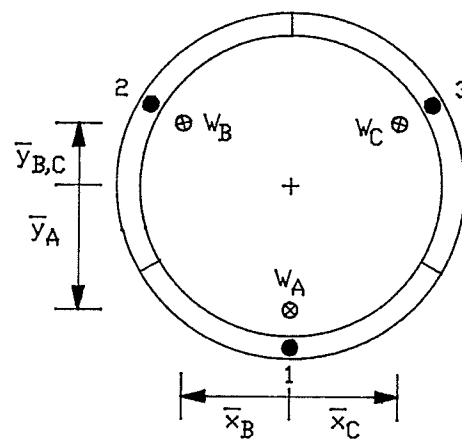


Figure C.4  
Wall sections A, B and C

The bin wall was divided into three 120 degree sections as shown in Figure C.4. The sections were again assumed to be acted upon by uniform vertical loads which were represented as point loads at the centroid of each section. Static equilibrium then defined these three wall loads as functions of the wall transducer loads only.

Equations defining the centroids of the circular arcs:

$$\bar{y}_A = \frac{r \sin \theta}{\theta} = \frac{499 * \sin(\pi/3)}{\pi/3} = 413 \text{ mm}$$

$$\bar{y}_{B,C} = \bar{y}_A \cos \theta = 499 * \cos(\pi/3) = 206 \text{ mm}$$

$$\bar{x}_{B,C} = \bar{y}_A \sin \theta = 413 * \sin(\pi/3) = 357 \text{ mm}$$

$$\Sigma M_x = 0 \text{ about line BC}$$

$$- (531+206)*T_1 + (265+206)*(T_2+T_3) + (413+206)*W_A = 0$$

$$W_A = \frac{737*T_1 - 59*(T_2+T_3)}{619} = 1.191*T_1 - 0.095*T_2 - 0.095*T_3 \quad [6]$$

$$\Sigma M_y = 0 \text{ about line 1A}$$

$$- 456*T_2 + 462*T_3 + 357*(W_B+W_C) = 0$$

$$\Sigma F_z = 0$$

$$- T_1 - T_2 - T_3 + W_A + W_B + W_C = 0$$

Solving for  $W_B$  and substituting for  $W_A$  gives:

$$W_B = 1.277*T_2 - 1.294*T_3 + W_C \quad [7]$$

$$W_B = - 0.191*T_1 + 1.095*(T_2+T_3) - W_C \quad [8]$$

Equating (2) and (3) and solving for  $W_C$  gives:

$$W_C = - 0.095*T_1 - 0.091*T_2 + 1.195*T_3 \quad [9]$$

Substituting (9) into (7) for  $W_C$  and solving for  $W_B$  gives:

$$W_B = - 0.095*T_1 + 1.186*T_2 - 0.099*T_3 \quad [10]$$

Equations [1], [4], [5], [6], [9] and [10] can be represented in matrix format as follows:

$$\begin{bmatrix} 1.191 & -0.095 & -0.095 & 0 & 0 & 0 \\ -0.095 & 1.1863 & -0.099 & 0 & 0 & 0 \\ -0.095 & -0.091 & 1.195 & 0 & 0 & 0 \\ -1.620 & 0.308 & 0.308 & -1.172 & 1.068 & 1.068 \\ 0.301 & -1.612 & 0.317 & 1.086 & -1.158 & 1.084 \\ 0.301 & 0.304 & -1.624 & 1.086 & 1.090 & -1.152 \end{bmatrix} \begin{Bmatrix} T_1 \\ T_2 \\ T_3 \\ T_4 \\ T_5 \\ T_6 \end{Bmatrix} = \begin{Bmatrix} W_A \\ W_B \\ W_C \\ F_A \\ F_B \\ F_C \end{Bmatrix}$$

The inverse bin-to-transducer load conversion matrix is as follows:

$$\begin{Bmatrix} T_1 \\ T_2 \\ T_3 \\ T_4 \\ T_5 \\ T_6 \end{Bmatrix} = \begin{bmatrix} 0.852 & 0.074 & 0.074 & 0 & 0 & 0 \\ 0.075 & 0.855 & 0.077 & 0 & 0 & 0 \\ 0.074 & 0.071 & 0.849 & 0 & 0 & 0 \\ -0.119 & 0.550 & 0.550 & 0.030 & 0.477 & 0.477 \\ 0.558 & -0.110 & 0.559 & 0.484 & 0.038 & 0.484 \\ 0.561 & 0.560 & -0.109 & 0.486 & 0.485 & 0.039 \end{bmatrix} \begin{Bmatrix} W_A \\ W_B \\ W_C \\ F_A \\ F_B \\ F_C \end{Bmatrix}$$

## APPENDIX D

### BIN LOADS VS. TIME GRAPHS - SERIES #1

The graphs on the following pages are plots of floor and wall loads vs. discharge time for the sixteen discharge conditions (4 flow rates X 4 locations), from series #1. Three colors, (black, red and blue), are used to differentiate between loads on sections A, B and C respectively. Although similar colors are used for both the floor and the wall loads, wall loads can always be distinguished as the lower set of curves. In tests using the 100 mm orifice there is only 45 s of data plotted, since the discharge gate had to be shut early to prevent grain spillage from the hopper cart.

45 mm ORIFICE DIAMETER - CENTRE DISCHARGE

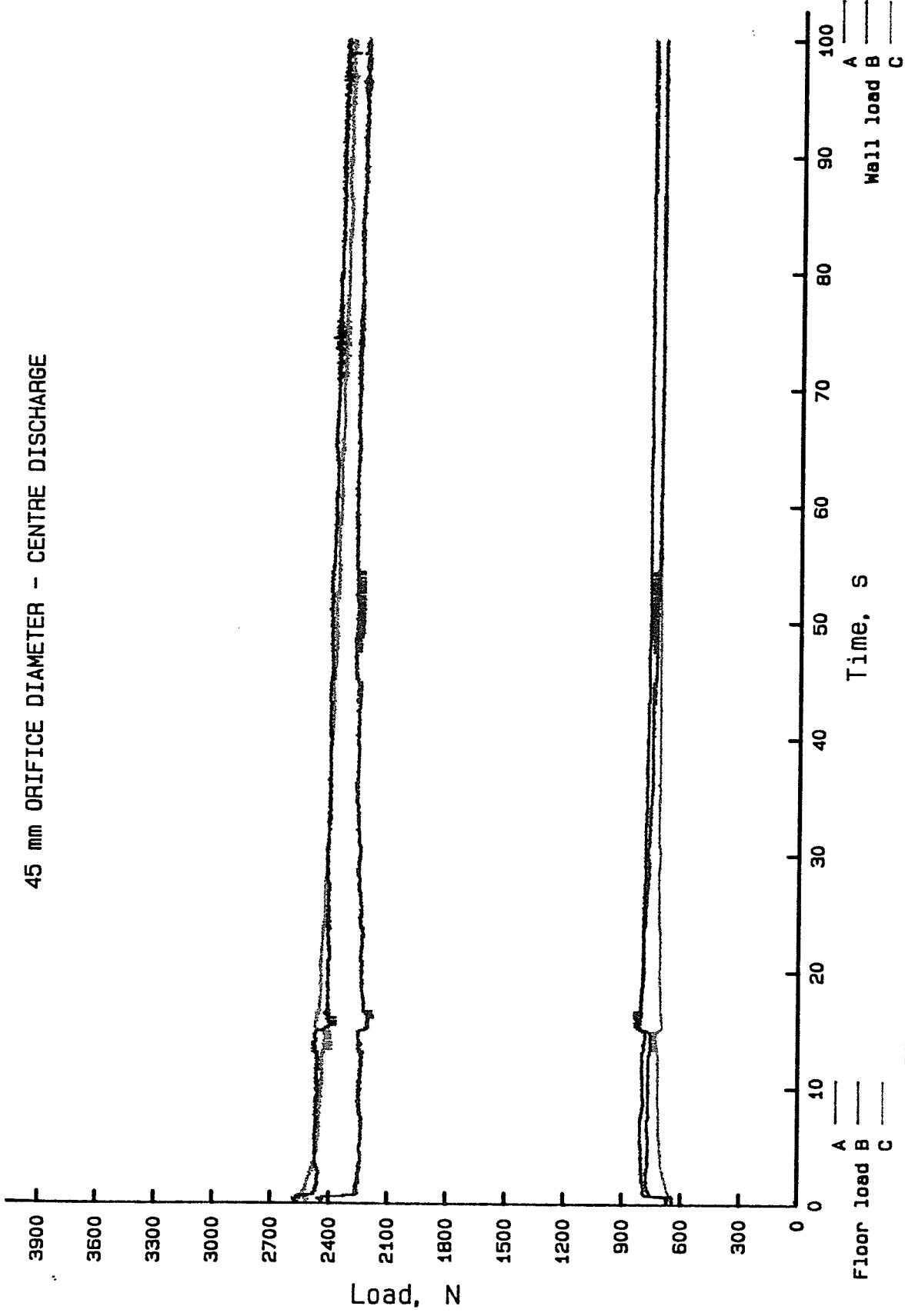


FIGURE D.1 - FLOOR AND WALL LOADS VS. DISCHARGE TIME - test D45E0S1

45 mm ORIFICE DIAMETER - 30% ECCENTRIC DISCHARGE

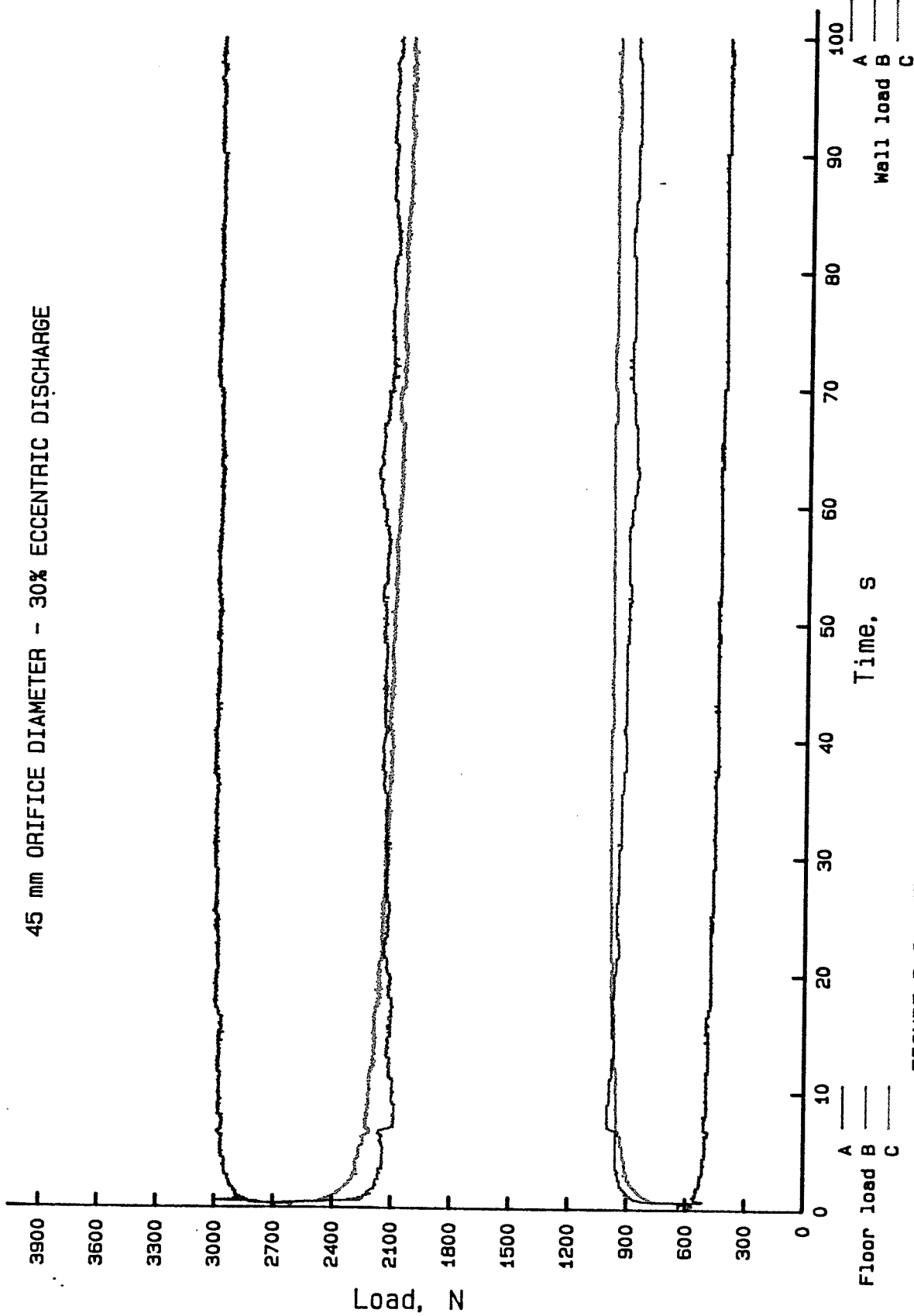


FIGURE D.2 - FLOOR AND WALL LOADS VS. DISCHARGE TIME - test D45E1S1

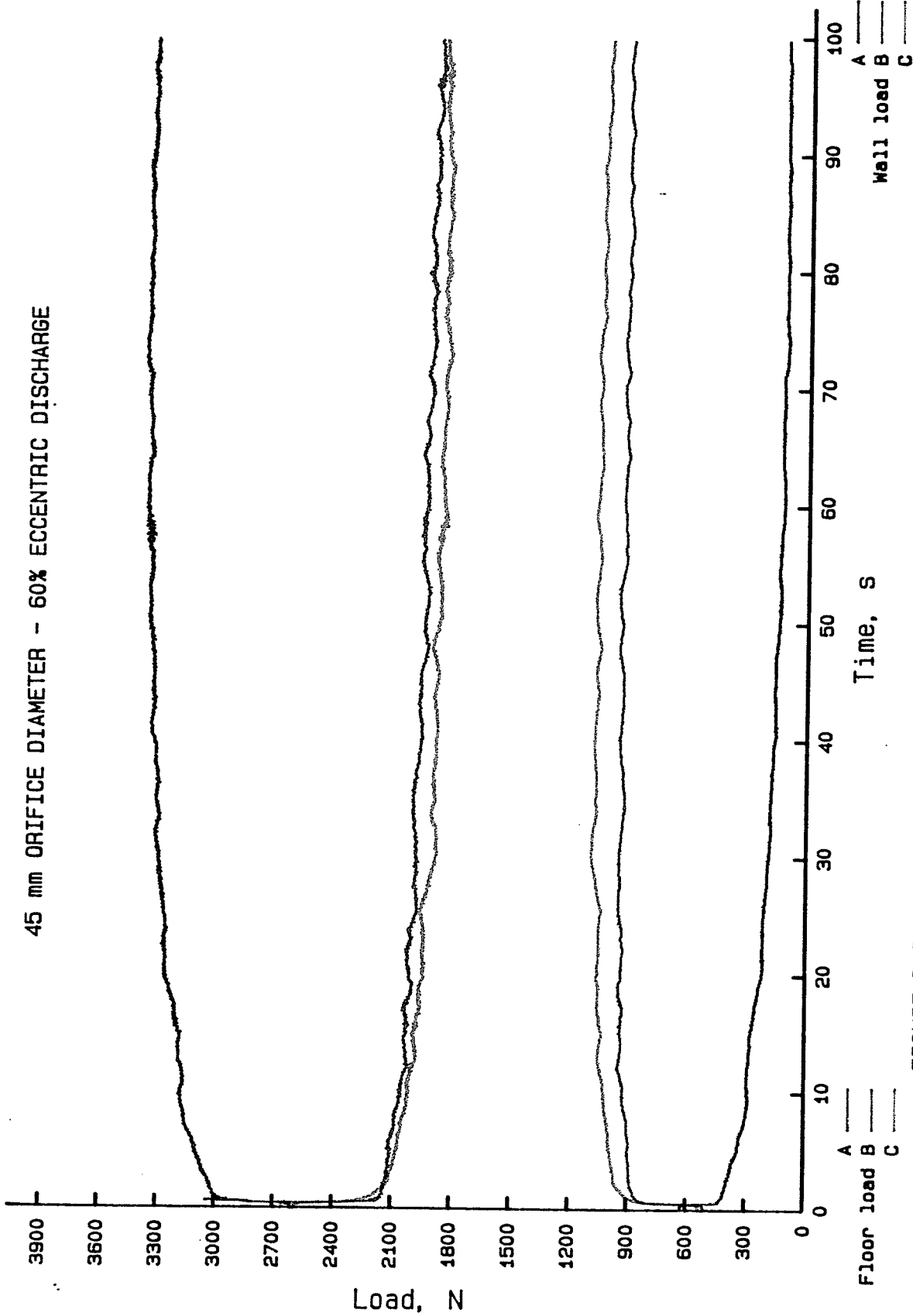


FIGURE D.3 - FLOOR AND WALL LOADS VS. DISCHARGE TIME - test D45E2S1

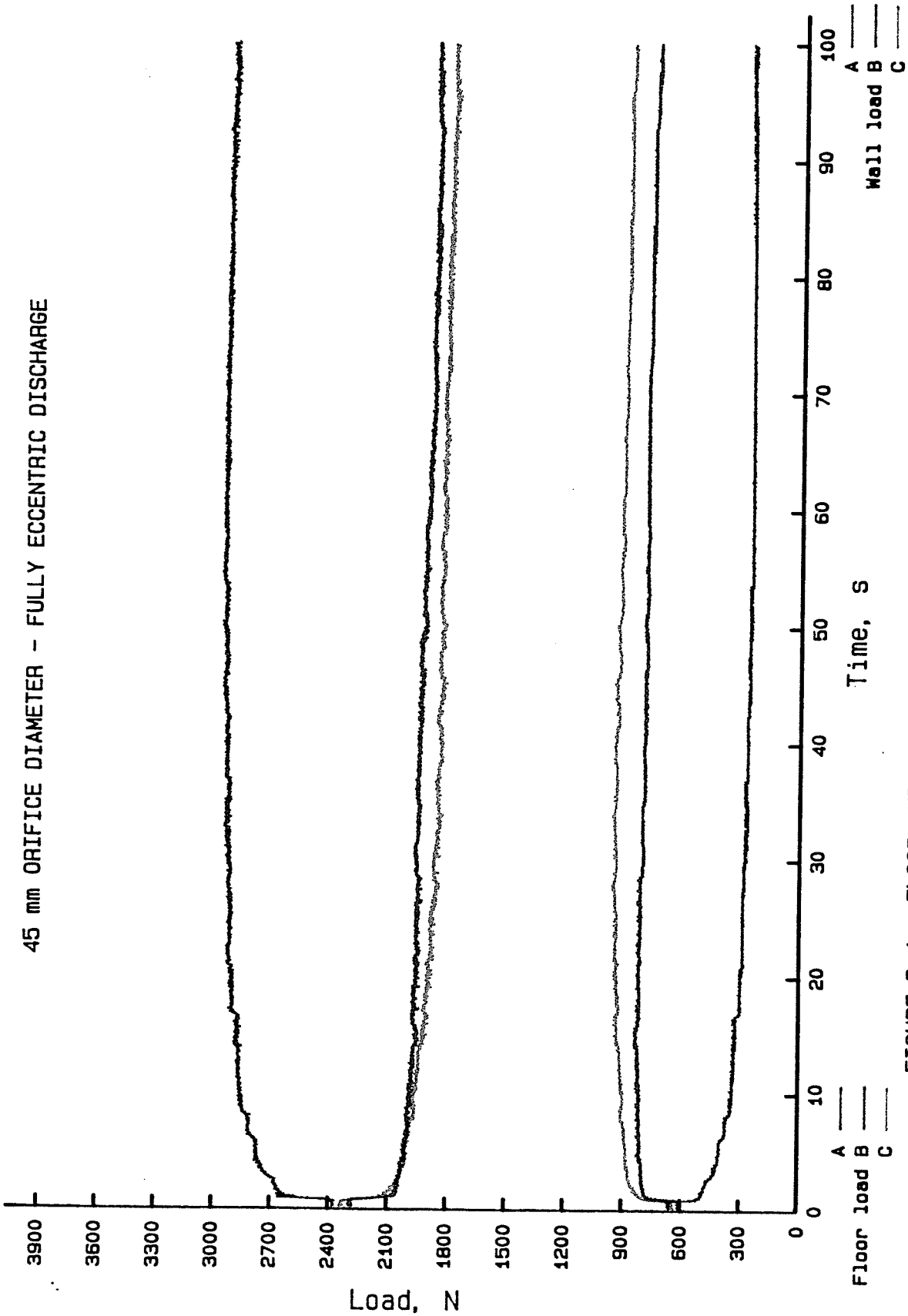


FIGURE D.4 - FLOOR AND WALL LOADS VS. DISCHARGE TIME - test D45E3S1

60 mm ORIFICE DIAMETER - CENTRE DISCHARGE

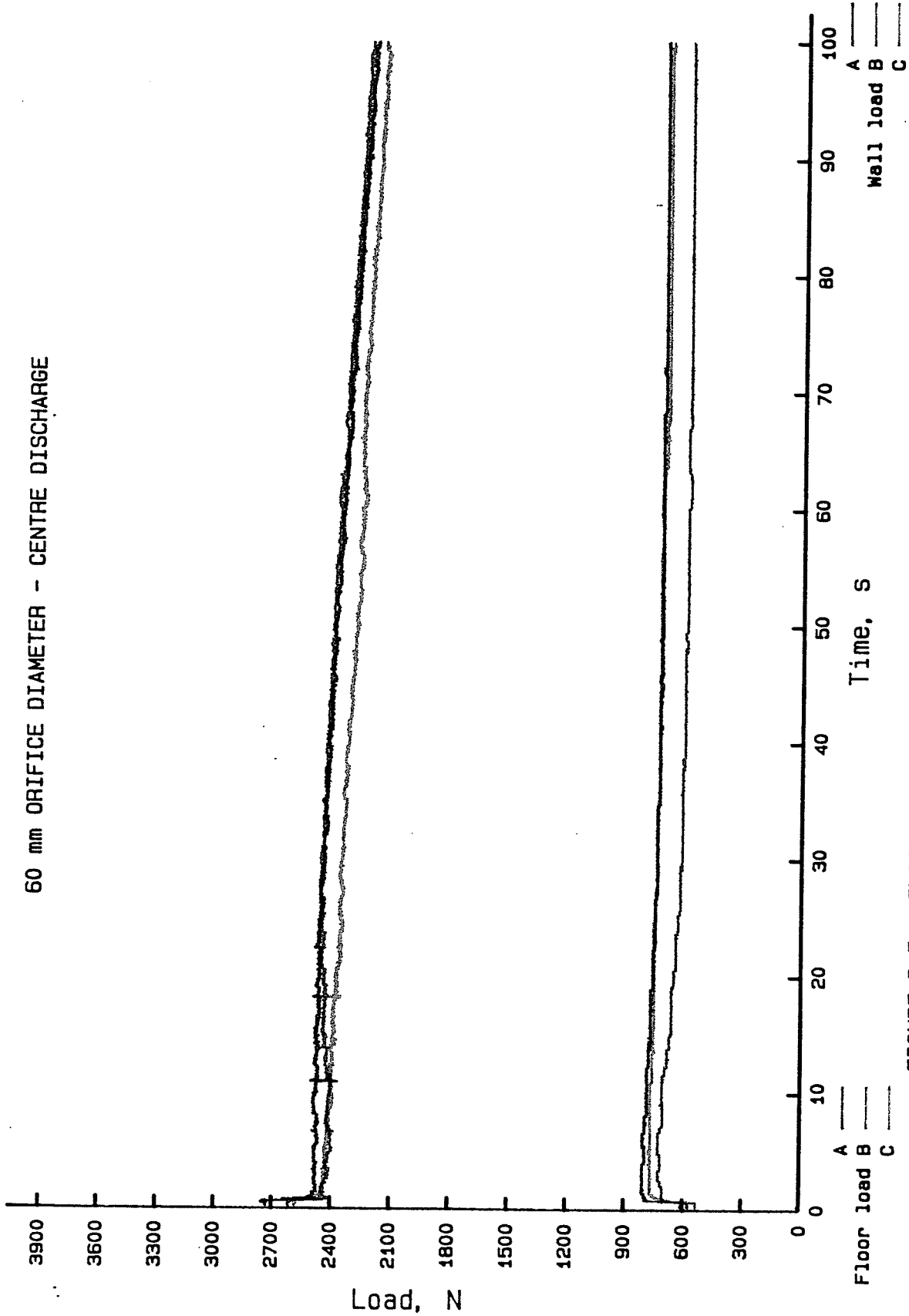


FIGURE D.5 - FLOOR AND WALL LOADS VS. DISCHARGE TIME - test D60E0S1

60 mm ORIFICE DIAMETER - 30% ECCENTRIC DISCHARGE

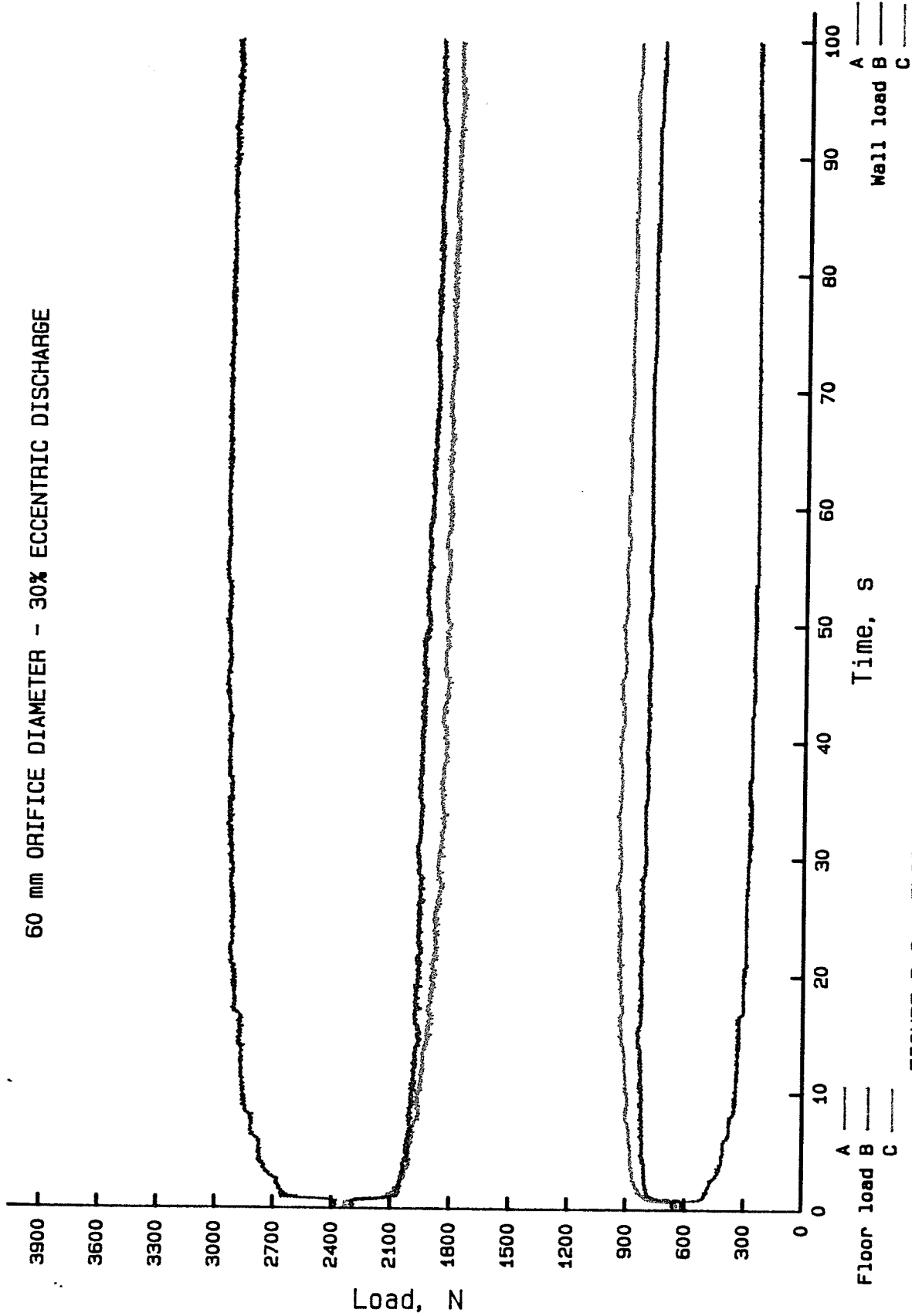


FIGURE D.6 - FLOOR AND WALL LOADS VS. DISCHARGE TIME - test D60E1S1

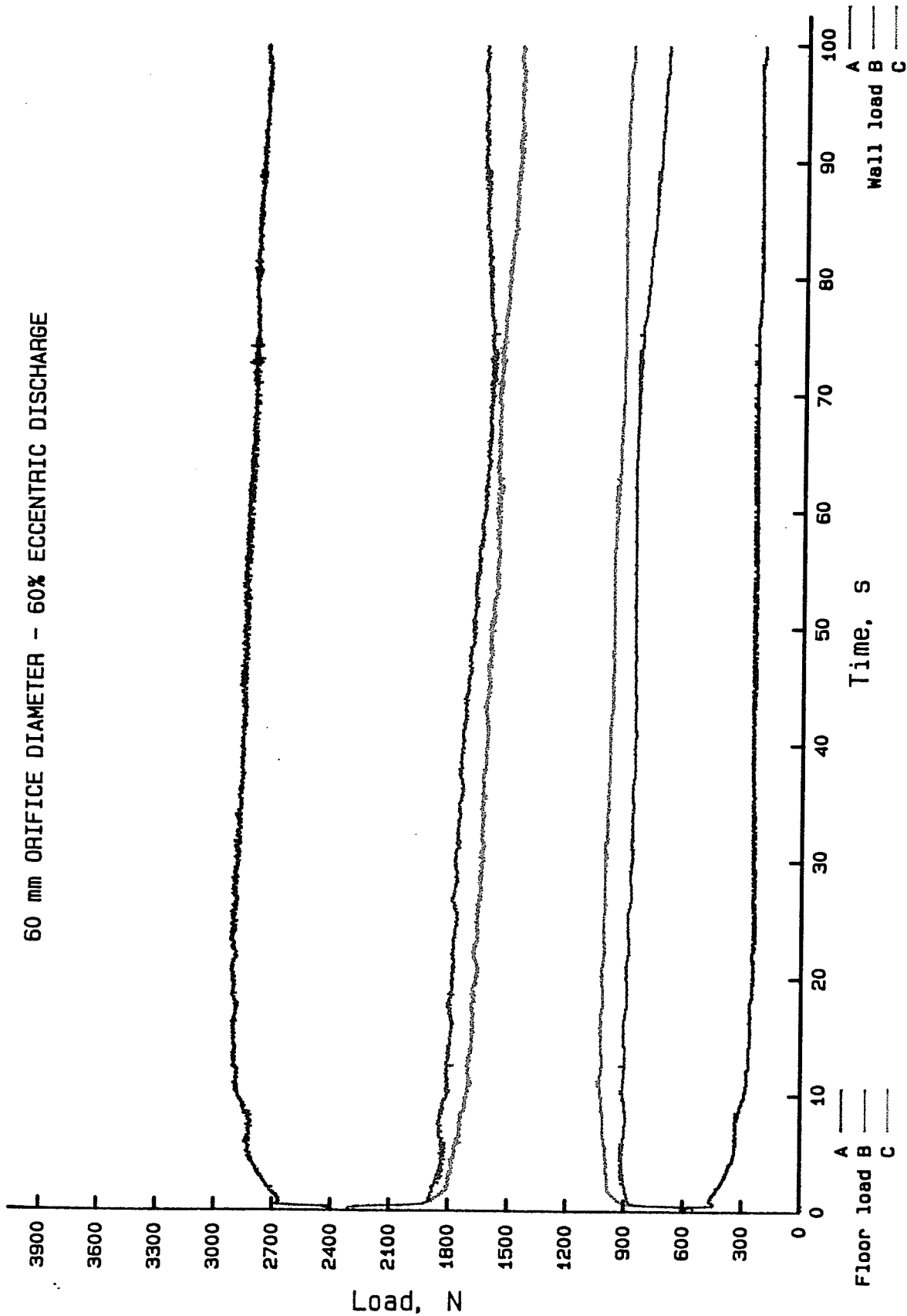


FIGURE D.7 - FLOOR AND WALL LOADS VS. DISCHARGE TIME - test D60E2S1

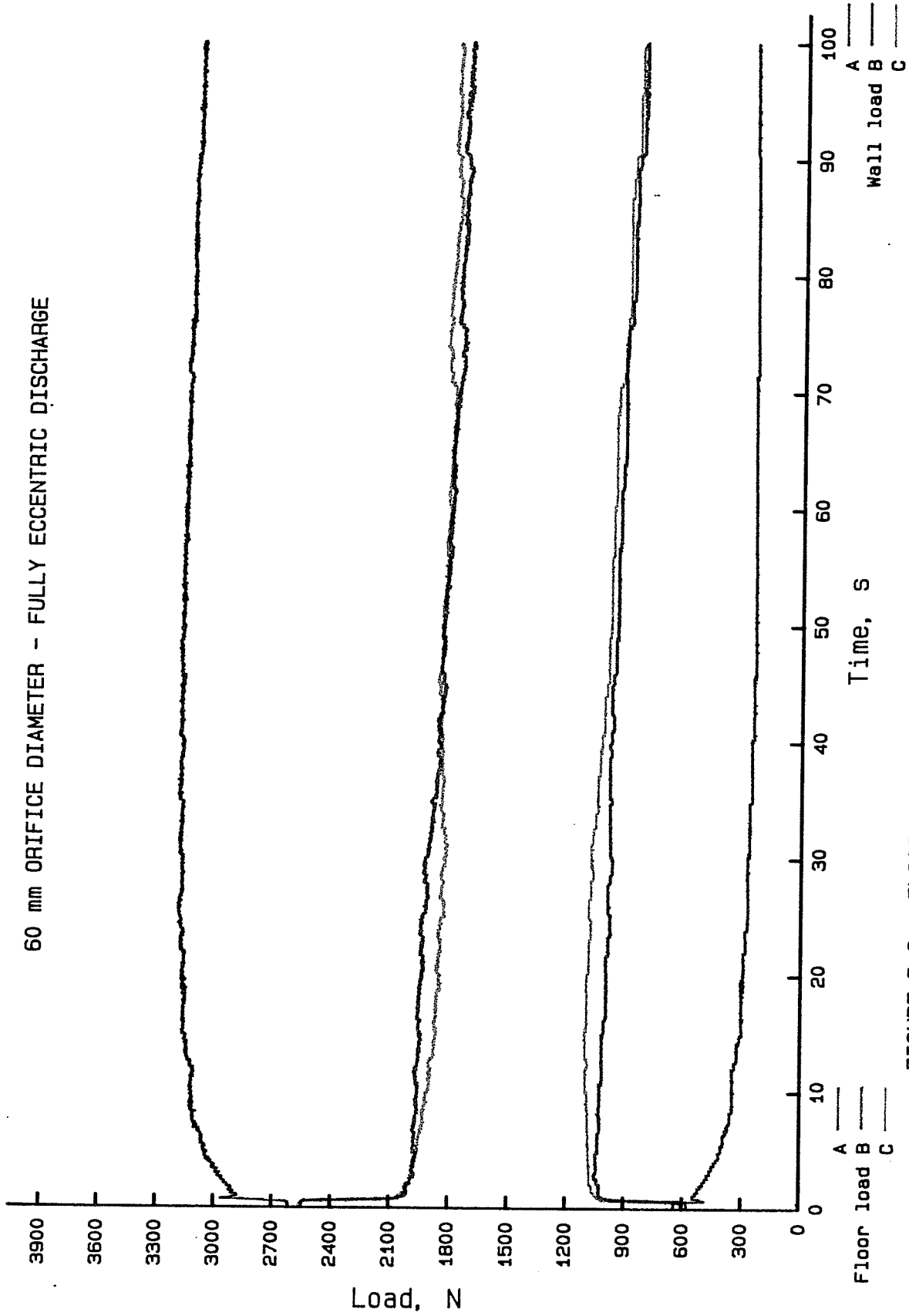


FIGURE D.8 - FLOOR AND WALL LOADS VS. DISCHARGE TIME - test D60E3S1

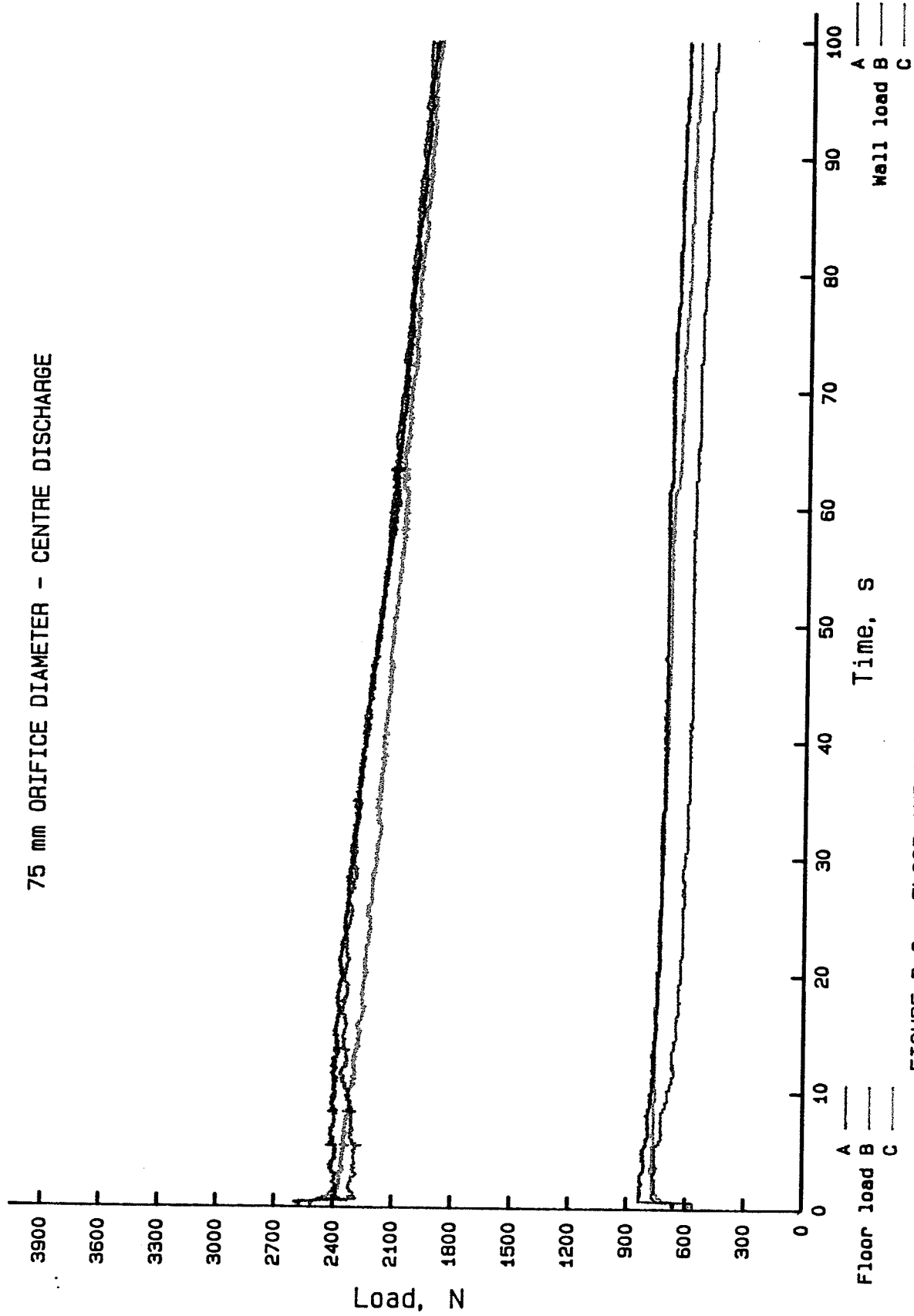


FIGURE D.9 - FLOOR AND WALL LOADS VS. DISCHARGE TIME - test D75E0S1

75 mm ORIFICE DIAMETER - 30% ECCENTRIC DISCHARGE

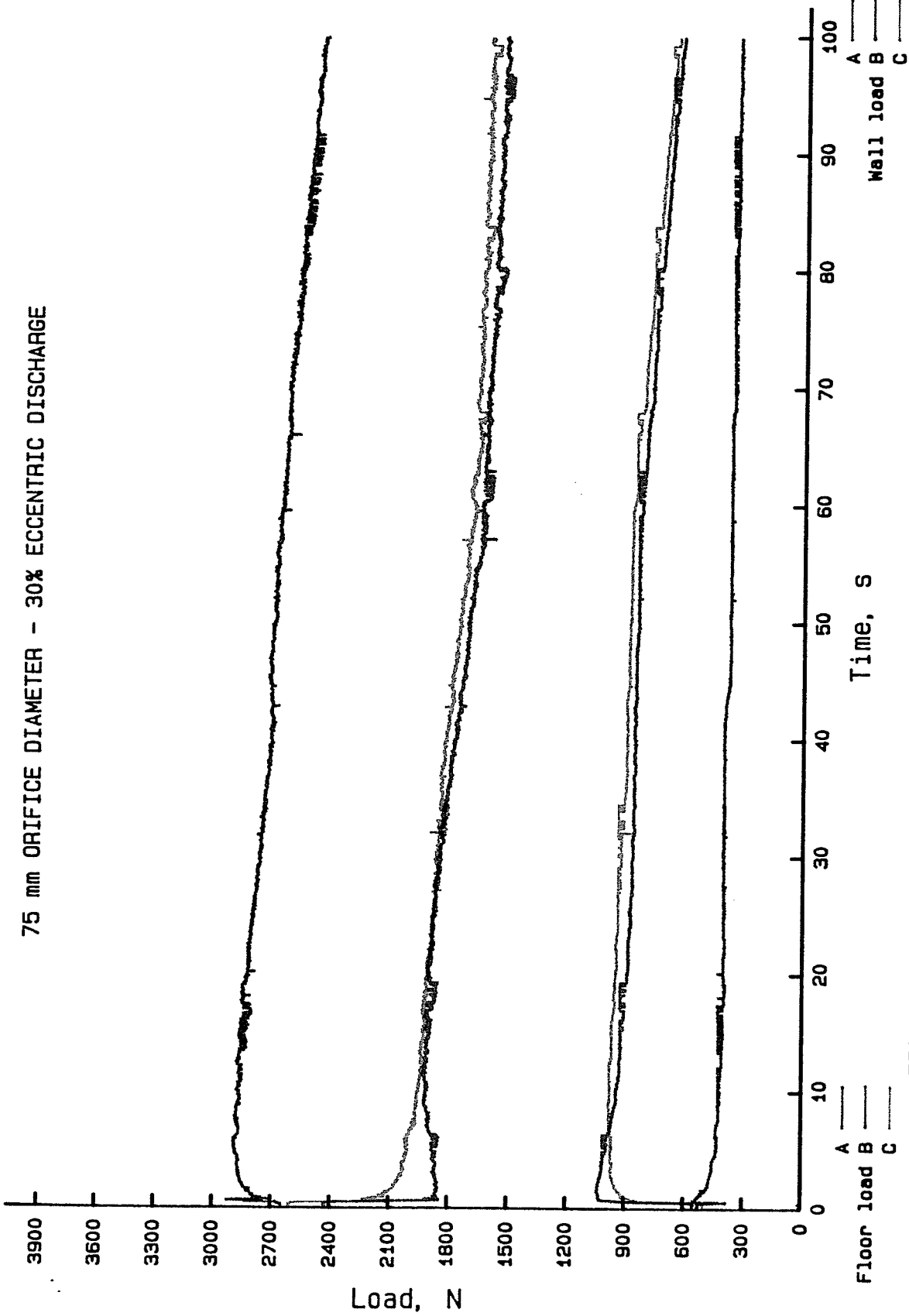


FIGURE D.10 - FLOOR AND WALL LOADS VS. DISCHARGE TIME - test D75E1S1

75 mm ORIFICE DIAMETER - 60% ECCENTRIC DISCHARGE

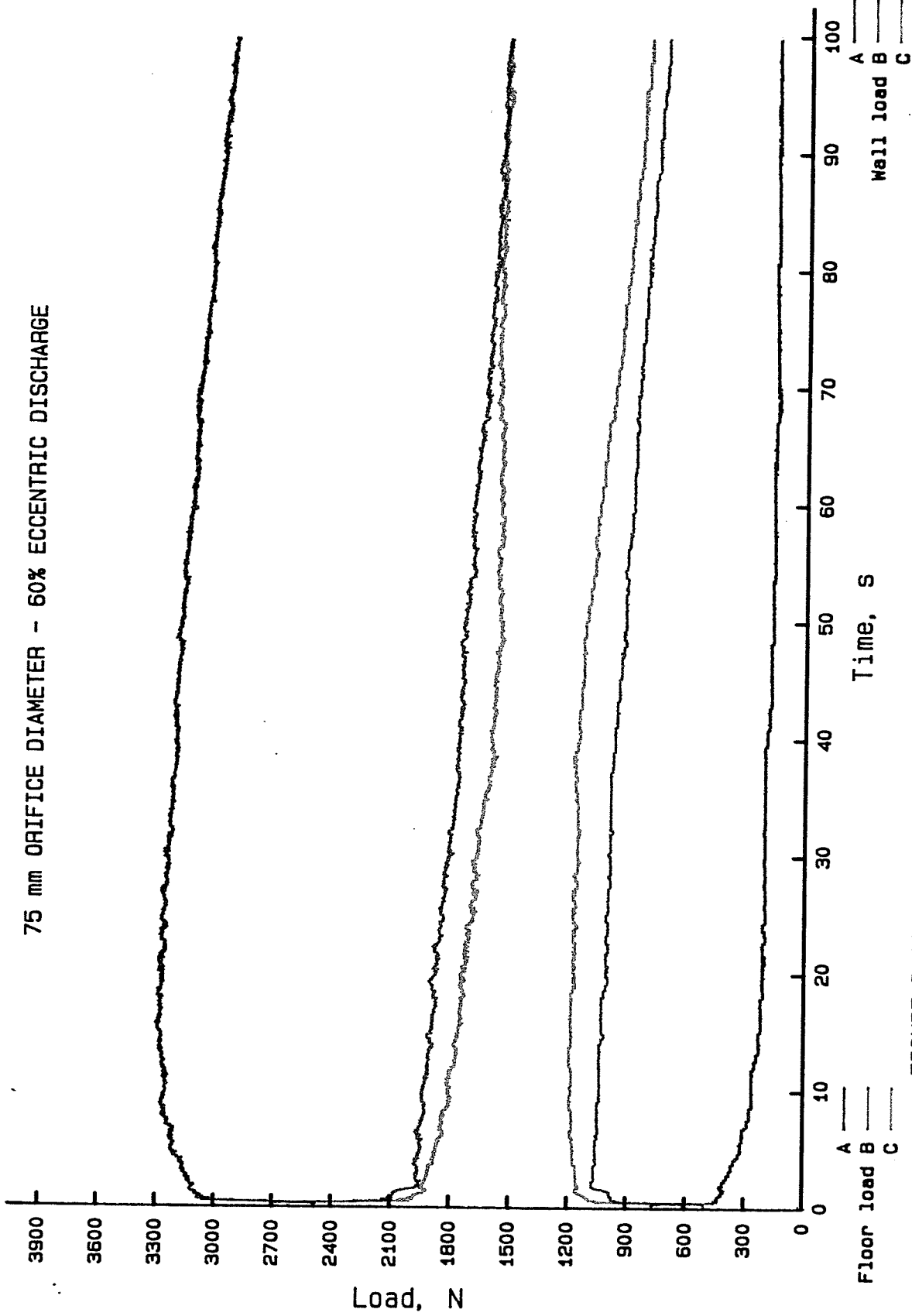


FIGURE D.11 - FLOOR AND WALL LOADS VS. DISCHARGE TIME - test D75E2S1

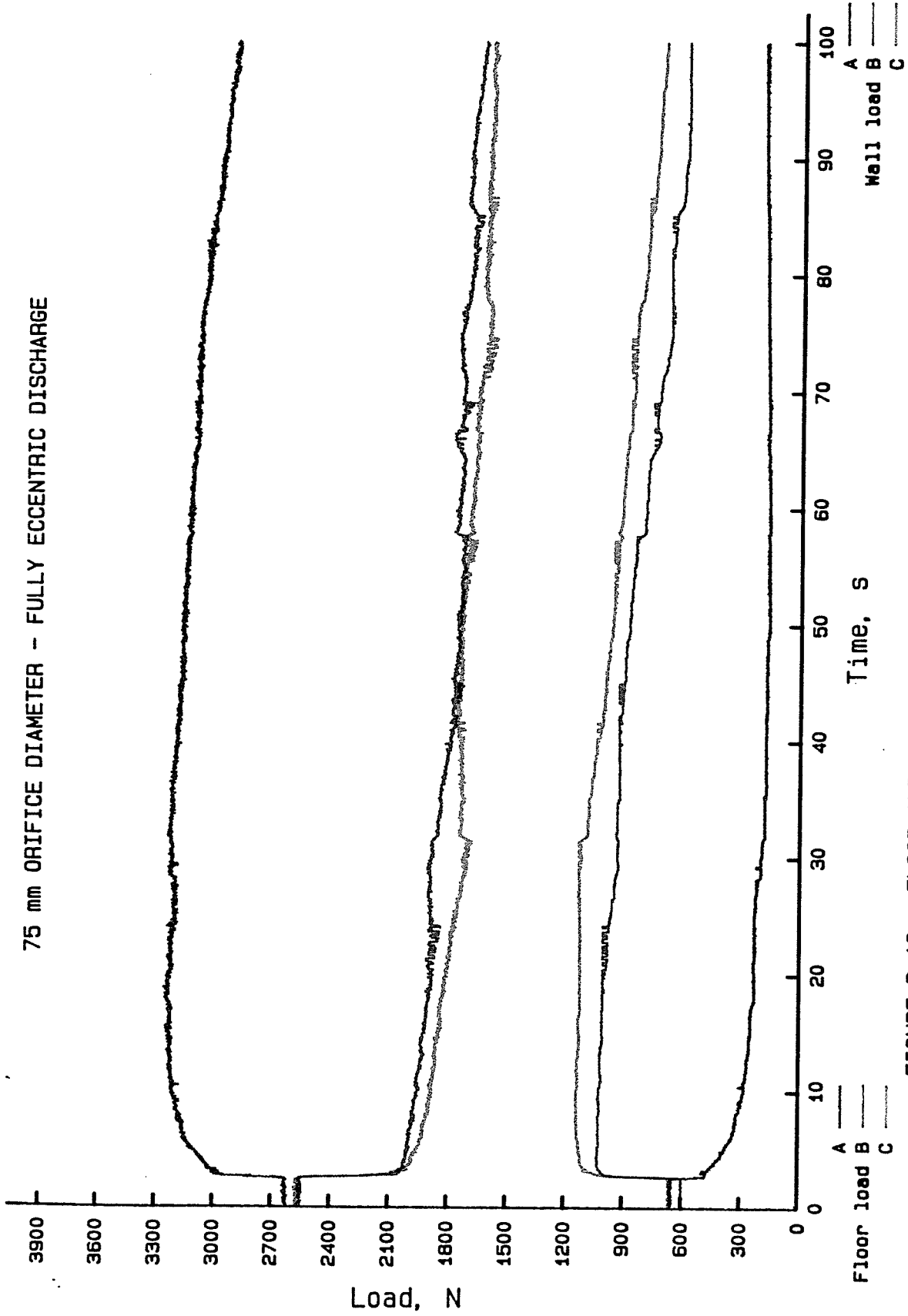


FIGURE D.12 - FLOOR AND WALL LOADS VS. DISCHARGE TIME - test D75E3S1

100 mm ORIFICE DIAMETER - CENTRE DISCHARGE

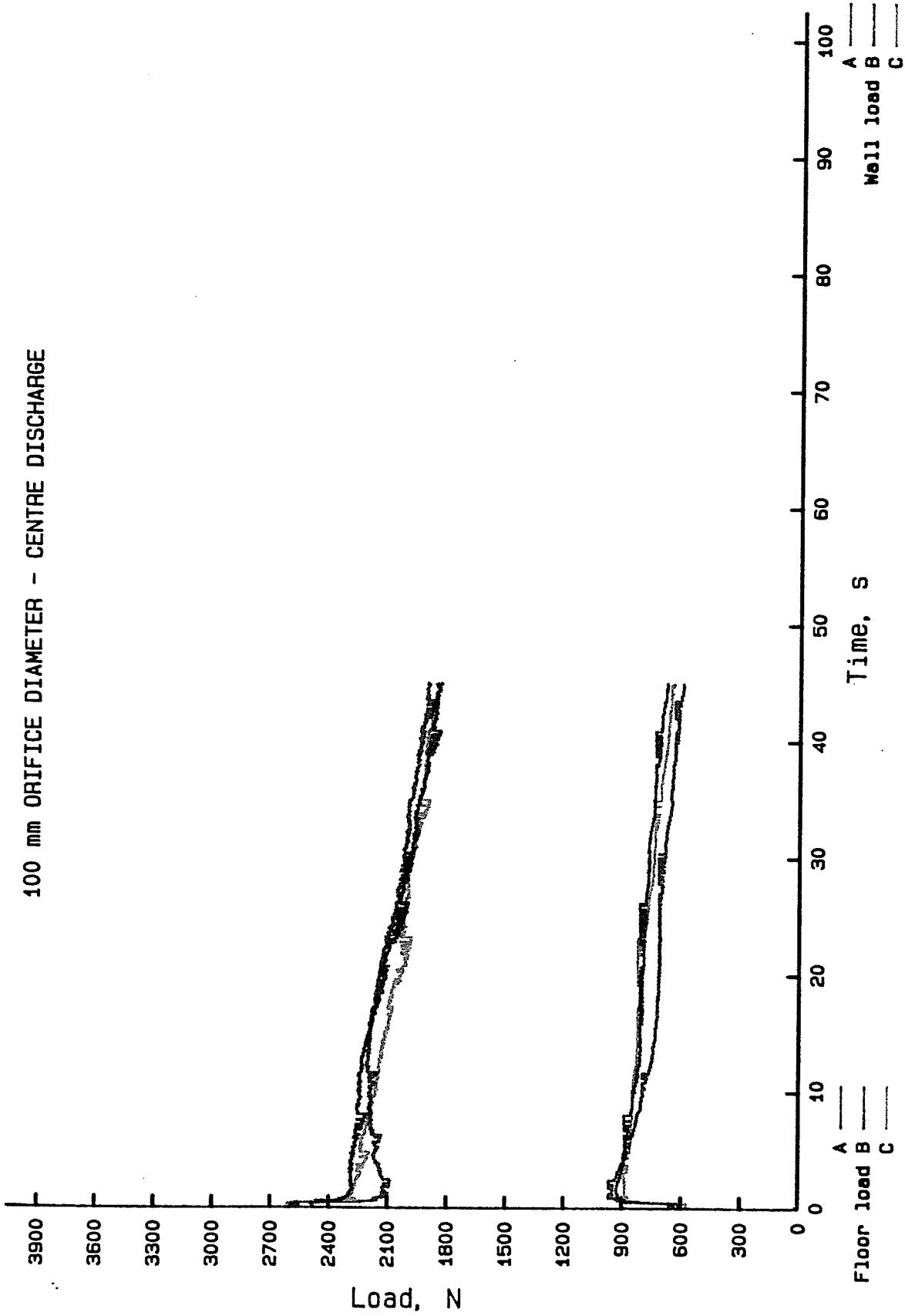


FIGURE D.13 - FLOOR AND WALL LOADS VS. DISCHARGE TIME - test D100E0S1

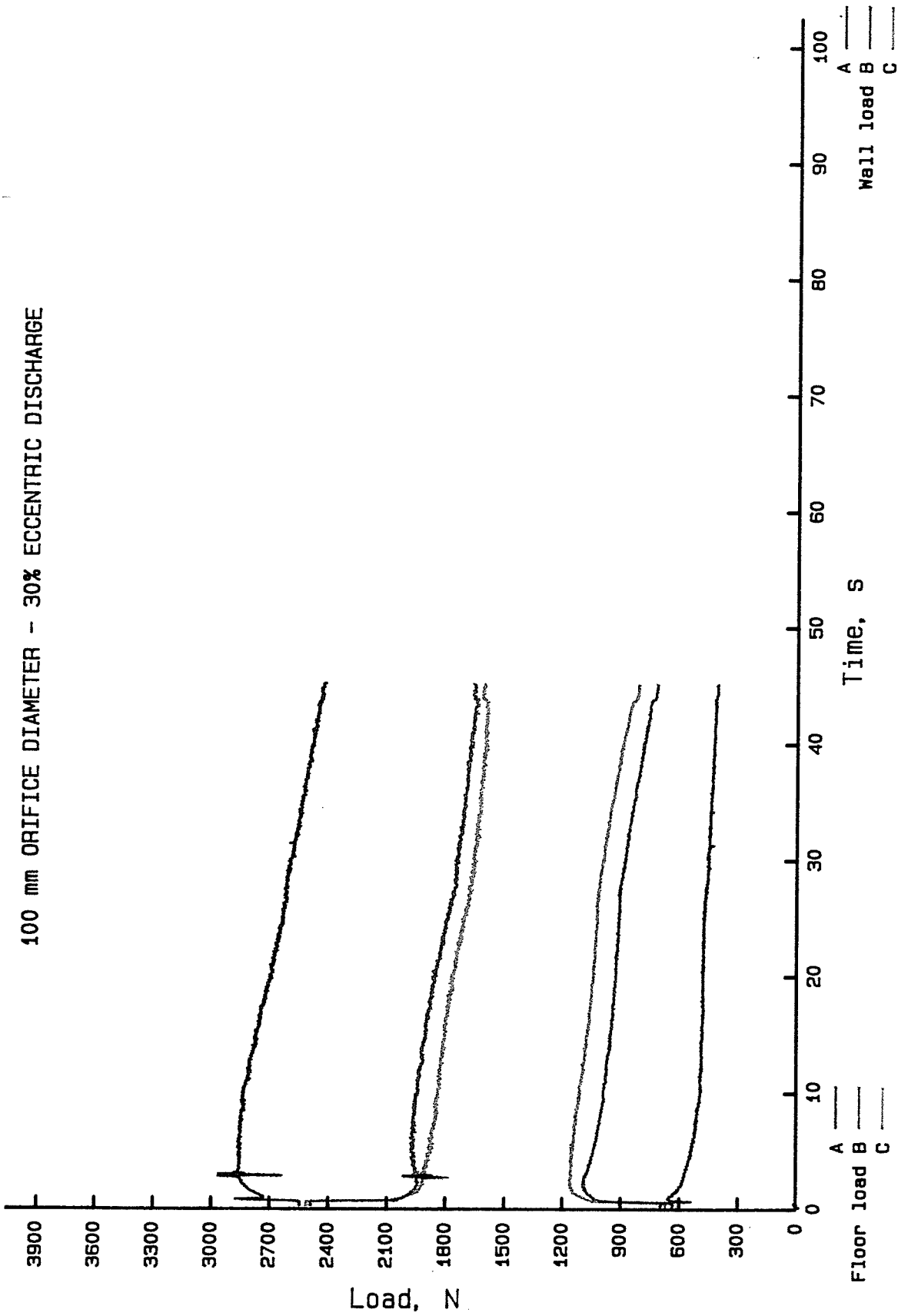


FIGURE D.14 - FLOOR AND WALL LOADS VS. DISCHARGE TIME - test D100E1S1

100 mm ORIFICE DIAMETER - 60% ECCENTRIC DISCHARGE

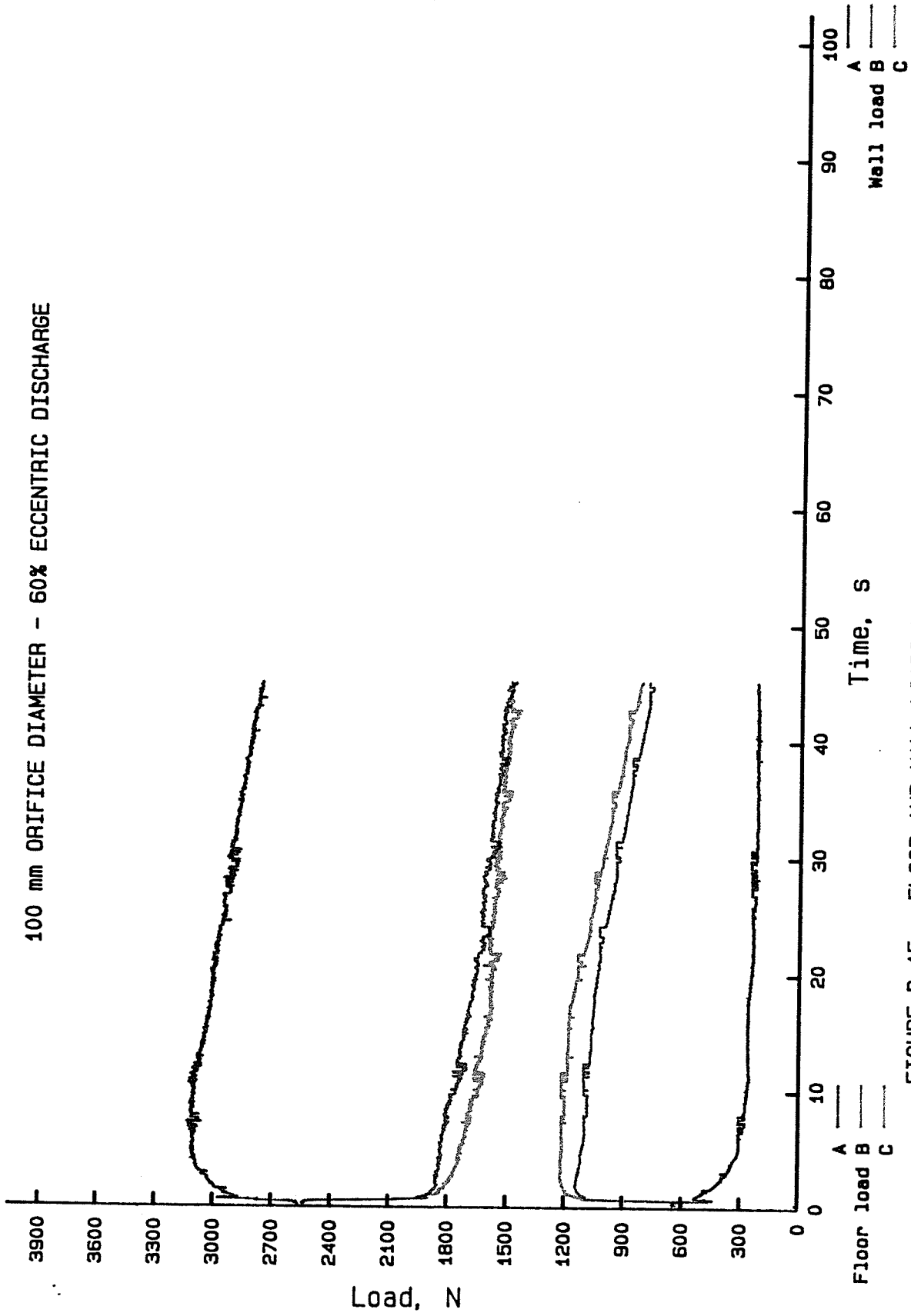


FIGURE D.15 - FLOOR AND WALL LOADS VS. DISCHARGE TIME - test D100E2S1

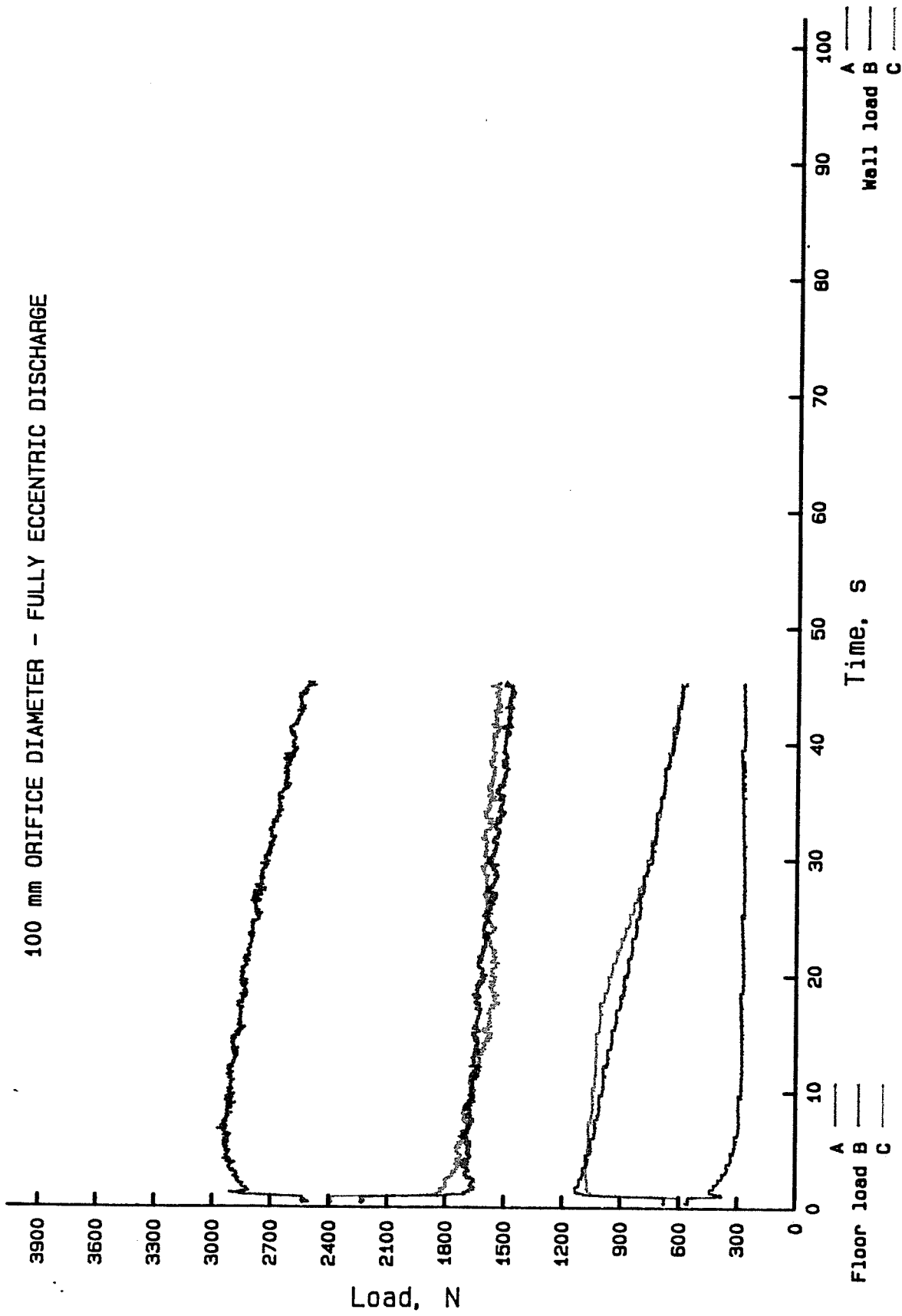


FIGURE D.16 - FLOOR AND WALL LOADS VS. DISCHARGE TIME - test D100E3S1

APPENDIX E

STATIC LOAD ANALYSIS RESULTS

The following tables list the static transducer loads measured during the testing procedure for both the main test series #1 to #3, and the supplemental settling test series #0. For each test, there are three rows of data. The first row corresponds to static loads measured immediately after the bin was filled. The second row corresponds to the transducer loads measured immediately prior to discharge, with the wall and floor values corresponding to percentages of the bin loads listed in the row above. The last row of data lists the transducer readings taken once the bin had been completely discharged.

STATIC RESULTS FOR TEST SERIES 0

	TRANSDUCER LOADS, N						WALL LOADS, N				FLOOR LOADS, N			
	1	2	3	4	5	6	A	B	C	TOTAL	A	B	C	TOTAL
D45E1S0	560	586	585	3265	3426	3399	555	584	592	1731	2914	2677	2768	8360
	499	467	483	3270	3430	3404	32.1%	33.7%	34.2%	17.2%	34.9%	32.0%	33.1%	82.8%
	-2	-2	0	7	10	17								
D60E1S0	606	615	595	3309	3455	3423	606	613	597	1816	2857	2688	2827	8372
	506	471	466	3316	3469	3438	33.4%	33.7%	32.9%	17.8%	34.1%	32.1%	33.8%	82.2%
	0	5	0	0	7	12								
D75E1S0	625	576	546	3345	3503	3469	637	569	540	1747	2857	2775	2939	8571
	424	389	398	3345	3503	3471	36.5%	32.6%	30.9%	16.9%	33.3%	32.4%	34.3%	83.1%
	0	7	-2	7	10	10								
AVERAGE PERCENTAGES:							34.0%	33.4%	32.7%	17.3%	34.1%	32.2%	33.7%	82.7%

STATIC RESULTS FOR TEST SERIES 1

	TRANSDUCER LOADS, N						WALL LOADS, N				FLOOR LOADS, N			
	1	2	3	4	5	6	A	B	C	TOTAL	A	B	C	TOTAL
D45E0S1	661	649	648	3048	3202	3175	663	643	652	1958	2565	2408	2494	7468
	661	644	636	3051	3202	3175	33.9%	32.8%	33.3%	20.8%	34.4%	32.2%	33.4%	79.2%
	2	0	0	0	0	0								
D45E1S1	620	581	561	3152	3292	3283	629	574	558	1762	2674	2603	2689	7966
	618	581	561	3154	3299	3286	35.7%	32.6%	31.7%	18.1%	33.6%	32.7%	33.8%	81.9%
	7	17	0	14	17	10								
D45E2S1	637	557	570	3116	3270	3242	651	543	570	1764	2617	2592	2656	7865
	632	547	556	3128	3279	3259	36.9%	30.8%	32.3%	18.3%	33.3%	33.0%	33.8%	81.7%
	0	17	0	19	19	17								
D45E3S1	674	644	655	2918	3055	3035	679	635	660	1973	2391	2300	2345	7036
	669	634	646	2918	3055	3035	34.4%	32.2%	33.4%	21.9%	34.0%	32.7%	33.3%	78.1%
	0	15	-2	0	-2	-2								
D60E0S1	589	561	609	3152	3299	3288	590	549	620	1759	2745	2638	2597	7981
	589	561	609	3149	3304	3288	33.5%	31.2%	35.3%	18.1%	34.4%	33.1%	32.5%	81.9%
	0	5	0	7	0	7								
D60E1S1	572	532	548	3116	3258	3240	578	522	552	1652	2692	2617	2654	7963
	579	535	551	3113	3258	3242	35.0%	31.6%	33.4%	17.2%	33.8%	32.9%	33.3%	82.8%
	-2	-2	0	0	-2	-2								
D60E2S1	586	569	616	2836	2965	2955	585	558	628	1771	2413	2309	2263	6986
	589	569	612	2836	2965	2955	33.0%	31.5%	35.5%	20.2%	34.5%	33.1%	32.4%	79.8%
	10	24	2	-2	-2	-10								
D60E3S1	627	581	599	3077	3216	3211	634	570	603	1807	2604	2546	2548	7698
	627	581	599	3077	3219	3211	35.1%	31.5%	33.4%	19.0%	33.8%	33.1%	33.1%	81.0%
	-2	7	-2	10	19	17								
D75E0S1	695	629	638	3094	3250	3230	707	617	639	1962	2557	2502	2554	7613
	661	591	599	3096	3250	3230	36.0%	31.4%	32.6%	20.5%	33.6%	32.9%	33.5%	79.5%
	5	-2	0	2	0	7								
D75E1S1	531	557	510	3007	3158	3129	531	559	508	1598	2657	2429	2611	7697
	533	557	510	3007	3158	3129	33.2%	35.0%	31.8%	17.2%	34.5%	31.6%	33.9%	82.8%
	5	5	2	17	17	22								
D75E2S1	531	523	483	3133	3279	3259	536	522	479	1537	2759	2613	2763	8135
	540	523	493	3133	3279	3261	34.9%	34.0%	31.2%	15.9%	33.9%	32.1%	34.0%	84.1%
	0	7	0	0	-2	0								
D75E3S1	661	617	658	3154	3296	3273	665	604	667	1936	2640	2575	2573	7788
	661	617	655	3152	3299	3271	34.4%	31.2%	34.5%	19.9%	33.9%	33.1%	33.0%	80.1%
	0	5	-2	0	7	7								
D100E0S1	635	632	585	3104	3231	3225	640	631	581	1852	2602	2489	2618	7709
	637	629	587	3104	3233	3228	34.6%	34.1%	31.4%	19.4%	33.7%	32.3%	34.0%	80.6%
	0	5	0	10	7	10								
D100E1S1	681	644	660	3084	3221	3206	687	633	665	1985	2546	2477	2504	7527
	681	639	655	3084	3221	3206	34.6%	31.9%	33.5%	20.9%	33.8%	32.9%	33.3%	79.1%
	0	5	0	31	37	36								
D100E2S1	632	600	621	3089	3204	3201	636	590	627	1853	2571	2540	2531	7642
	644	605	624	3089	3206	3201	34.3%	31.8%	33.8%	19.5%	33.6%	33.2%	33.1%	80.5%
	5	0	-2	10	17	10								
D100E3S1	557	659	595	2916	3034	3025	544	670	598	1811	2536	2231	2397	7165
	560	661	595	2916	3036	3025	30.0%	37.0%	33.0%	20.2%	35.4%	31.1%	33.5%	79.8%
	0	12	0	0	5	10								
AVERAGE PERCENTAGES:							34.3%	32.5%	33.1%	19.2%	34.0%	32.6%	33.4%	80.8%

STATIC RESULTS FOR TEST SERIES 2

	TRANSDUCER LOADS, N						WALL LOADS, N				FLOOR LOADS, N			
	1	2	3	4	5	6	A	B	C	TOTAL	A	B	C	TOTAL
D45E0S2	480	479	502	3152	3301	3278	478	473	510	1461	2855	2690	2726	8271
	482	481	502	3152	3299	3278	32.7%	32.3%	34.9%	15.0%	34.5%	32.5%	33.0%	85.0%
	-2	-7	-2	0	-2	0								
D45E1S2	695	661	626	3277	3416	3404	705	656	621	1982	2712	2641	2763	8116
	695	661	626	3277	3416	3404	35.6%	33.1%	31.4%	19.6%	33.4%	32.5%	34.0%	80.4%
	0	0	0	-12	-5	-2								
D45E2S2	516	489	497	3299	3450	3435	520	482	500	1502	2953	2840	2890	8683
	516	491	500	3297	3455	3438	34.6%	32.1%	33.3%	14.7%	34.0%	32.7%	33.3%	85.3%
	-2	-2	0	-7	-7	-2								
D45E3S2	502	493	502	3224	3387	3360	503	487	507	1497	2919	2741	2815	8475
	504	491	502	3224	3391	3360	33.6%	32.5%	33.9%	15.0%	34.4%	32.3%	33.2%	85.0%
	7	0	0	5	0	0								
D60E0S2	623	586	568	3171	3321	3300	632	579	566	1777	2699	2604	2713	8016
	627	588	575	3169	3321	3302	35.6%	32.6%	31.8%	18.1%	33.7%	32.5%	33.8%	81.9%
	2	7	0	-2	0	0								
D60E1S2	627	561	551	3123	3275	3249	641	551	547	1739	2633	2586	2690	7909
	627	557	551	3118	3279	3249	36.8%	31.7%	31.5%	18.0%	33.3%	32.7%	34.0%	82.0%
	-2	-2	-2	-12	-10	-19								
D60E2S2	550	474	619	3217	3370	3348	551	448	644	1643	2849	2823	2621	8293
	550	474	619	3219	3372	3346	33.5%	27.3%	39.2%	16.5%	34.4%	34.0%	31.6%	83.5%
	7	-2	0	7	12	17								
D60E3S2	487	467	466	3222	3374	3346	491	461	468	1420	2898	2765	2860	8523
	487	467	466	3222	3374	3346	34.6%	32.5%	32.9%	14.3%	34.0%	32.4%	33.6%	85.7%
	0	0	0	-2	0	0								
D75E0S2	548	506	478	3152	3314	3288	559	501	473	1532	2771	2655	2797	8223
	550	506	481	3152	3314	3290	36.5%	32.7%	30.9%	15.7%	33.7%	32.3%	34.0%	84.3%
	0	7	0	-2	-2	-2								
D75E1S2	627	523	629	3256	3426	3397	637	498	644	1779	2808	2802	2691	8301
	603	508	604	3256	3426	3399	35.8%	28.0%	36.2%	17.6%	33.8%	33.8%	32.4%	82.4%
	0	-2	0	-2	7	0								
D75E2S2	652	581	561	3222	3384	3355	667	571	555	1794	2715	2661	2792	8168
	654	581	561	3222	3384	3355	37.2%	31.8%	30.9%	18.0%	33.2%	32.6%	34.2%	82.0%
	7	-5	0	7	7	0								
D75E3S2	526	503	478	3217	3370	3348	533	499	475	1507	2853	2724	2852	8429
	526	503	478	3215	3370	3348	35.4%	33.1%	31.5%	15.2%	33.8%	32.3%	33.8%	84.8%
	0	7	-2	0	0	7								
D100E0S2	468	454	478	3157	3314	3298	468	446	485	1400	2889	2731	2750	8370
	472	462	483	3162	3314	3298	33.5%	31.9%	34.7%	14.3%	34.5%	32.6%	32.9%	85.7%
	0	-2	2	7	0	7								
D100E1S2	618	542	578	2988	3136	3117	629	527	582	1738	2519	2493	2492	7504
	608	532	565	2990	3136	3117	36.2%	30.3%	33.5%	18.8%	33.6%	33.2%	33.2%	81.2%
	-19	5	0	0	0	0								
D100E2S2	589	561	512	3253	3423	3399	599	558	505	1662	2848	2694	2872	8414
	589	559	510	3253	3426	3394	36.0%	33.6%	30.4%	16.5%	33.9%	32.0%	34.1%	83.5%
	2	-10	0	0	0	0								
D100E3S2	611	525	529	3142	3299	3278	627	512	526	1665	2675	2656	2724	8055
	613	527	531	3140	3301	3281	37.7%	30.8%	31.6%	17.1%	33.2%	33.0%	33.8%	82.9%
	5	7	0	-2	0	-7								
AVERAGE PERCENTAGES:							35.3%	31.6%	33.0%	16.5%	33.8%	32.7%	33.4%	83.5%

STATIC RESULTS FOR TEST SERIES 3

	TRANSDUCER LOADS, N						WALL LOADS, N				FLOOR LOADS, N			
	1	2	3	4	5	6	A	B	C	TOTAL	A	B	C	TOTAL
D45E0S3	620	576	570	3316	3479	3447	629	568	569	1766	2858	2753	2866	8477
	620	576	573	3318	3477	3450	35.6%	32.1%	32.2%	17.2%	33.7%	32.5%	33.8%	82.8%
	-5	-2	0	-2	0	0								
D45E1S3	511	493	481	3316	3472	3442	516	488	481	1485	2968	2828	2950	8746
	511	493	483	3316	3472	3447	34.7%	32.9%	32.4%	14.5%	33.9%	32.3%	33.7%	85.5%
	-2	7	0	-2	-2	-2								
D45E2S3	521	493	505	3318	3474	3438	525	485	509	1519	2955	2834	2923	8712
	521	493	512	3313	3474	3442	34.6%	31.9%	33.5%	14.8%	33.9%	32.5%	33.5%	85.2%
	-2	-12	0	-2	-2	0								
D45E3S3	492	476	517	3325	3489	3452	491	466	527	1485	3023	2862	2897	8782
	492	476	517	3316	3494	3452	33.1%	31.4%	35.5%	14.5%	34.4%	32.6%	33.0%	85.5%
	7	5	-2	5	0	0								
D60E0S3	521	537	522	3325	3484	3442	519	536	525	1580	2981	2769	2922	8672
	526	537	522	3325	3484	3438	32.9%	33.9%	33.2%	15.4%	34.4%	31.9%	33.7%	84.6%
	0	12	-2	0	0	0								
D60E1S3	434	457	459	3263	3423	3394	429	455	465	1350	3034	2802	2895	8731
	453	454	461	3260	3413	3392	31.8%	33.7%	34.5%	13.4%	34.7%	32.1%	33.2%	86.6%
	-2	-41	0	-10	-10	-10								
D60E2S3	550	493	495	3265	3416	3389	561	483	494	1538	2853	2796	2884	8533
	560	496	502	3265	3416	3389	36.5%	31.4%	32.1%	15.3%	33.4%	32.8%	33.8%	84.7%
	0	5	0	2	7	5								
D60E3S3	472	593	531	3217	3362	3336	455	606	535	1596	2963	2575	2781	8320
	480	593	534	3219	3362	3336	28.5%	38.0%	33.5%	16.1%	35.6%	31.0%	33.4%	83.9%
	0	5	-2	0	-2	0								
D75E0S3	598	513	493	3282	3435	3397	616	503	485	1604	2790	2784	2938	8511
	598	513	493	3284	3433	3397	38.4%	31.3%	30.3%	15.9%	32.8%	32.7%	34.5%	84.1%
	0	0	0	0	2	0								
D75E1S3	598	547	551	3328	3494	3462	607	537	552	1696	2896	2799	2893	8589
	598	547	551	3330	3491	3457	35.8%	31.7%	32.5%	16.5%	33.7%	32.6%	33.7%	83.5%
	-2	0	0	7	0	2								
D75E2S3	642	591	599	3325	3482	3452	651	580	601	1832	2834	2757	2837	8428
	642	588	599	3325	3479	3452	35.5%	31.7%	32.8%	17.9%	33.6%	32.7%	33.7%	82.1%
	0	0	0	0	0	0								
D75E3S3	482	435	473	3325	3469	3435	487	423	480	1390	2974	2916	2951	8840
	492	435	473	3325	3469	3438	35.1%	30.4%	34.5%	13.6%	33.6%	33.0%	33.4%	86.4%
	7	0	0	-2	0	0								
D100E0S3	627	535	551	3306	3464	3423	643	520	550	1713	2798	2796	2887	8481
	627	532	551	3304	3467	3425	37.5%	30.4%	32.1%	16.8%	33.0%	33.0%	34.0%	83.2%
	-2	7	-2	0	10	10								
D100E1S3	521	600	476	3328	3477	3447	518	615	464	1597	2980	2670	3006	8656
	521	600	478	3325	3477	3447	32.4%	38.5%	29.1%	15.6%	34.4%	30.8%	34.7%	84.4%
	2	2	0	7	7	7								
D100E2S3	635	615	575	3275	3426	3404	643	612	570	1825	2792	2667	2822	8281
	632	610	575	3272	3426	3401	35.2%	33.5%	31.3%	18.1%	33.7%	32.2%	34.1%	81.9%
	0	27	0	0	0	7								
D100E3S3	463	454	417	3299	3455	3425	468	453	413	1334	2998	2838	3009	8846
	470	464	425	3301	3455	3428	35.1%	34.0%	30.9%	13.1%	33.9%	32.1%	34.0%	86.9%
	-2	5	0	-2	0	0								
AVERAGE PERCENTAGES:							34.5%	32.9%	32.5%	15.5%	33.9%	32.3%	33.8%	84.5%

APPENDIX F  
DYNAMIC LOAD ANALYSIS RESULTS

DYNAMIC LOAD ANALYSIS FOR SETTLING TESTS

PEAK LOCATION	DELTA	WALL SECTION				FLOOR SECTION				TOTAL LOAD	DISCHARGE TIME, s	
		A	B	C	TOTAL	A	B	C	TOTAL			
D45E1S0	STATIC LOAD, N		555	584	592	1731	2914	2677	2768	8359	10090	-0.63
DELTA	LOAD, N	735	218	893	1013	2124	3443	2282	2188	7913	10037	14.17
	PERCENTAGE		10.3	42.0	47.7	21.2	43.5	28.8	27.7	78.8		
	DSR		0.39	1.53	1.71	1.23	1.18	0.85	0.79	0.95		
B	LOAD, N	732	216	951	945	2112	3481	2204	2315	8000	10112	1.15
	PERCENTAGE		10.2	45.0	44.7	20.9	43.5	27.6	28.9	79.1		
	DSR		0.39	1.63	1.60	1.22	1.19	0.82	0.84	0.96		
C	LOAD, N	730	219	872	1026	2117	3450	2294	2155	7899	10016	19.28
	PERCENTAGE		10.3	41.2	48.5	21.1	43.7	29.0	27.3	78.9		
	DSR		0.39	1.49	1.73	1.22	1.18	0.86	0.78	0.94		
B+C	LOAD, N	726	229	955		2139	3456	2261	2228	7945	10084	6.68
	PERCENTAGE		10.7	44.6		21.2	43.5	28.5	28.0	78.8		
	DSR		0.41	1.62		1.24	1.19	0.84	0.80	0.95		
D60E1S0	STATIC LOAD, N		606	613	597	1816	2857	2688	2827	8372	10188	-0.59
DELTA	LOAD, N	831	165	965	1026	2156	3565	2230	2253	8048	10204	0.86
	PERCENTAGE		7.7	44.8	47.6	21.1	44.3	27.7	28.0	78.9		
	DSR		0.27	1.57	1.72	1.19	1.25	0.83	0.80	0.96		
B	LOAD, N	826	212	1024	1051	2287	3517	2158	2232	7907	10194	2.56
	PERCENTAGE		9.3	44.8	46.0	22.4	44.5	27.3	28.2	77.6		
	DSR		0.35	1.67	1.76	1.26	1.23	0.80	0.79	0.94		
C	LOAD, N	807	217	967	1081	2265	3485	2214	2156	7855	10120	9.11
	PERCENTAGE		9.6	42.7	47.7	22.4	44.4	28.2	27.4	77.6		
	DSR		0.36	1.58	1.81	1.25	1.22	0.82	0.76	0.94		
B+C	LOAD, N	823	217	1040		2296	3511	2166	2221	7898	10194	2.82
	PERCENTAGE		9.5	45.3		22.5	44.5	27.4	28.1	77.5		
	DSR		0.36	1.72		1.26	1.23	0.81	0.79	0.94		
D75E1S0	STATIC LOAD, N		637	569	540	1746	2857	2775	2939	8571	10317	-1.45
DELTA	LOAD, N	1009	8	982	1052	2042	3795	2160	2169	8124	10166	6.47
	PERCENTAGE		0.4	48.1	51.5	20.1	46.7	26.6	26.7	79.9		
	DSR		0.01	1.73	1.95	1.17	1.33	0.78	0.74	0.95		
B	LOAD, N	937	82	1037	1001	2120	3719	2134	2314	8167	10287	1.70
	PERCENTAGE		3.9	48.9	47.2	20.6	45.5	26.1	28.3	79.4		
	DSR		0.13	1.82	1.85	1.21	1.30	0.77	0.79	0.95		
C	LOAD, N	919	65	908	1059	2032	3676	2264	2123	8063	10095	11.34
	PERCENTAGE		3.2	44.7	52.1	20.1	45.6	28.1	26.3	79.9		
	DSR		0.10	1.60	1.96	1.16	1.29	0.82	0.72	0.94		
B+C	LOAD, N	925	103	1028		2159	3697	2147	2257	8101	10260	3.20
	PERCENTAGE		4.8	47.6		21.0	45.6	26.5	27.9	79.0		
	DSR		0.16	1.85		1.24	1.29	0.77	0.77	0.95		

DYNAMIC LOAD ANALYSIS FOR TEST NUMBER D45E0

PEAK LOCATION	DELTA	WALL SECTION				FLOOR SECTION				TOTAL LOAD	DISCHARGE TIME, s	
		A	B	C	TOTAL	A	B	C	TOTAL			
SERIES1	STATIC LOAD, N		663	643	652	1958	2565	2408	2494	7467	9425	-0.52
A	LOAD, N	-84	829	807	684	2320	2361	2195	2474	7030	9350	14.69
	PERCENTAGE		35.7	34.8	29.5	24.8	33.6	31.2	35.2	75.2		
	DSR		1.25	1.26	1.05	1.18	0.92	0.91	0.99	0.94		
B	LOAD, N	-36	793	827	688	2308	2412	2168	2476	7056	9364	14.47
	PERCENTAGE		34.4	35.8	29.8	24.6	34.2	30.7	35.1	75.4		
	DSR		1.20	1.29	1.06	1.18	0.94	0.90	0.99	0.94		
C	LOAD, N	11	747	772	743	2262	2473	2243	2387	7103	9365	13.20
	PERCENTAGE		33.0	34.1	32.8	24.2	34.8	31.6	33.6	75.8		
	DSR		1.13	1.20	1.14	1.16	0.96	0.93	0.96	0.95		
B+C	LOAD, N	4	758	762		2282	2468	2238	2385	7091	9373	11.49
	PERCENTAGE		33.2	33.4		24.3	34.8	31.6	33.6	75.7		
	DSR		1.14	1.18		1.17	0.96	0.93	0.96	0.95		
SERIES2	STATIC LOAD, N		478	473	510	1461	2855	2690	2726	8271	9732	-0.80
A	LOAD, N	-93	837	700	789	2326	2469	2485	2439	7393	9719	2.25
	PERCENTAGE		36.0	30.1	33.9	23.9	33.4	33.6	33.0	76.1		
	DSR		1.75	1.48	1.55	1.59	0.86	0.92	0.89	0.89		
B	LOAD, N	-91	835	701	787	2323	2472	2484	2442	7398	9721	2.24
	PERCENTAGE		35.9	30.2	33.9	23.9	33.4	33.6	33.0	76.1		
	DSR		1.75	1.48	1.54	1.59	0.87	0.92	0.90	0.89		
C	LOAD, N	-93	813	610	830	2253	2485	2605	2379	7469	9722	1.93
	PERCENTAGE		36.1	27.1	36.8	23.2	33.3	34.9	31.9	76.8		
	DSR		1.70	1.29	1.63	1.54	0.87	0.97	0.87	0.90		
B+C	LOAD, N	-88	834	747		2327	2471	2477	2443	7391	9718	2.31
	PERCENTAGE		35.8	32.1		23.9	33.4	33.5	33.1	76.1		
	DSR		1.74	1.52		1.59	0.87	0.92	0.90	0.89		
SERIES3	STATIC LOAD, N		629	568	569	1766	2858	2753	2866	8477	10243	-0.46
A	LOAD, N	-145	785	707	573	2065	2674	2605	2904	8183	10248	0.50
	PERCENTAGE		38.0	34.2	27.7	20.2	32.7	31.8	35.5	79.8		
	DSR		1.25	1.24	1.01	1.17	0.94	0.95	1.01	0.97		
B	LOAD, N	-48	756	753	663	2172	2725	2544	2782	8051	10223	5.11
	PERCENTAGE		34.8	34.7	30.5	21.2	33.8	31.6	34.6	78.8		
	DSR		1.20	1.33	1.17	1.23	0.95	0.92	0.97	0.95		
C	LOAD, N	-38	749	740	682	2171	2714	2564	2744	8022	10193	9.15
	PERCENTAGE		34.5	34.1	31.4	21.3	33.8	32.0	34.2	78.7		
	DSR		1.19	1.30	1.20	1.23	0.95	0.93	0.96	0.95		
B+C	LOAD, N	-38	749	712		2172	2737	2542	2770	8049	10221	5.86
	PERCENTAGE		34.5	32.8		21.3	34.0	31.6	34.4	78.7		
	DSR		1.19	1.25		1.23	0.96	0.92	0.97	0.95		

DYNAMIC LOAD ANALYSIS FOR TEST NUMBER D45E1

PEAK LOCATION	DELTA	WALL SECTION				FLOOR SECTION				TOTAL LOAD	DISCHARGE TIME, s	
		A	B	C	TOTAL	A	B	C	TOTAL			
SERIES1	STATIC LOAD, N		629	574	558	1761	2674	2603	2689	7966	9727	-0.38
DELTA	LOAD, N	535	403	903	973	2279	3001	2080	2038	7119	9398	69.96
	PERCENTAGE		17.7	39.6	42.7	24.2	42.2	29.2	28.6	75.8		
	DSR		0.64	1.57	1.74	1.29	1.12	0.80	0.76	0.89		
B	LOAD, N	472	499	997	945	2441	2960	2079	2228	7267	9708	6.87
	PERCENTAGE		20.4	40.8	38.7	25.1	40.7	28.6	30.7	74.9		
	DSR		0.79	1.74	1.69	1.39	1.11	0.80	0.83	0.91		
C	LOAD, N	511	445	927	985	2357	2998	2129	2096	7223	9580	32.83
	PERCENTAGE		18.9	39.3	41.8	24.6	41.5	29.5	29.0	75.4		
	DSR		0.71	1.61	1.77	1.34	1.12	0.82	0.78	0.91		
B+C	LOAD, N	486	488	974		2435	2982	2082	2205	7269	9704	7.91
	PERCENTAGE		20.0	40.0		25.1	41.0	28.6	30.3	74.9		
	DSR		0.78	1.72		1.38	1.12	0.80	0.82	0.91		
SERIES2	STATIC LOAD, N		705	656	621	1982	2712	2641	2763	8116	10098	-0.38
DELTA	LOAD, N	636	310	911	980	2201	3269	2269	2233	7771	9972	26.81
	PERCENTAGE		14.1	41.4	44.5	22.1	42.1	29.2	28.7	77.9		
	DSR		0.44	1.39	1.58	1.11	1.21	0.86	0.81	0.96		
B	LOAD, N	552	422	976	971	2369	3191	2225	2291	7707	10076	4.58
	PERCENTAGE		17.8	41.2	41.0	23.5	41.4	28.9	29.7	76.5		
	DSR		0.60	1.49	1.56	1.20	1.18	0.84	0.83	0.95		
C	LOAD, N	610	358	939	997	2294	3258	2255	2238	7751	10045	12.93
	PERCENTAGE		15.6	40.9	43.5	22.8	42.0	29.1	28.9	77.2		
	DSR		0.51	1.43	1.61	1.16	1.20	0.85	0.81	0.96		
B+C	LOAD, N	590	385	975		2335	3218	2240	2261	7719	10054	8.13
	PERCENTAGE		16.5	41.8		23.2	41.7	29.0	29.3	76.8		
	DSR		0.55	1.53		1.18	1.19	0.85	0.82	0.95		
SERIES3	STATIC LOAD, N		516	488	481	1485	2968	2828	2950	8746	10231	-0.64
DELTA	LOAD, N	618	289	805	1008	2102	3345	2362	2158	7865	9967	54.22
	PERCENTAGE		13.7	38.3	48.0	21.1	42.5	30.0	27.4	78.9		
	DSR		0.56	1.65	2.10	1.42	1.13	0.84	0.73	0.90		
B	LOAD, N	461	467	918	938	2323	3166	2327	2402	7895	10218	3.01
	PERCENTAGE		20.1	39.5	40.4	22.7	40.1	29.5	30.4	77.3		
	DSR		0.91	1.88	1.95	1.56	1.07	0.82	0.81	0.90		
C	LOAD, N	539	412	881	1020	2313	3233	2371	2273	7877	10190	8.32
	PERCENTAGE		17.8	38.1	44.1	22.7	41.0	30.1	28.9	77.3		
	DSR		0.80	1.81	2.12	1.56	1.09	0.84	0.77	0.90		
B+C	LOAD, N	539	414	953		2320	3243	2357	2276	7876	10196	7.57
	PERCENTAGE		17.8	41.1		22.8	41.2	29.9	28.9	77.2		
	DSR		0.80	1.97		1.56	1.09	0.83	0.77	0.90		

DYNAMIC LOAD ANALYSIS FOR TEST NUMBER D45E2

PEAK LOCATION	DELTA	WALL SECTION				FLOOR SECTION				TOTAL LOAD	DISCHARGE TIME, s	
		A	B	C	TOTAL	A	B	C	TOTAL			
SERIES1	STATIC LOAD, N		651	543	570	1764	2617	2592	2656	7865	9629	-0.50
DELTA	LOAD, N	900	121	958	1084	2163	3392	1928	1843	7163	9326	73.47
	PERCENTAGE		5.6	44.3	50.1	23.2	47.4	26.9	25.7	76.8		
	DSR		0.19	1.76	1.90	1.23	1.30	0.74	0.69	0.91		
B	LOAD, N	798	228	984	1067	2279	3301	1994	1976	7271	9550	25.36
	PERCENTAGE		10.0	43.2	46.8	23.9	45.4	27.4	27.2	76.1		
	DSR		0.35	1.81	1.87	1.29	1.26	0.77	0.74	0.92		
C	LOAD, N	841	205	976	1116	2297	3327	2007	1899	7233	9530	30.14
	PERCENTAGE		8.9	42.5	48.6	24.1	46.0	27.7	26.3	75.9		
	DSR		0.31	1.80	1.96	1.30	1.27	0.77	0.71	0.92		
B+C	LOAD, N	842	207	1049	2304	3327	1997	1904	7228	9532	9532	29.47
	PERCENTAGE		9.0	45.5	24.2	46.0	27.6	26.3	75.8			
	DSR		0.32	1.88	1.31	1.27	0.77	0.72	0.92			
SERIES2	STATIC LOAD, N		520	482	500	1502	2953	2840	2890	8683	10185	-0.44
DELTA	LOAD, N	1047	17	1009	1118	2144	3737	2023	1966	7726	9870	63.71
	PERCENTAGE		0.8	47.1	52.1	21.7	48.4	26.2	25.4	78.3		
	DSR		0.03	2.09	2.24	1.43	1.27	0.71	0.68	0.89		
B	LOAD, N	907	164	1038	1103	2305	3546	2131	2114	7791	10096	15.67
	PERCENTAGE		7.1	45.0	47.9	22.8	45.5	27.4	27.1	77.2		
	DSR		0.32	2.15	2.21	1.53	1.20	0.75	0.73	0.90		
C	LOAD, N	985	96	983	1179	2258	3660	2167	1964	7791	10049	29.13
	PERCENTAGE		4.3	43.5	52.2	22.5	47.0	27.8	25.2	77.5		
	DSR		0.18	2.04	2.36	1.50	1.24	0.76	0.68	0.90		
B+C	LOAD, N	984	101	1085	2270	3638	2144	2007	7789	10059	10059	27.51
	PERCENTAGE		4.4	47.8	22.6	46.7	27.5	25.8	77.4			
	DSR		0.19	2.21	1.51	1.23	0.75	0.69	0.90			
SERIES3	STATIC LOAD, N		525	485	509	1519	2955	2834	2923	8712	10231	-0.49
DELTA	LOAD, N	1087	-6	983	1179	2156	3772	2135	1943	7850	10006	46.48
	PERCENTAGE		-0.3	45.6	54.7	21.5	48.1	27.2	24.8	78.5		
	DSR		-0.01	2.03	2.32	1.42	1.28	0.75	0.66	0.90		
B	LOAD, N	1018	50	1012	1123	2185	3719	2113	2059	7891	10076	29.63
	PERCENTAGE		2.3	46.3	51.4	21.7	47.1	26.8	26.1	78.3		
	DSR		0.10	2.09	2.21	1.44	1.26	0.75	0.70	0.91		
C	LOAD, N	1087	-6	983	1179	2156	3772	2135	1943	7850	10006	46.48
	PERCENTAGE		-0.3	45.6	54.7	21.5	48.1	27.2	24.8	78.5		
	DSR		-0.01	2.03	2.32	1.42	1.28	0.75	0.66	0.90		
B+C	LOAD, N	1084	2	1086	2174	3758	2116	1964	7838	10012	10012	45.27
	PERCENTAGE		0.1	50.0	21.7	47.9	27.0	25.1	78.3			
	DSR		0.00	2.19	1.43	1.27	0.75	0.67	0.90			

DYNAMIC LOAD ANALYSIS FOR TEST NUMBER D45E3

PEAK LOCATION	DELTA	WALL SECTION				FLOOR SECTION				TOTAL LOAD	DISCHARGE TIME, s
		A	B	C	TOTAL	A	B	C	TOTAL		
SERIES1	STATIC LOAD, N	679	635	660	1974	2391	2300	2345	7036	9010	-0.63
DELTA	LOAD, N	621	264	818	952	2034	2980	1935	1827	6742	8776
	PERCENTAGE		13.0	40.2	46.8	23.2	44.2	28.7	27.1	76.8	
	DSR		0.39	1.29	1.44	1.03	1.25	0.84	0.78	0.96	
B	LOAD, N	558	339	859	934	2132	2902	1970	1947	6819	8951
	PERCENTAGE		15.9	40.3	43.8	23.8	42.6	28.9	28.6	76.2	
	DSR		0.50	1.35	1.42	1.08	1.21	0.86	0.83	0.97	
C	LOAD, N	618	282	826	973	2081	2963	1971	1840	6774	8855
	PERCENTAGE		13.6	39.7	46.8	23.5	43.7	29.1	27.2	76.5	
	DSR		0.42	1.30	1.47	1.05	1.24	0.86	0.78	0.96	
B+C	LOAD, N	612	297	909	2115	2950	1949	1866	6765	8880	27.04
	PERCENTAGE		14.0	43.0	23.8	43.6	28.8	27.6	76.2		
	DSR		0.44	1.40	1.07	1.23	0.85	0.80	0.96		
SERIES2	STATIC LOAD, N	503	487	507	1497	2919	2741	2815	8475	9972	-0.38
DELTA	LOAD, N	825	74	824	974	1872	3583	2204	2083	7870	9742
	PERCENTAGE		4.0	44.0	52.0	19.2	45.5	28.0	26.5	80.8	
	DSR		0.15	1.69	1.92	1.25	1.23	0.80	0.74	0.93	
B	LOAD, N	783	153	884	988	2025	3515	2204	2149	7868	9893
	PERCENTAGE		7.6	43.7	48.8	20.5	44.7	28.0	27.3	79.5	
	DSR		0.30	1.82	1.95	1.35	1.20	0.80	0.76	0.93	
C	LOAD, N	800	141	859	1022	2022	3512	2263	2075	7850	9872
	PERCENTAGE		7.0	42.5	50.5	20.5	44.7	28.8	26.4	79.5	
	DSR		0.28	1.76	2.02	1.35	1.20	0.83	0.74	0.93	
B+C	LOAD, N	797	151	948	2047	3498	2223	2118	7839	9886	17.99
	PERCENTAGE		7.4	46.3	20.7	44.6	28.4	27.0	79.3		
	DSR		0.30	1.91	1.37	1.20	0.81	0.75	0.92		
SERIES3	STATIC LOAD, N	491	466	527	1484	3023	2862	2897	8782	10266	-2.06
DELTA	LOAD, N	954	91	956	1133	2180	3665	2144	2035	7844	10024
	PERCENTAGE		4.2	43.9	52.0	21.7	46.7	27.3	25.9	78.3	
	DSR		0.19	2.05	2.15	1.47	1.21	0.75	0.70	0.89	
B	LOAD, N	551	454	992	1018	2464	3261	2239	2303	7803	10267
	PERCENTAGE		18.4	40.3	41.3	24.0	41.8	28.7	29.5	76.0	
	DSR		0.92	2.13	1.93	1.66	1.08	0.78	0.79	0.89	
C	LOAD, N	876	183	970	1147	2300	3559	2216	2097	7872	10172
	PERCENTAGE		8.0	42.2	49.9	22.6	45.2	28.2	26.6	77.4	
	DSR		0.37	2.08	2.18	1.55	1.18	0.77	0.72	0.90	
B+C	LOAD, N	925	137	1062	2261	3610	2168	2081	7859	10120	33.24
	PERCENTAGE		6.1	47.0	22.3	45.9	27.6	26.5	77.7		
	DSR		0.28	2.14	1.52	1.19	0.76	0.72	0.89		

DYNAMIC LOAD ANALYSIS FOR TEST NUMBER D60E0

PEAK LOCATION	DELTA	WALL SECTION				FLOOR SECTION				TOTAL LOAD	DISCHARGE TIME, s	
		A	B	C	TOTAL	A	B	C	TOTAL			
SERIES1	STATIC LOAD, N		590	549	620	1759	2745	2638	2597	7980	9739	-0.48
A	LOAD, N	-73	832	741	778	2351	2479	2431	2447	7357	9708	2.29
	PERCENTAGE		35.4	31.5	33.1	24.2	33.7	33.0	33.3	75.8		
	DSR		1.41	1.35	1.25	1.34	0.90	0.92	0.94	0.92		
B	LOAD, N	-63	821	743	773	2337	2500	2428	2460	7388	9725	2.05
	PERCENTAGE		35.1	31.8	33.1	24.0	33.8	32.9	33.3	76.0		
	DSR		1.39	1.35	1.25	1.33	0.91	0.92	0.95	0.93		
C	LOAD, N	-54	815	730	792	2337	2505	2442	2422	7369	9706	3.11
	PERCENTAGE		34.9	31.2	33.9	24.1	34.0	33.1	32.9	75.9		
	DSR		1.38	1.33	1.28	1.33	0.91	0.93	0.93	0.92		
B+C	LOAD, N	-45	811	767		2344	2502	2421	2429	7352	9696	4.17
	PERCENTAGE		34.6	32.7		24.2	34.0	32.9	33.0	75.8		
	DSR		1.37	1.31		1.33	0.91	0.92	0.94	0.92		
SERIES2	STATIC LOAD, N		632	579	566	1777	2699	2604	2713	8016	9793	-0.49
A	LOAD, N	-71	919	853	844	2616	2389	2327	2429	7145	9761	3.24
	PERCENTAGE		35.1	32.6	32.3	26.8	33.4	32.6	34.0	73.2		
	DSR		1.45	1.47	1.49	1.47	0.89	0.89	0.90	0.89		
B	LOAD, N	-47	896	855	843	2594	2425	2298	2388	7111	9705	7.63
	PERCENTAGE		34.5	33.0	32.5	26.7	34.1	32.3	33.6	73.3		
	DSR		1.42	1.48	1.49	1.46	0.90	0.88	0.88	0.89		
C	LOAD, N	-63	913	847	853	2613	2406	2328	2417	7151	9764	2.65
	PERCENTAGE		34.9	32.4	32.6	26.8	33.6	32.6	33.8	73.2		
	DSR		1.44	1.46	1.51	1.47	0.89	0.89	0.89	0.89		
B+C	LOAD, N	-63	913	850		2613	2406	2328	2417	7151	9764	2.65
	PERCENTAGE		34.9	32.5		26.8	33.6	32.6	33.8	73.2		
	DSR		1.44	1.48		1.47	0.89	0.89	0.89	0.89		
SERIES3	STATIC LOAD, N		519	536	525	1580	2981	2769	2922	8672	10252	-0.54
A	LOAD, N	-98	870	767	778	2415	2593	2563	2683	7839	10254	0.34
	PERCENTAGE		36.0	31.8	32.2	23.6	33.1	32.7	34.2	76.4		
	DSR		1.68	1.43	1.48	1.53	0.87	0.93	0.92	0.90		
B	LOAD, N	-45	833	786	791	2410	2618	2492	2625	7735	10145	9.47
	PERCENTAGE		34.6	32.6	32.8	23.8	33.8	32.2	33.9	76.2		
	DSR		1.61	1.47	1.51	1.53	0.88	0.90	0.90	0.89		
C	LOAD, N	-47	833	774	798	2405	2630	2518	2629	7777	10182	6.38
	PERCENTAGE		34.6	32.2	33.2	23.6	33.8	32.4	33.8	76.4		
	DSR		1.61	1.44	1.52	1.52	0.88	0.91	0.90	0.90		
B+C	LOAD, N	-45	833	789		2410	2618	2492	2625	7735	10145	9.47
	PERCENTAGE		34.6	32.7		23.8	33.8	32.2	33.9	76.2		
	DSR		1.61	1.49		1.53	0.88	0.90	0.90	0.89		

DYNAMIC LOAD ANALYSIS FOR TEST NUMBER D60E1

PEAK LOCATION	DELTA	WALL SECTION				FLOOR SECTION				TOTAL LOAD	DISCHARGE TIME, s	
		A	B	C	TOTAL	A	B	C	TOTAL			
SERIES1	STATIC LOAD, N		578	522	552	1652	2692	2617	2654	7963	9615	-0.32
DELTA	LOAD, N	554	371	859	991	2221	3001	2092	1978	7071	9292	28.96
	PERCENTAGE		16.7	38.7	44.6	23.9	42.4	29.6	28.0	76.1		
	DSR		0.64	1.65	1.80	1.34	1.11	0.80	0.75	0.89		
B	LOAD, N	455	502	912	1001	2415	2917	2155	2097	7169	9584	2.58
	PERCENTAGE		20.8	37.8	41.4	25.2	40.7	30.1	29.3	74.8		
	DSR		0.87	1.75	1.81	1.46	1.08	0.82	0.79	0.90		
C	LOAD, N	521	434	879	1030	2343	2993	2169	2028	7190	9533	8.21
	PERCENTAGE		18.5	37.5	44.0	24.6	41.6	30.2	28.2	75.4		
	DSR		0.75	1.68	1.87	1.42	1.11	0.83	0.76	0.90		
B+C	LOAD, N	505	458	963	2384	2976	2162	2037	7175	9559	5.86	
	PERCENTAGE		19.2	40.4	24.9	41.5	30.1	28.4	75.1			
	DSR		0.79	1.79	1.44	1.11	0.83	0.77	0.90			
SERIES2	STATIC LOAD, N		641	551	547	1739	2633	2586	2690	7909	9648	-0.35
DELTA	LOAD, N	514	343	807	906	2056	3003	2098	2058	7159	9215	38.52
	PERCENTAGE		16.7	39.3	44.1	22.3	41.9	29.3	28.7	77.7		
	DSR		0.54	1.46	1.66	1.18	1.14	0.81	0.77	0.91		
B	LOAD, N	478	450	920	936	2306	2977	2104	2187	7268	9574	6.33
	PERCENTAGE		19.5	39.9	40.6	24.1	41.0	28.9	30.1	75.9		
	DSR		0.70	1.67	1.71	1.33	1.13	0.81	0.81	0.92		
C	LOAD, N	489	419	864	952	2235	3014	2156	2131	7301	9536	11.17
	PERCENTAGE		18.7	38.7	42.6	23.4	41.3	29.5	29.2	76.6		
	DSR		0.65	1.57	1.74	1.29	1.14	0.83	0.79	0.92		
B+C	LOAD, N	478	450	928	2306	2977	2104	2187	7268	9574	6.33	
	PERCENTAGE		19.5	40.2	24.1	41.0	28.9	30.1	75.9			
	DSR		0.70	1.69	1.33	1.13	0.81	0.81	0.92			
SERIES3	STATIC LOAD, N		429	455	465	1349	3034	2802	2895	8731	10080	-0.40
DELTA	LOAD, N	657	312	875	1063	2250	3276	2271	2100	7647	9897	13.65
	PERCENTAGE		13.9	38.9	47.2	22.7	42.8	29.7	27.5	77.3		
	DSR		0.73	1.92	2.29	1.67	1.08	0.81	0.73	0.88		
B	LOAD, N	514	435	980	918	2333	3156	2192	2381	7729	10062	0.66
	PERCENTAGE		18.6	42.0	39.3	23.2	40.8	28.4	30.8	76.8		
	DSR		1.01	2.15	1.97	1.73	1.04	0.78	0.82	0.89		
C	LOAD, N	654	313	869	1064	2246	3277	2276	2101	7654	9900	13.57
	PERCENTAGE		13.9	38.7	47.4	22.7	42.8	29.7	27.4	77.3		
	DSR		0.73	1.91	2.29	1.66	1.08	0.81	0.73	0.88		
B+C	LOAD, N	608	382	990	2361	3220	2187	2259	7666	10027	2.51	
	PERCENTAGE		16.2	41.9	23.5	42.0	28.5	29.5	76.5			
	DSR		0.89	2.15	1.75	1.06	0.78	0.78	0.88			

DYNAMIC LOAD ANALYSIS FOR TEST NUMBER D60E2

PEAK LOCATION	DELTA	WALL SECTION				FLOOR SECTION				TOTAL LOAD	DISCHARGE TIME, s	
		A	B	C	TOTAL	A	B	C	TOTAL			
SERIES1	STATIC LOAD, N		585	558	628	1771	2413	2309	2263	6985	8756	-0.32
DELTA	LOAD, N	720	237	894	1020	2151	2921	1769	1648	6338	8489	24.25
	PERCENTAGE		11.0	41.6	47.4	25.3	46.1	27.9	26.0	74.7		
	DSR		0.41	1.60	1.62	1.21	1.21	0.77	0.73	0.91		
B	LOAD, N	707	268	934	1016	2218	2914	1782	1712	6408	8626	12.08
	PERCENTAGE		12.1	42.1	45.8	25.7	45.5	27.8	26.7	74.3		
	DSR		0.46	1.67	1.62	1.25	1.21	0.77	0.76	0.92		
C	LOAD, N	702	274	905	1047	2226	2912	1821	1673	6406	8632	11.87
	PERCENTAGE		12.3	40.7	47.0	25.8	45.5	28.4	26.1	74.2		
	DSR		0.47	1.62	1.67	1.26	1.21	0.79	0.74	0.92		
B+C	LOAD, N	698	289	987	2263	2263	2894	1800	1694	6388	8651	9.72
	PERCENTAGE		12.8	43.6	26.2	26.2	45.3	28.2	26.5	73.8		
	DSR		0.49	1.66	1.28	1.28	1.20	0.78	0.75	0.91		
SERIES2	STATIC LOAD, N		551	448	644	1643	2849	2823	2621	8293	9936	-0.43
DELTA	LOAD, N	1051	-3	977	1119	2093	3616	1939	1810	7365	9458	42.54
	PERCENTAGE		-0.1	46.7	53.5	22.1	49.1	26.3	24.6	77.9		
	DSR		-0.01	2.18	1.74	1.27	1.27	0.69	0.69	0.89		
B	LOAD, N	814	245	1051	1066	2362	3391	2034	2107	7532	9894	3.71
	PERCENTAGE		10.4	44.5	45.1	23.9	45.0	27.0	28.0	76.1		
	DSR		0.44	2.35	1.66	1.44	1.19	0.72	0.80	0.91		
C	LOAD, N	993	95	1000	1175	2270	3568	2039	1860	7467	9737	18.58
	PERCENTAGE		4.2	44.1	51.8	23.3	47.8	27.3	24.9	76.7		
	DSR		0.17	2.23	1.82	1.38	1.25	0.72	0.71	0.90		
B+C	LOAD, N	1001	96	1097	2289	2289	3567	2015	1868	7450	9739	17.33
	PERCENTAGE		4.2	47.9	23.5	23.5	47.9	27.0	25.1	76.5		
	DSR		0.17	2.01	1.39	1.39	1.25	0.71	0.71	0.90		
SERIES3	STATIC LOAD, N		561	483	494	1538	2853	2796	2884	8533	10071	-0.54
DELTA	LOAD, N	1075	-16	1001	1116	2101	3661	1912	1848	7421	9522	49.77
	PERCENTAGE		-0.8	47.6	53.1	22.1	49.3	25.8	24.9	77.9		
	DSR		-0.03	2.07	2.26	1.37	1.28	0.68	0.64	0.87		
B	LOAD, N	1047	56	1054	1151	2261	3646	1983	1932	7561	9822	22.04
	PERCENTAGE		2.5	46.6	50.9	23.0	48.2	26.2	25.6	77.0		
	DSR		0.10	2.18	2.33	1.47	1.28	0.71	0.67	0.89		
C	LOAD, N	997	114	1028	1194	2336	3588	2074	1921	7583	9919	13.32
	PERCENTAGE		4.9	44.0	51.1	23.6	47.3	27.4	25.3	76.4		
	DSR		0.20	2.13	2.42	1.52	1.26	0.74	0.67	0.89		
B+C	LOAD, N	997	121	1118	2357	2357	3581	2053	1922	7556	9913	14.00
	PERCENTAGE		5.1	47.4	23.8	23.8	47.4	27.2	25.4	76.2		
	DSR		0.22	2.29	1.53	1.53	1.26	0.73	0.67	0.89		

DYNAMIC LOAD ANALYSIS FOR TEST NUMBER D60E3

PEAK LOCATION	DELTA	WALL SECTION				FLOOR SECTION				TOTAL LOAD	DISCHARGE TIME, s
		A	B	C	TOTAL	A	B	C	TOTAL		
SERIES1	STATIC LOAD, N	634	570	603	1807	2604	2546	2548	7698	9505	-0.54
DELTA	LOAD, N	770	261	980	1082	2323	3184	1909	1827	6920	9243
	PERCENTAGE		11.2	42.2	46.6	25.1	46.0	27.6	26.4	74.9	
	DSR		0.41	1.72	1.79	1.29	1.22	0.75	0.72	0.90	
B	LOAD, N	591	462	1044	1062	2568	2971	1958	1994	6923	9491
	PERCENTAGE		18.0	40.7	41.4	27.1	42.9	28.3	28.8	72.9	
	DSR		0.73	1.83	1.76	1.42	1.14	0.77	0.78	0.90	
C	LOAD, N	753	303	1008	1104	2415	3143	1937	1860	6940	9355
	PERCENTAGE		12.5	41.7	45.7	25.8	45.3	27.9	26.8	74.2	
	DSR		0.48	1.77	1.83	1.34	1.21	0.76	0.73	0.90	
B+C	LOAD, N	595	462	1057	2576	2973	1960	1982	6915	9491	9491
	PERCENTAGE		17.9	41.0	27.1	43.0	28.3	28.7	72.9		
	DSR		0.73	1.80	1.43	1.14	0.77	0.78	0.90	2.08	
SERIES2	STATIC LOAD, N	491	461	468	1420	2898	2765	2860	8523	9943	-0.43
DELTA	LOAD, N	888	94	900	1063	2057	3524	2098	1967	7589	9646
	PERCENTAGE		4.6	43.8	51.7	21.3	46.4	27.6	25.9	78.7	
	DSR		0.19	1.95	2.27	1.45	1.22	0.76	0.69	0.89	
B	LOAD, N	717	284	978	1023	2285	3323	2128	2166	7617	9902
	PERCENTAGE		12.4	42.8	44.8	23.1	43.6	27.9	28.4	76.9	
	DSR		0.58	2.12	2.19	1.61	1.15	0.77	0.76	0.89	
C	LOAD, N	854	159	937	1089	2185	3464	2126	2008	7598	9783
	PERCENTAGE		7.3	42.9	49.8	22.3	45.6	28.0	26.4	77.7	
	DSR		0.32	2.03	2.33	1.54	1.20	0.77	0.70	0.89	
B+C	LOAD, N	826	195	1021	2236	3427	2120	2059	7606	9842	9842
	PERCENTAGE		8.7	45.6	22.7	45.1	27.9	27.1	77.3		
	DSR		0.40	2.20	1.57	1.18	0.77	0.72	0.89	8.92	
SERIES3	STATIC LOAD, N	455	606	535	1596	2963	2575	2781	8319	9915	-0.75
DELTA	LOAD, N	880	168	1004	1091	2263	3451	2046	2016	7513	9776
	PERCENTAGE		7.4	44.4	48.2	23.1	45.9	27.2	26.8	76.9	
	DSR		0.37	1.66	2.04	1.42	1.16	0.79	0.72	0.90	
B	LOAD, N	575	445	1039	1001	2485	3137	2081	2229	7447	9932
	PERCENTAGE		17.9	41.8	40.3	25.0	42.1	27.9	29.9	75.0	
	DSR		0.98	1.71	1.87	1.56	1.06	0.81	0.80	0.90	
C	LOAD, N	862	190	1002	1101	2293	3417	2060	2022	7499	9792
	PERCENTAGE		8.3	43.7	48.0	23.4	45.6	27.5	27.0	76.6	
	DSR		0.42	1.65	2.06	1.44	1.15	0.80	0.73	0.90	
B+C	LOAD, N	831	223	1054	2331	3385	2057	2050	7492	9823	9823
	PERCENTAGE		9.6	45.2	23.7	45.2	27.5	27.4	76.3		
	DSR		0.49	1.85	1.46	1.14	0.80	0.74	0.90	8.60	

DYNAMIC LOAD ANALYSIS FOR TEST NUMBER D75E0

PEAK LOCATION	DELTA	WALL SECTION				FLOOR SECTION				TOTAL LOAD	DISCHARGE TIME, s	
		A	B	C	TOTAL	A	B	C	TOTAL			
SERIES1	STATIC LOAD, N		707	617	639	1963	2557	2502	2554	7613	9576	-0.41
A	LOAD, N	-103	856	768	739	2363	2445	2299	2429	7173	9536	0.14
	PERCENTAGE		36.2	32.5	31.3	24.8	34.1	32.1	33.9	75.2		
	DSR		1.21	1.24	1.16	1.20	0.96	0.92	0.95	0.94		
B	LOAD, N	-82	850	788	749	2387	2404	2329	2467	7200	9587	0.35
	PERCENTAGE		35.6	33.0	31.4	24.9	33.4	32.3	34.3	75.1		
	DSR		1.20	1.28	1.17	1.22	0.94	0.93	0.97	0.95		
C	LOAD, N	-49	831	765	799	2395	2429	2326	2372	7127	9522	2.85
	PERCENTAGE		34.7	31.9	33.4	25.2	34.1	32.6	33.3	74.8		
	DSR		1.18	1.24	1.25	1.22	0.95	0.93	0.93	0.94		
B+C	LOAD, N	-47	833	786		2405	2428	2315	2364	7107	9512	2.64
	PERCENTAGE		34.6	32.7		25.3	34.2	32.6	33.3	74.7		
	DSR		1.18	1.25		1.23	0.95	0.93	0.93	0.93		
SERIES2	STATIC LOAD, N		559	501	473	1533	2771	2655	2797	8223	9756	-0.45
A	LOAD, N	-48	819	819	724	2362	2510	2316	2540	7366	9728	1.17
	PERCENTAGE		34.7	34.7	30.7	24.3	34.1	31.4	34.5	75.7		
	DSR		1.47	1.63	1.53	1.54	0.91	0.87	0.91	0.90		
B	LOAD, N	-26	801	829	722	2352	2531	2278	2543	7352	9704	2.63
	PERCENTAGE		34.1	35.2	30.7	24.2	34.4	31.0	34.6	75.8		
	DSR		1.43	1.65	1.53	1.53	0.91	0.86	0.91	0.89		
C	LOAD, N	-21	788	804	731	2323	2534	2310	2506	7350	9673	4.07
	PERCENTAGE		33.9	34.6	31.5	24.0	34.5	31.4	34.1	76.0		
	DSR		1.41	1.60	1.55	1.52	0.91	0.87	0.90	0.89		
B+C	LOAD, N	-22	800	778		2356	2542	2295	2529	7366	9722	1.75
	PERCENTAGE		34.0	33.0		24.2	34.5	31.2	34.3	75.8		
	DSR		1.43	1.60		1.54	0.92	0.86	0.90	0.90		
SERIES3	STATIC LOAD, N		616	503	485	1604	2790	2784	2938	8512	10116	-0.20
A	LOAD, N	-268	968	693	707	2368	2384	2538	2629	7551	9919	0.44
	PERCENTAGE		40.9	29.3	29.9	23.9	31.6	33.6	34.8	76.1		
	DSR		1.57	1.38	1.46	1.48	0.85	0.91	0.89	0.89		
B	LOAD, N	-134	938	798	810	2546	2465	2496	2591	7552	10098	1.71
	PERCENTAGE		36.8	31.3	31.8	25.2	32.6	33.1	34.3	74.8		
	DSR		1.52	1.59	1.67	1.59	0.88	0.90	0.88	0.89		
C	LOAD, N	-141	939	786	811	2536	2463	2507	2583	7553	10089	1.42
	PERCENTAGE		37.0	31.0	32.0	25.1	32.6	33.2	34.2	74.9		
	DSR		1.52	1.56	1.67	1.58	0.88	0.90	0.88	0.89		
B+C	LOAD, N	-134	938	804		2546	2465	2496	2591	7552	10098	1.71
	PERCENTAGE		36.8	31.6		25.2	32.6	33.1	34.3	74.8		
	DSR		1.52	1.63		1.59	0.88	0.90	0.88	0.89		

DYNAMIC LOAD ANALYSIS FOR TEST NUMBER D75E1

PEAK LOCATION	DELTA	WALL SECTION				FLOOR SECTION				TOTAL LOAD	DISCHARGE TIME, s	
		A	B	C	TOTAL	A	B	C	TOTAL			
SERIES1	STATIC LOAD, N		531	559	508	1598	2657	2429	2611	7697	9295	-0.41
DELTA	LOAD, N	576	382	976	940	2298	2828	2044	2252	7124	9422	0.11
	PERCENTAGE		16.6	42.5	40.9	24.4	39.7	28.7	31.6	75.6		
	DSR		0.72	1.75	1.85	1.44	1.06	0.84	0.86	0.93		
B	LOAD, N	487	497	1042	925	2464	2823	1836	2148	6807	9271	1.05
	PERCENTAGE		20.2	42.3	37.5	26.6	41.5	27.0	31.6	73.4		
	DSR		0.94	1.86	1.82	1.54	1.06	0.76	0.82	0.88		
C	LOAD, N	556	424	968	992	2384	2891	1902	1970	6763	9147	7.31
	PERCENTAGE		17.8	40.6	41.6	26.1	42.7	28.1	29.1	73.9		
	DSR		0.80	1.73	1.95	1.49	1.09	0.78	0.75	0.88		
B+C	LOAD, N	530	471	1001		2473	2869	1864	2049	6782	9255	2.07
	PERCENTAGE		19.0	40.5		26.7	42.3	27.5	30.2	73.3		
	DSR		0.89	1.88		1.55	1.08	0.77	0.78	0.88		
SERIES2	STATIC LOAD, N		637	498	644	1779	2808	2802	2691	8301	10080	-1.58
DELTA	LOAD, N	635	330	868	1062	2260	3239	2239	2052	7530	9790	14.53
	PERCENTAGE		14.6	38.4	47.0	23.1	43.0	29.7	27.3	76.9		
	DSR		0.52	1.74	1.65	1.27	1.15	0.80	0.76	0.91		
B	LOAD, N	589	414	958	1047	2419	3248	2219	2177	7644	10063	1.17
	PERCENTAGE		17.1	39.6	43.3	24.0	42.5	29.0	28.5	76.0		
	DSR		0.65	1.92	1.63	1.36	1.16	0.79	0.81	0.92		
C	LOAD, N	620	366	891	1080	2337	3248	2263	2080	7591	9928	7.09
	PERCENTAGE		15.7	38.1	46.2	23.5	42.8	29.8	27.4	76.5		
	DSR		0.57	1.79	1.68	1.31	1.16	0.81	0.77	0.91		
B+C	LOAD, N	589	414	1003		2419	3248	2219	2177	7644	10063	1.17
	PERCENTAGE		17.1	41.4		24.0	42.5	29.0	28.5	76.0		
	DSR		0.65	1.76		1.36	1.16	0.79	0.81	0.92		
SERIES3	STATIC LOAD, N		607	537	552	1696	2896	2799	2893	8588	10284	-1.11
DELTA	LOAD, N	661	287	875	1020	2182	3355	2232	2143	7730	9912	18.39
	PERCENTAGE		13.2	40.1	46.7	22.0	43.4	28.9	27.7	78.0		
	DSR		0.47	1.63	1.85	1.29	1.16	0.80	0.74	0.90		
B	LOAD, N	485	483	981	954	2418	3102	2335	2413	7850	10268	0.26
	PERCENTAGE		20.0	40.6	39.5	23.5	39.5	29.7	30.7	76.5		
	DSR		0.80	1.83	1.73	1.43	1.07	0.83	0.83	0.91		
C	LOAD, N	624	361	926	1043	2330	3325	2292	2209	7826	10156	6.79
	PERCENTAGE		15.5	39.7	44.8	22.9	42.5	29.3	28.2	77.1		
	DSR		0.59	1.72	1.89	1.37	1.15	0.82	0.76	0.91		
B+C	LOAD, N	614	386	1000		2386	3267	2245	2292	7804	10190	4.46
	PERCENTAGE		16.2	41.9		23.4	41.9	28.8	29.4	76.6		
	DSR		0.64	1.84		1.41	1.13	0.80	0.79	0.91		

DYNAMIC LOAD ANALYSIS FOR TEST NUMBER D75E2

PEAK LOCATION	DELTA	WALL SECTION				FLOOR SECTION				TOTAL LOAD	DISCHARGE TIME, s	
		A	B	C	TOTAL	A	B	C	TOTAL			
SERIES1	STATIC LOAD, N		536	522	479	1537	2759	2613	2763	8135	9672	-0.42
DELTA	LOAD, N	901	218	1042	1195	2455	3289	1884	1749	6922	9377	17.51
	PERCENTAGE		8.9	42.4	48.7	26.2	47.5	27.2	25.3	73.8		
	DSR		0.41	2.00	2.49	1.60	1.19	0.72	0.63	0.85		
B	LOAD, N	695	423	1085	1151	2659	3127	1962	1956	7045	9704	1.38
	PERCENTAGE		15.9	40.8	43.3	27.4	44.4	27.8	27.8	72.6		
	DSR		0.79	2.08	2.40	1.73	1.13	0.75	0.71	0.87		
C	LOAD, N	892	236	1051	1204	2491	3295	1916	1771	6982	9473	12.80
	PERCENTAGE		9.5	42.2	48.3	26.3	47.2	27.4	25.4	73.7		
	DSR		0.44	2.01	2.51	1.62	1.19	0.73	0.64	0.86		
B+C	LOAD, N	820	312	1132	2576	2576	3239	1961	1850	7050	9626	5.71
	PERCENTAGE		12.1	43.9	26.8	26.8	45.9	27.8	26.2	73.2		
	DSR		0.58	2.26	1.68	1.68	1.17	0.75	0.67	0.87		
SERIES2	STATIC LOAD, N		667	571	555	1793	2715	2661	2792	8168	9961	-1.27
DELTA	LOAD, N	1008	110	1043	1193	2346	3525	1920	1820	7265	9611	17.22
	PERCENTAGE		4.7	44.5	50.9	24.4	48.5	26.4	25.1	75.6		
	DSR		0.16	1.83	2.15	1.31	1.30	0.72	0.65	0.89		
B	LOAD, N	866	274	1113	1167	2554	3350	1958	1989	7297	9851	5.05
	PERCENTAGE		10.7	43.6	45.7	25.9	45.9	26.8	27.3	74.1		
	DSR		0.41	1.95	2.10	1.42	1.23	0.74	0.71	0.89		
C	LOAD, N	992	141	1059	1206	2406	3499	1946	1845	7290	9696	12.66
	PERCENTAGE		5.9	44.0	50.1	24.8	48.0	26.7	25.3	75.2		
	DSR		0.21	1.85	2.17	1.34	1.29	0.73	0.66	0.89		
B+C	LOAD, N	963	189	1152	2493	2493	3462	1917	1909	7288	9781	8.38
	PERCENTAGE		7.6	46.2	25.5	25.5	47.5	26.3	26.2	74.5		
	DSR		0.28	2.05	1.39	1.39	1.28	0.72	0.68	0.89		
SERIES3	STATIC LOAD, N		651	580	601	1832	2834	2757	2837	8428	10260	-1.75
DELTA	LOAD, N	1151	-54	1016	1178	2140	3649	1835	1742	7226	9366	42.66
	PERCENTAGE		-2.5	47.5	55.0	22.8	50.5	25.4	24.1	77.2		
	DSR		-0.08	1.75	1.96	1.17	1.29	0.67	0.61	0.86		
B	LOAD, N	864	226	1065	1115	2406	3439	2285	2261	7985	10391	0.14
	PERCENTAGE		9.4	44.3	46.3	23.2	43.1	28.6	28.3	76.8		
	DSR		0.35	1.84	1.86	1.31	1.21	0.83	0.80	0.95		
C	LOAD, N	989	142	1012	1250	2404	3656	2166	1902	7724	10128	6.67
	PERCENTAGE		5.9	42.1	52.0	23.7	47.3	28.0	24.6	76.3		
	DSR		0.22	1.74	2.08	1.31	1.29	0.79	0.67	0.92		
B+C	LOAD, N	1073	71	1144	2358	2358	3647	2121	1911	7679	10037	10.54
	PERCENTAGE		3.0	48.5	23.5	23.5	47.5	27.6	24.9	76.5		
	DSR		0.11	1.94	1.29	1.29	1.29	0.77	0.67	0.91		

DYNAMIC LOAD ANALYSIS FOR TEST NUMBER D75E3

PEAK LOCATION	DELTA	WALL SECTION				FLOOR SECTION				TOTAL LOAD	DISCHARGE TIME, s	
		A	B	C	TOTAL	A	B	C	TOTAL			
SERIES1	STATIC LOAD, N		665	604	667	1936	2640	2575	2573	7788	9724	-2.39
DELTA	LOAD, N	849	194	943	1142	2279	3250	1889	1692	6831	9110	29.20
	PERCENTAGE		8.5	41.4	50.1	25.0	47.6	27.7	24.8	75.0		
	DSR		0.29	1.56	1.71	1.18	1.23	0.73	0.66	0.88		
B	LOAD, N	670	415	1043	1126	2584	3084	2020	1997	7101	9685	1.79
	PERCENTAGE		16.1	40.4	43.6	26.7	43.4	28.4	28.1	73.3		
	DSR		0.62	1.73	1.69	1.33	1.17	0.78	0.78	0.91		
C	LOAD, N	814	276	1029	1150	2455	3232	1957	1882	7071	9526	9.16
	PERCENTAGE		11.2	41.9	46.8	25.8	45.7	27.7	26.6	74.2		
	DSR		0.42	1.70	1.72	1.27	1.22	0.76	0.73	0.91		
B+C	LOAD, N	795	299	1094		2486	3211	1977	1900	7088	9574	6.76
	PERCENTAGE		12.0	44.0		26.0	45.3	27.9	26.8	74.0		
	DSR		0.45	1.72		1.28	1.22	0.77	0.74	0.91		
SERIES2	STATIC LOAD, N		533	499	475	1507	2853	2724	2852	8429	9936	-3.98
DELTA	LOAD, N	885	116	950	1051	2117	3424	1921	1874	7219	9336	31.13
	PERCENTAGE		5.5	44.9	49.6	22.7	47.4	26.6	26.0	77.3		
	DSR		0.22	1.90	2.21	1.40	1.20	0.71	0.66	0.86		
B	LOAD, N	572	465	1090	983	2538	3108	2028	2256	7392	9930	0.49
	PERCENTAGE		18.3	42.9	38.7	25.6	42.0	27.4	30.5	74.4		
	DSR		0.87	2.18	2.07	1.68	1.09	0.74	0.79	0.88		
C	LOAD, N	859	207	1019	1112	2338	3404	2020	1968	7392	9730	11.05
	PERCENTAGE		8.9	43.6	47.6	24.0	46.0	27.3	26.6	76.0		
	DSR		0.39	2.04	2.34	1.55	1.19	0.74	0.69	0.88		
B+C	LOAD, N	838	237	1075		2387	3384	2006	2015	7405	9792	7.48
	PERCENTAGE		9.9	45.0		24.4	45.7	27.1	27.2	75.6		
	DSR		0.44	2.21		1.58	1.19	0.74	0.71	0.88		
SERIES3	STATIC LOAD, N		487	423	480	1390	2974	2916	2951	8841	10231	-0.74
DELTA	LOAD, N	975	120	1006	1183	2309	3571	2099	1911	7581	9890	16.43
	PERCENTAGE		5.2	43.6	51.2	23.3	47.1	27.7	25.2	76.7		
	DSR		0.25	2.38	2.46	1.66	1.20	0.72	0.65	0.86		
B	LOAD, N	832	296	1132	1123	2551	3372	2102	2170	7644	10195	0.38
	PERCENTAGE		11.6	44.4	44.0	25.0	44.1	27.5	28.4	75.0		
	DSR		0.61	2.68	2.34	1.84	1.13	0.72	0.74	0.86		
C	LOAD, N	963	121	970	1198	2289	3541	2102	1904	7547	9836	18.41
	PERCENTAGE		5.3	42.4	52.3	23.3	46.9	27.9	25.2	76.7		
	DSR		0.25	2.29	2.50	1.65	1.19	0.72	0.65	0.85		
B+C	LOAD, N	727	413	1140		2692	3290	2108	2112	7510	10202	1.24
	PERCENTAGE		15.3	42.3		26.4	43.8	28.1	28.1	73.6		
	DSR		0.85	2.52		1.94	1.11	0.72	0.72	0.85		

DYNAMIC LOAD ANALYSIS FOR TEST NUMBER D100E0

PEAK LOCATION	DELTA	WALL SECTION				FLOOR SECTION				TOTAL LOAD	DISCHARGE TIME, s	
		A	B	C	TOTAL	A	B	C	TOTAL			
SERIES1	STATIC LOAD, N		640	631	581	1852	2602	2489	2618	7709	9561	-0.38
A	LOAD, N	-16	942	960	893	2795	2293	2136	2284	6713	9508	1.12
	PERCENTAGE		33.7	34.3	31.9	29.4	34.2	31.8	34.0	70.6		
	DSR		1.47	1.52	1.54	1.51	0.88	0.86	0.87	0.87		
B	LOAD, N	-1	928	980	875	2783	2322	2114	2319	6755	9538	0.47
	PERCENTAGE		33.3	35.2	31.4	29.2	34.4	31.3	34.3	70.8		
	DSR		1.45	1.55	1.51	1.50	0.89	0.85	0.89	0.88		
C	LOAD, N	-3	899	889	903	2691	2295	2184	2215	6694	9385	3.97
	PERCENTAGE		33.4	33.0	33.6	28.7	34.3	32.6	33.1	71.3		
	DSR		1.40	1.41	1.55	1.45	0.88	0.88	0.85	0.87		
B+C	LOAD, N	15	921	936		2793	2332	2120	2296	6748	9541	0.39
	PERCENTAGE		33.0	33.5		29.3	34.6	31.4	34.0	70.7		
	DSR		1.44	1.54		1.51	0.90	0.85	0.88	0.88		
SERIES2	STATIC LOAD, N		468	446	485	1399	2889	2731	2750	8370	9769	-0.41
A	LOAD, N	-51	863	828	796	2487	2482	2323	2420	7225	9712	0.29
	PERCENTAGE		34.7	33.3	32.0	25.6	34.4	32.2	33.5	74.4		
	DSR		1.84	1.86	1.64	1.78	0.86	0.85	0.88	0.86		
B	LOAD, N	31	754	857	712	2323	2728	2416	2583	7727	10050	0.10
	PERCENTAGE		32.5	36.9	30.7	23.1	35.3	31.3	33.4	76.9		
	DSR		1.61	1.92	1.47	1.66	0.94	0.88	0.94	0.92		
C	LOAD, N	-18	831	818	809	2458	2487	2311	2396	7194	9652	2.43
	PERCENTAGE		33.8	33.3	32.9	25.5	34.6	32.1	33.3	74.5		
	DSR		1.78	1.83	1.67	1.76	0.86	0.85	0.87	0.86		
B+C	LOAD, N	-25	849	824		2497	2492	2318	2431	7241	9738	0.83
	PERCENTAGE		34.0	33.0		25.6	34.4	32.0	33.6	74.4		
	DSR		1.81	1.77		1.78	0.86	0.85	0.88	0.87		
SERIES3	STATIC LOAD, N		643	520	550	1713	2798	2796	2887	8481	10194	-0.44
A	LOAD, N	3	874	864	890	2628	2580	2399	2485	7464	10092	2.18
	PERCENTAGE		33.3	32.9	33.9	26.0	34.6	32.1	33.3	74.0		
	DSR		1.36	1.66	1.62	1.53	0.92	0.86	0.86	0.88		
B	LOAD, N	78	771	892	805	2468	2675	2307	2551	7533	10001	0.16
	PERCENTAGE		31.2	36.1	32.6	24.7	35.5	30.6	33.9	75.3		
	DSR		1.20	1.72	1.46	1.44	0.96	0.83	0.88	0.89		
C	LOAD, N	26	859	864	905	2628	2624	2465	2507	7596	10224	0.34
	PERCENTAGE		32.7	32.9	34.4	25.7	34.5	32.5	33.0	74.3		
	DSR		1.34	1.66	1.65	1.53	0.94	0.88	0.87	0.90		
B+C	LOAD, N	21	867	888		2643	2605	2397	2499	7501	10144	1.25
	PERCENTAGE		32.8	33.6		26.1	34.7	32.0	33.3	73.9		
	DSR		1.35	1.66		1.54	0.93	0.86	0.87	0.88		

DYNAMIC LOAD ANALYSIS FOR TEST NUMBER D100E1

PEAK LOCATION	DELTA	WALL SECTION				FLOOR SECTION				TOTAL LOAD	DISCHARGE TIME, s	
		A	B	C	TOTAL	A	B	C	TOTAL			
SERIES1	STATIC LOAD, N		687	633	665	1985	2546	2477	2504	7527	9512	-0.39
DELTA	LOAD, N	565	486	992	1110	2588	2838	1929	1834	6601	9189	9.60
	PERCENTAGE		18.8	38.3	42.9	28.2	43.0	29.2	27.8	71.8		
	DSR		0.71	1.57	1.67	1.30	1.11	0.78	0.73	0.88		
B	LOAD, N	528	593	1093	1149	2835	2824	1933	1923	6680	9515	1.34
	PERCENTAGE		20.9	38.6	40.5	29.8	42.3	28.9	28.8	70.2		
	DSR		0.86	1.73	1.73	1.43	1.11	0.78	0.77	0.89		
C	LOAD, N	545	578	1085	1160	2823	2843	1944	1905	6692	9515	1.74
	PERCENTAGE		20.5	38.4	41.1	29.7	42.5	29.0	28.5	70.3		
	DSR		0.84	1.71	1.74	1.42	1.12	0.78	0.76	0.89		
B+C	LOAD, N	542	581	1123		2827	2843	1938	1904	6685	9512	1.56
	PERCENTAGE		20.6	39.7		29.7	42.5	29.0	28.5	70.3		
	DSR		0.85	1.73		1.42	1.12	0.78	0.76	0.89		
SERIES2	STATIC LOAD, N		629	527	582	1738	2519	2493	2492	7504	9242	-0.36
DELTA	LOAD, N	507	431	892	983	2306	2849	1986	1924	6759	9065	3.87
	PERCENTAGE		18.7	38.7	42.6	25.4	42.2	29.4	28.5	74.6		
	DSR		0.69	1.69	1.69	1.33	1.13	0.80	0.77	0.90		
B	LOAD, N	436	529	961	969	2459	2775	1956	2021	6752	9211	0.72
	PERCENTAGE		21.5	39.1	39.4	26.7	41.1	29.0	29.9	73.3		
	DSR		0.84	1.82	1.66	1.41	1.10	0.78	0.81	0.90		
C	LOAD, N	477	489	934	997	2420	2803	1981	1962	6746	9166	1.73
	PERCENTAGE		20.2	38.6	41.2	26.4	41.6	29.4	29.1	73.6		
	DSR		0.78	1.77	1.71	1.39	1.11	0.79	0.79	0.90		
B+C	LOAD, N	461	511	972		2454	2794	1957	1998	6749	9203	1.05
	PERCENTAGE		20.8	39.6		26.7	41.4	29.0	29.6	73.3		
	DSR		0.81	1.75		1.41	1.11	0.78	0.80	0.90		
SERIES3	STATIC LOAD, N		518	615	464	1597	2980	2670	3006	8656	10253	-0.52
DELTA	LOAD, N	662	350	1022	1002	2374	3154	2432	2611	8197	10571	0.11
	PERCENTAGE		14.7	43.0	42.2	22.5	38.5	29.7	31.9	77.5		
	DSR		0.68	1.66	2.16	1.49	1.06	0.91	0.87	0.95		
B	LOAD, N	514	532	1045	1047	2624	3112	2186	2280	7578	10202	0.97
	PERCENTAGE		20.3	39.8	39.9	25.7	41.1	28.8	30.1	74.3		
	DSR		1.03	1.70	2.26	1.64	1.04	0.82	0.76	0.88		
C	LOAD, N	591	443	990	1077	2510	3185	2212	2196	7593	10103	3.24
	PERCENTAGE		17.6	39.4	42.9	24.8	41.9	29.1	28.9	75.2		
	DSR		0.86	1.61	2.32	1.57	1.07	0.83	0.73	0.88		
B+C	LOAD, N	514	532	1046		2624	3112	2186	2280	7578	10202	0.97
	PERCENTAGE		20.3	39.9		25.7	41.1	28.8	30.1	74.3		
	DSR		1.03	1.94		1.64	1.04	0.82	0.76	0.88		

DYNAMIC LOAD ANALYSIS FOR TEST NUMBER D100E2

PEAK LOCATION	DELTA	WALL SECTION				FLOOR SECTION				TOTAL LOAD	DISCHARGE TIME, s	
		A	B	C	TOTAL	A	B	C	TOTAL			
SERIES1	STATIC LOAD, N		636	590	627	1853	2571	2540	2531	7642	9495	-0.31
DELTA	LOAD, N	907	251	1100	1216	2567	3097	1738	1622	6457	9024	10.43
	PERCENTAGE		9.8	42.9	47.4	28.4	48.0	26.9	25.1	71.6		
	DSR		0.39	1.86	1.94	1.39	1.20	0.68	0.64	0.84		
B	LOAD, N	744	430	1142	1205	2777	2997	1848	1810	6655	9432	1.30
	PERCENTAGE		15.5	41.1	43.4	29.4	45.0	27.8	27.2	70.6		
	DSR		0.68	1.94	1.92	1.50	1.17	0.73	0.72	0.87		
C	LOAD, N	798	376	1128	1220	2724	3044	1861	1769	6674	9398	2.21
	PERCENTAGE		13.8	41.4	44.8	29.0	45.6	27.9	26.5	71.0		
	DSR		0.59	1.91	1.95	1.47	1.18	0.73	0.70	0.87		
B+C	LOAD, N	787	390	1177	1205	2744	3034	1855	1783	6672	9416	1.90
	PERCENTAGE		14.2	42.9	29.1	29.1	45.5	27.8	26.7	70.9		
	DSR		0.61	1.93	1.48	1.48	1.18	0.73	0.70	0.87		
SERIES2	STATIC LOAD, N		599	558	505	1662	2848	2694	2872	8414	10076	-0.39
DELTA	LOAD, N	1032	135	1103	1231	2469	3492	1830	1739	7061	9530	11.97
	PERCENTAGE		5.5	44.7	49.9	25.9	49.5	25.9	24.6	74.1		
	DSR		0.23	1.98	2.44	1.49	1.23	0.68	0.61	0.84		
B	LOAD, N	829	374	1173	1233	2780	3332	1949	1960	7241	10021	1.29
	PERCENTAGE		13.5	42.2	44.4	27.7	46.0	26.9	27.1	72.3		
	DSR		0.62	2.10	2.44	1.67	1.17	0.72	0.68	0.86		
C	LOAD, N	993	214	1143	1270	2627	3471	1907	1834	7212	9839	5.04
	PERCENTAGE		8.1	43.5	48.3	26.7	48.1	26.4	25.4	73.3		
	DSR		0.36	2.05	2.51	1.58	1.22	0.71	0.64	0.86		
B+C	LOAD, N	993	214	1207	1270	2627	3471	1907	1834	7212	9839	5.04
	PERCENTAGE		8.1	45.9	26.7	26.7	48.1	26.4	25.4	73.3		
	DSR		0.36	2.27	1.58	1.58	1.22	0.71	0.64	0.86		
SERIES3	STATIC LOAD, N		643	612	570	1825	2792	2667	2822	8281	10106	-0.76
DELTA	LOAD, N	1069	62	1067	1195	2324	3554	1857	1772	7183	9507	12.53
	PERCENTAGE		2.7	45.9	51.4	24.4	49.5	25.9	24.7	75.6		
	DSR		0.10	1.74	2.10	1.27	1.27	0.70	0.63	0.87		
B	LOAD, N	852	312	1143	1184	2639	3401	1993	2039	7433	10072	0.84
	PERCENTAGE		11.8	43.3	44.9	26.2	45.8	26.8	27.4	73.8		
	DSR		0.49	1.87	2.08	1.45	1.22	0.75	0.72	0.90		
C	LOAD, N	1021	144	1099	1231	2474	3537	2000	1876	7413	9887	4.63
	PERCENTAGE		5.8	44.4	49.8	25.0	47.7	27.0	25.3	75.0		
	DSR		0.22	1.80	2.16	1.36	1.27	0.75	0.66	0.90		
B+C	LOAD, N	884	293	1177	1205	2646	3416	1991	1994	7401	10047	1.15
	PERCENTAGE		11.1	44.5	26.3	26.3	46.2	26.9	26.9	73.7		
	DSR		0.46	1.99	1.45	1.45	1.22	0.75	0.71	0.89		

DYNAMIC LOAD ANALYSIS FOR TEST NUMBER D100E3

PEAK LOCATION	DELTA	WALL SECTION				FLOOR SECTION				TOTAL LOAD	DISCHARGE TIME, s	
		A	B	C	TOTAL	A	B	C	TOTAL			
SERIES1	STATIC LOAD, N		544	670	598	1812	2536	2231	2397	7164	8976	-0.57
DELTA	LOAD, N	763	287	1030	1070	2387	2933	1675	1691	6299	8686	6.07
	PERCENTAGE		12.0	43.2	44.8	27.5	46.6	26.6	26.8	72.5		
	DSR		0.53	1.54	1.79	1.32	1.16	0.75	0.71	0.88		
B	LOAD, N	670	424	1133	1055	2612	2857	1676	1839	6372	8984	0.39
	PERCENTAGE		16.2	43.4	40.4	29.1	44.8	26.3	28.9	70.9		
	DSR		0.78	1.69	1.76	1.44	1.13	0.75	0.77	0.89		
C	LOAD, N	756	317	1057	1088	2462	2935	1683	1719	6337	8799	3.67
	PERCENTAGE		12.9	42.9	44.2	28.0	46.3	26.6	27.1	72.0		
	DSR		0.58	1.58	1.82	1.36	1.16	0.75	0.72	0.88		
B+C	LOAD, N	686	419	1105	2628	2848	1651	1809	6308	8936		0.78
	PERCENTAGE		15.9	42.0	29.4	45.1	26.2	28.7	70.6			
	DSR		0.77	1.74	1.45	1.12	0.74	0.75	0.88			
SERIES2	STATIC LOAD, N		627	512	526	1665	2675	2656	2724	8055	9720	-0.34
DELTA	LOAD, N	874	188	990	1133	2311	3313	1907	1787	7007	9318	8.64
	PERCENTAGE		8.1	42.8	49.0	24.8	47.3	27.2	25.5	75.2		
	DSR		0.30	1.93	2.15	1.39	1.24	0.72	0.66	0.87		
B	LOAD, N	658	428	1072	1100	2600	2903	2080	2014	6997	9597	0.17
	PERCENTAGE		16.5	41.2	42.3	27.1	41.5	29.7	28.8	72.9		
	DSR		0.68	2.09	2.09	1.56	1.09	0.78	0.74	0.87		
C	LOAD, N	725	370	1035	1154	2559	3190	1960	1940	7090	9649	1.53
	PERCENTAGE		14.5	40.4	45.1	26.5	45.0	27.6	27.4	73.5		
	DSR		0.59	2.02	2.19	1.54	1.19	0.74	0.71	0.88		
B+C	LOAD, N	693	406	1099	2604	3147	1978	1947	7072	9676		1.10
	PERCENTAGE		15.6	42.2	26.9	44.5	28.0	27.5	73.1			
	DSR		0.65	2.12	1.56	1.18	0.74	0.71	0.88			
SERIES3	STATIC LOAD, N		468	453	413	1334	2998	2838	3009	8845	10179	-3.62
DELTA	LOAD, N	1076	42	1049	1187	2278	3639	1966	1870	7475	9753	8.92
	PERCENTAGE		1.8	46.0	52.1	23.4	48.7	26.3	25.0	76.6		
	DSR		0.09	2.32	2.87	1.71	1.21	0.69	0.62	0.85		
B	LOAD, N	910	253	1155	1171	2579	3533	1986	2054	7573	10152	0.64
	PERCENTAGE		9.8	44.8	45.4	25.4	46.7	26.2	27.1	74.6		
	DSR		0.54	2.55	2.84	1.93	1.18	0.70	0.68	0.86		
C	LOAD, N	1066	82	1086	1209	2377	3634	2001	1913	7548	9925	5.75
	PERCENTAGE		3.4	45.7	50.9	23.9	48.1	26.5	25.3	76.1		
	DSR		0.18	2.40	2.93	1.78	1.21	0.71	0.64	0.85		
B+C	LOAD, N	932	247	1179	2605	3541	1989	2011	7541	10146		0.88
	PERCENTAGE		9.5	45.3	25.7	47.0	26.4	26.7	74.3			
	DSR		0.53	2.72	1.95	1.18	0.70	0.67	0.85			

APPENDIX G  
DATA ACQUISITION PROGRAM LISTING

```
1000 REM *****
1010 REM          COLLECT1
1020 REM    DATA ACQUISITION PROGRAM FOR THREE CHANNELS ON TAURUS ONE UNIT #1
1030 REM    A RESTART FEATURE ALLOWS PROGRAM TO BE RUN FROM LINE 1470 IF NECESSARY
1040 REM          WRITTEN BY DARRYL POKRANT
1050 REM          CREATION DATE: NOVEMBER 1986
1060 REM          LAST MODIFICATION DATE: DECEMBER 19,1986
1070 REM *****
1080 GOSUB 3000:REM          INITIALIZE TAURUS UNIT #1
1090 REM *****
1100 REM    CONTINUOUSLY READ CHANNELS AND DISPLAY.  ZERO THE AMPLIFIER OUTPUTS
1110 REM *****
1120 KEY OFF:DEFSTR U,V,D,M
1130 CLS:LOCATE 25,7
1140 PRINT "SET AMPLIFIER BALANCE FOR ZERO READING      PRESS ENTER TO CONTINUE"
1150 LOCATE 1,1:A$=INKEY$
1160 WHILE A$ <> CHR$(13)
1170   PRINT #1,"$A0 1 AA (1,0)":LINE INPUT #1,B$:LINE INPUT #1,B$
1180   PRINT #1,"$A0 1 AR (3)":INPUT #1,B$,N1$,N2$,N3$,E$
1190   PRINT TAB(19);:PRINT USING "\          \"";N1$;N2$;N3$
1200   A$=INKEY$
1210 WEND
1220 CLS:LOCATE 3,26:PRINT "BALANCING SEQUENCE COMPLETE"
1230 REM *****
1240 GOSUB 4000:REM    CHOOSE FILENAME AND OPEN INPUT FILES ON RAM DISK
1250 REM *****
1260 REM    SCAN EACH CHANNEL 25 TIMES WITH A 5 ms PERIOD FOR THE FOLLOWING CASES:
1270 REM    1)EMPTY BIN  2)FULL BIN AFTER LOADING  3)FULL BIN BEFORE UNLOADING
1280 REM    DISPLAY MAXIMUM, MINIMUM AND AVERAGE VALUES.  STORE AVERAGE VALUES
1290 REM *****
1300 CLS:LOCATE 13,20
1310 PRINT "YOU ARE NOW READY TO BEGIN TEST ";:COLOR 0,7:PRINT FILE$:COLOR 7,0
1320 LOCATE 25,18:PRINT "PRESS ENTER TO TAKE READINGS FROM EMPTY BIN"
1330 A$=INKEY$:IF A$ <> CHR$(13) GOTO 1330 ELSE CLS
1340 COUNT=1:GOSUB 5000
1350 LSET STATIC1$=MKI$(AVG(1))+MKI$(AVG(2))+MKI$(AVG(3))
1360 LOCATE 25,18:PRINT "    PRESS ENTER ONCE BIN HAS BEEN FILLED      "
1370 GOSUB 6000
1380 COUNT=2:GOSUB 5000
1390 LSET STATIC2$=MKI$(AVG(1))+MKI$(AVG(2))+MKI$(AVG(3))
1400 LOCATE 25,18:PRINT "    PRESS ENTER WHEN YOU ARE READY TO UNLOAD    "
1410 GOSUB 6000
1420 COUNT=3:GOSUB 5000
1430 LSET STATIC3$=MKI$(AVG(1))+MKI$(AVG(2))+MKI$(AVG(3))
1440 PUT #2,546
1450 GOTO 1480
1460 REM *****
1470 GOSUB 3000:DEFSTR D,M,U,V:CLS:GOSUB 4000:REM          RESTART FEATURE
1480 REM *****
1490 REM    PERFORM 109 SECONDS OF DATA ACQUISITION - 21800 SCANS AT 5 ms INTERVALS
1500 REM    ACQUISITION TRIGGERS WHEN DISCHARGE GATE OPENS (TAURUS CHANNEL 7 RISES)
1510 REM          TRANSFER DATA TO RANDOM ACCESS FILE ON DRIVE C
1520 REM *****
1530 PRINT #1,"$A0 1 AA CA(21800,5,1)":LINE INPUT #1,B$
1540 CLS:LOCATE 12,32:COLOR 26,0:PRINT "READY TO UNLOAD":COLOR 7,0
1550 LOCATE 14,14:PRINT "DATA ACQUISITION TRIGGERS WHEN DISCHARGE GATE OPENS"
1560 IF EOF(1) GOTO 1560
1570 CLS:LOCATE 11,27:PRINT "DATA ACQUISITION TRIGGERED"
1580 LOCATE 13,20:PRINT "TRANSFER TAKES APPROXIMATELY 2.5 MINUTES"
1590 LOCATE 15,32:COLOR 26,0:PRINT "<DO NOT DISTURB>":COLOR 7,0
```

```
1600 FOR I=1 TO 545
1610   LSET DYNAMIC$=INPUT$(240,#1)
1620   PUT #2,I
1630 NEXT I
1640 LINE INPUT #1,B$
1650 CLS:LOCATE 13,20:PRINT "DATA ACQUISITION AND TRANSFER COMPLETED"
1660 REM *****
1670 REM   AFTER UNLOADING, SCAN EACH CHANNEL 25 TIMES WITH A 5 ms PERIOD
1680 REM   DISPLAY MAXIMUM, MINIMUM AND AVERAGE VALUES.  STORE AVERAGE VALUES
1690 REM *****
1700 LOCATE 25,18:PRINT "PRESS ENTER WHEN BIN IS COMPLETELY UNLOADED"
1710 GOSUB 6000
1720 CLS:COUNT=4:GOSUB 5000
1730 GET #2,546
1740 LSET STATIC4$=MKI$(AVG(1))+MKI$(AVG(2))+MKI$(AVG(3))
1750 PUT #2,546
1760 CLOSE #1,#2
1770 CLS:LOCATE 11,28
1780 PRINT "TEST ";:COLOR 0,7:PRINT FILE$;:COLOR 7,0:PRINT " IS COMPLETE"
1790 LOCATE 13,20:PRINT "RESULTS ARE CURRENTLY STORED ON DRIVE C"
1800 LOCATE 15,13:COLOR 26,0
1810 PRINT "INSERT DATA DISKETTE FROM OTHER COMPUTER INTO DRIVE B":COLOR 7,0
1820 LOCATE 25,20:PRINT " PRESS ENTER TO UPLOAD DATA INTO DRIVE C"
1830 A$=INKEY$: IF A$ <> CHR$(13) GOTO 1830
1840 REM *****
1850 REM   CREATE RANDOM FILES TO UPLOAD DATA FROM DRIVE B TO DRIVE C
1860 REM *****
1870 OPEN "R",#3,"B:"+FILE$+".456",4096
1880 OPEN "R",#4,"C:"+FILE$+".456",4096
1890 DIM U(17),V(17),X$(436),Y$(436),Z$(436):I=250
1900 FIELD #3,I AS U(1),I AS U(2),I AS U(3),I AS U(4),I AS U(5),I AS U(6),
      I AS U(7),I AS U(8),I AS U(9),I AS U(10),I AS U(11),I AS U(12),
      I AS U(13),I AS U(14),I AS U(15),I AS U(16),96 AS U(17)
1910 FIELD #4,I AS V(1),I AS V(2),I AS V(3),I AS V(4),I AS V(5),I AS V(6),
      I AS V(7),I AS V(8),I AS V(9),I AS V(10),I AS V(11),I AS V(12),
      I AS V(13),I AS V(14),I AS V(15),I AS V(16),96 AS V(17)
1920 CLS:LOCATE 11,29:PRINT "UPLOADING IN PROGRESS"
1930 LOCATE 13,21:PRINT "TRANSFER TAKES APPROXIMATELY 1 MINUTE"
1940 LOCATE 15,32:COLOR 26,0:PRINT "<DO NOT DISTURB>":COLOR 7,0
1950 FOR I=1 TO 32
1960   GET #3,I
1970   FOR J=1 TO 17
1980     LSET V(J)=U(J)
1990   NEXT J
2000   PUT #4,I
2010 NEXT I
2020 CLOSE #3,#4:KILL "B:"+FILE$+".456"
2030 CLS:LOCATE 13,22:PRINT "UPLOADING COMPLETE - PLEASE STAND BY"
2040 REM *****
2050 REM   OPEN RANDOM FILES ON DRIVE C WITH RECORD LENGTHS OF 2616-BYTES
2060 REM   MERGE DATA FROM FILES TESTNAME.123 AND TESTNAME.456
2070 REM   DOWNLOAD STATIC AND DYNAMIC DATA TO SEPARATE FILES ON DRIVE B
2080 REM *****
2090 OPEN "R",#5,"C:"+FILE$+".123",2616
2100 OPEN "R",#6,"C:"+FILE$+".456",2616
2110 OPEN "R",#7,"B:"+FILE$+".DYN",5232
```

```
2120 FOR I=0 TO 217 STEP 2
2130   FIELD #5,I AS DUM1,I AS DUM2,I AS DUM3,I AS DUM4,I AS DUM5,I AS DUM6,
      I AS DUM7,I AS DUM8,I AS DUM9,I AS DUM10,I AS DUM11,I AS DUM12,
      6 AS X$(2*I),6 AS X$(2*I+1),6 AS X$(2*I+2),6 AS X$(2*I+3)
2140   FIELD #6,I AS DUM1,I AS DUM2,I AS DUM3,I AS DUM4,I AS DUM5,I AS DUM6,
      I AS DUM7,I AS DUM8,I AS DUM9,I AS DUM10,I AS DUM11,I AS DUM12,
      6 AS Y$(2*I),6 AS Y$(2*I+1),6 AS Y$(2*I+2),6 AS Y$(2*I+3)
2150   FIELD #7,I AS D1,I AS D2,I AS D3,I AS D4,I AS D5,I AS D6,I AS D7,I AS D8
      ,I AS U1,I AS U2,I AS U3,I AS U4,I AS U5,I AS U6,I AS U7,I AS U8,I AS M1
      ,I AS M2,I AS M3,I AS M4,I AS M5,I AS M6,I AS M7,I AS M8,48 AS Z$(2*I)
2160 NEXT I
2170 CLS:LOCATE 11,24:PRINT "MERGE AND DOWNLOAD IN PROGRESS"
2180 LOCATE 13,20:PRINT "TRANSFER TAKES APPROXIMATELY 8 MINUTES"
2190 LOCATE 15,32:COLOR 26,0:PRINT "<DO NOT DISTURB>":COLOR 7,0
2200 FOR I=1 TO 50
2210   GET #5,I
2220   GET #6,I
2230   FOR J=0 TO 435 STEP 4
2240     LSET Z$(J)=X$(J)+Y$(J)+X$(J+1)+Y$(J+1)+X$(J+2)+Y$(J+2)+X$(J+3)+Y$(J+3)
2250   NEXT J
2260   PUT #7,I
2270 NEXT I
2280 CLOSE #7
2290 OPEN "R",#8,"B:"+FILE$+".STA",48
2300 FIELD #8,48 AS STATIC$
2310 GET #5,51
2320 GET #6,51
2330 LSET STATIC$=X$(0)+Y$(0)+X$(1)+Y$(1)+X$(2)+Y$(2)+X$(3)+Y$(3)
2340 PUT #8,1
2350 CLS:LOCATE 13,30:PRINT "DOWNLOADING COMPLETE"
2360 CLEAR:KILL "C:*.*)"
2370 OPEN "COM1:9600,N,8,1,RS,CS,DS"AS #1
2380 LOCATE 25,13:PRINT "PRESS ENTER TO RETURN TO AMPLIFIER BALANCING SEQUENCE"
2390 A$=INKEY$:IF A$ <> CHR$(13) GOTO 2390 ELSE GOTO 1120
3000 REM *****
3010 REM           SUBROUTINE: GOSUB 3000
3020 REM SUBROUTINE FOR OPENING COMMUNICATION TO AND INITIALIZING TAURUS ONE #1
3030 REM *****
3040 OPEN "COM1:9600,N,8,1,RS,CS,DS" AS #1
3050 REM UPDATE COMMUNICATION PARAMETERS: SEND LINE FEED WITH CARRIAGE RETURN
3060 PRINT #1,"$A0 1 UC CA (18,10)":LINE INPUT #1,B$
3070 REM SETUP SCAN TABLE: BUS ADDRESS=0, START CHANNEL=0, NUMBER OF CHANNELS=3
3080 PRINT #1,"$A0 1 AS CL(0,0,3)":LINE INPUT #1,B$
3090 REM SETUP TRIGGER ON CHANNEL NUMBER 7 AS RISE OF 500 TAURUS NUMBERS
3100 PRINT #1,"$A0 1 TS (0,7,+500)":LINE INPUT #1,B$
3110 RETURN
4000 REM *****
4010 REM           SUBROUTINE: GOSUB 4000
4020 REM SUBROUTINE FOR CHOOSING FILENAME AND OPENING INPUT FILE ON DRIVE C
4030 REM *****
4040 LOCATE 9,20:PRINT "CHOOSE FILENAME FOR DATA STORAGE USING:"
4050 LOCATE 11,26:PRINT "DIAMETER (D45,D60,D75,D100)"
4060 LOCATE 13,26:PRINT "ECCENTRICITY (E0-E3)"
4070 LOCATE 15,26:PRINT "SERIES NUMBER (S1-S6)"
4080 LOCATE 18,26:COLOR 26,0:INPUT "WHAT IS FILENAME";FILE$:COLOR 7,0
4090 OPEN "R",#2,"C:"+FILE$+".123",240
4100 FIELD #2,240 AS DYNAMIC$
4110 FIELD #2,6 AS STATIC1$,6 AS STATIC2$,6 AS STATIC3$,6 AS STATIC4$
4120 RETURN
```

```
5000 REM *****
5010 REM                SUBROUTINE: GOSUB 5000
5020 REM                SUBROUTINE FOR TAKING READINGS AT A GIVEN STATIC CONDITION
5030 REM                25 READINGS PER CHANNEL ARE AVERAGED AND THE RESULTS ARE DISPLAYED
5040 REM *****
5050 LOCATE 17,1:PRINT SPACE$(160)
5060 LOCATE 25,16:COLOR 26,0
5070 PRINT "  COMPUTER TAKING READINGS - PLEASE STAND BY  ":COLOR 7,0
5080 PRINT #1,"$A0 1 AA (25,5)":LINE INPUT #1,B$:LINE INPUT #1,B$
5090 FOR I=1 TO 3
5100     SUM(I)=0:HIGH(I)=-2048:LOW(I)=2047
5110 NEXT I
5120 FOR I=1 TO 25
5130     PRINT #1,"$A0 1 AR(3)"
5140     INPUT #1,B$,N(1),N(2),N(3),E$
5150     FOR J=1 TO 3
5160         SUM(J)=SUM(J)+N(J)
5170         IF N(J) > HIGH(J) THEN HIGH(J)=N(J)
5180         IF N(J) < LOW(J) THEN LOW(J)=N(J)
5190     NEXT J
5200 NEXT I
5210 FOR I=1 TO 3
5220     AVG(I)=SUM(I)/25\1
5230 NEXT I
5240 ON COUNT GOTO 5250,5260,5270,5280
5250 LOCATE 1,34:PRINT "TRANSDUCER 1  TRANSDUCER 2  TRANSDUCER 3":LOCATE 5,7:
      PRINT "EMPTY BIN":GOTO 5290
5260 LOCATE 11,7:PRINT "FULL BIN":LOCATE 12,9:PRINT "AFTER":LOCATE 13,8:PRINT
      "LOADING":GOTO 5290
5270 LOCATE 18,7:PRINT "FULL BIN":LOCATE 19,7:PRINT "PRIOR TO":LOCATE 20,7:PRINT
      "UNLOADING":GOTO 5290
5280 LOCATE 1,34:PRINT "TRANSDUCER 1  TRANSDUCER 2  TRANSDUCER 3":LOCATE 4,7:
      PRINT "EMPTY BIN":LOCATE 5,9:PRINT "AFTER":LOCATE 6,7:PRINT "UNLOADING"
5290 ROW=((COUNT-1) MOD 3)+1)*7
5300 LOCATE ROW-4,23
5310 PRINT "MAXIMUM";:PRINT USING "      #### " ;HIGH(1);HIGH(2);HIGH(3)
5320 LOCATE ROW-2,23
5330 PRINT "MINIMUM";:PRINT USING "      #### " ;LOW(1);LOW(2);LOW(3)
5340 LOCATE ROW,23
5350 PRINT "AVERAGE";:PRINT USING "      #### " ;AVG(1);AVG(2);AVG(3)
5360 LOCATE 25,18:PRINT "      ARE THESE READINGS OKAY? (Y/N)      "
5370 A$=INKEY$
5380 IF A$<>"N" AND A$<>"Y" AND A$<>CHR$(13) GOTO 5370 ELSE IF A$="N" GOTO 5060
5390 RETURN
6000 REM *****
6010 REM                SUBROUTINE: GOSUB 6000
6020 REM                SUBROUTINE TO DISPLAY CURRENT TAURUS VALUES FROM EACH CHANNEL
6030 REM *****
6040 A$=INKEY$:LOCATE 17,11:COLOR 15,0:PRINT"CURRENT TAURUS VALUE":COLOR 7,0
6050 WHILE A$ <> CHR$(13)
6060     PRINT #1,"$A0 1 AA (1,0)":LINE INPUT #1,B$:LINE INPUT #1,B$
6070     PRINT #1,"$A0 1 AR (3)"
6080     INPUT #1,B$,N(1),N(2),N(3),E$
6090     TOTAL=N(1)+N(2)+N(3)
6100     IF TOTAL=0 THEN PCENT(1)=0:PCENT(2)=0:PCENT(3)=0:GOTO 6140
6110     FOR I=1 TO 3
6120         PCENT (I)=N(I)/TOTAL*100
6130     NEXT I
6140     LOCATE 17,37:PRINT USING "#### " ;N(1);N(2);N(3)
6150     LOCATE 18,37:PRINT USING " #### " ;PCENT(1);PCENT(2);PCENT(3)
6160     A$=INKEY$:WEND
6170 RETURN
```